

UC Davis

UC Davis Electronic Theses and Dissertations

Title

The Synergistic Inactivation of Bacteria with the Combined Ultrasound and Food Grade Antimicrobial Treatment

Permalink

<https://escholarship.org/uc/item/61q6b98t>

Author

Nguyen, Cuong Huu

Publication Date

2022

Peer reviewed|Thesis/dissertation

The Synergistic Inactivation of Bacteria with the Combined Ultrasound and Food Grade Antimicrobial Treatment

By

CUONG HUU NGUYEN
DISSERTATION

Submitted in partial satisfaction of the requirements for the degree of

DOCTOR OF PHILOSOPHY

in

Food Science

in the

OFFICE OF GRADUATE STUDIES

of the

UNIVERSITY OF CALIFORNIA

DAVIS

Approved:

Nitin Nitin, Chair

Gang Sun

Glenn M. Young

Committee in Charge

2022

ACKNOWLEDGEMENTS

I would like to express my gratitude to all the people who have made the research presented in this dissertation possible. I would be remiss not to show appreciation to the University of California, Davis, and to the Robert Mondavi Institute for Wine and Food Science. Not only to these institutions but to their faculty and staff, who have provided me with countless opportunities, and fellowships, and have facilitated my learning and progression as a scientist.

I owe a significant debt of gratitude to my advisor, Dr. Nitin Nitin. Your encouragement, whether gentle nudges or forceful shoves, has always led me down the path to success and personal growth. I aspire to one day be as great of a mentor as you have been to me.

Thank you to Dr. Juliana Bell and Dr. Gang Sun for your guidance and patience through my qualifying exam and through the length of this dissertation work.

I would like to thank my Nitin Lab family, especially Dr. Rewa Rai, a kind and compassionate instructor, Dr. Stephen Young, an exceedingly intelligent role model, and my sushi buffet partner, and Erick and Maha, who keep me together through the frustrating and emotional times.

A special thank you to my family, my wife, and two of my sons, who are my greatest source of motivation to fulfill my Ph.D. journey. And to those who have passed on in my life; I hope you are smiling down as I am smiling up at you.

And to the most important person in my life, my mother and father. My gratitude for all you have done for me exceeds the number of stars in the universe; the debt I owe you can never be summed up or repaid. Thank you for your love, your sacrifice, your inspiration, and thank you for never doubting me or my potential. I owe everything to you.

The Synergistic Inactivation of Bacteria with the Combined Ultrasound and Food Grade Antimicrobial Treatment

ABSTRACT

Despite being able to attain commercial sterility, thermal processing can promote reactions that could lower the overall quality of foods. Non-thermal processing was developed to solve some of the fundamental constraints of thermal processing, which reduces food nutrition and sensory quality. Non-thermal processing systems do, however, have some inherent limitations, such as a low rate of bacterial inactivation and the necessity for a lengthy treatment period. To increase the efficacy and shorten the treatment time needed of non-thermal processing, this study assessed the combination of two common non-thermal processing techniques, namely UV light irradiation and ultrasound treatment with food grade antimicrobial compounds.

This study evaluated a synergistic antimicrobial treatment using a combination of ultrasound in a low frequency (LFU, 40kHz) or a high-frequency domain (HFU, 1 MHz) and a food-grade antioxidant, propyl gallate (PG, 10 mM), against a model gram-positive (*Listeria innocua*) and the gram-negative bacteria (*Escherichia coli* O157:H7) in water and a model beverage (apple juice). Treatment times ranged from 5 to 15 minutes for HFU and 5 to 45 minutes for LFU. Bacterial inactivation kinetic measurements were complemented by characterization of biophysical changes in liposomes, changes in bacterial membrane permeability, morphological changes in bacterial cells, and intracellular oxidative stress upon treatment with LFU/HFU, PG, and a combination of LFU/HFU + PG.

This study also evaluated the effects of a synergistic antimicrobial combination of high-frequency ultrasounds and the food-grade antioxidant, propyl gallate, against mono-species biofilms from *L. innocua* and multispecies biofilms formed using a raw milk sample and *L. innocua*.

This study also examines the antibacterial activity of combining UV-A light treatment or high-frequency (HFU) ultrasound treatment with three different classes of phenolic compounds (gallate derivatives, cinnamic acid derivatives, and other polyphenolic compounds such as quercetin, flavone,

and grape seed extract) against *E. coli* O157:H7 and *L. innocua*. This study was motivated by the need to develop compounds that can work synergistically with UV-A light treatment or HFU.

The result of this study indicated that the combination of ultrasound, both LFU and HFU, with PG resulted in a significant enhanced bacterial inactivation of 5 log CFU/mL, $P < 0.05$, within 10 (HFU) to 30 minutes (LFU) of treatment time. The inactivation kinetic of HFU is significantly faster compared to LFU with the same PG concentration. Combined treatment of HFU + PG also significantly (> 5 log CFU/mL, $P < 0.05$) enhanced the inactivation of both *L. innocua* and multispecies biofilm as compared to single treatments of HFU or PG, after 30 minutes of treatment time. Upon extended treatment of cells with LFU/HFU and PG, a significant increase in membrane damage was observed compared to LFU/HFU or PG single treatments. Although oxidative stress was not the primary mechanism responsible for synergistic inactivation by LFU+PG, it was one of the factors contributing to bacterial inactivation in HFU+PG treatment. Overall, the study illustrates synergistic inactivation of various bacteria targets using a combination of LFU/HFU and PG based on enhanced membrane damage, oxidative stress and metabolic activity suppression and its potential for applications in the food and environmental systems.

On the screening study, six photo-activated compounds were found to have a synergistic interaction with UV-A inactivating *E. coli* O157:H7, and four compounds were confirmed in the case of *L. innocua*, all of which belong to cinnamic acid derivatives. Of six photosensitizers confirmed in UV-A treatment, there were four retained their antimicrobial effectiveness when combined with HFU. Sinapic acid (SA) demonstrated the highest bacterial inactivation efficiency of the 18 chemicals tested when combined with either UV-A or HFU treatment. A "cause and effect" relationship between the physiochemical responses of the targeted bacteria to the combined treatments was observed, where intracellular oxidative stress could be a direct result of membrane damage, and membrane damage could also contribute to the inactivation of membrane-associated dehydrogenase enzyme families.

Chapter 1

Introduction

1. The motivation for this study

1.1. Thermal technologies for food processing

1.1.1. Overall view of thermal processing:

Thermal processing is currently the most widely used food preservation method for microbial inactivation in the food industry. Thermal inactivation of bacteria and enzymes results in shelf-stable, safe products. The extent of thermal treatment required for a food product depends on whether it is an acid product, an acidified product, or a low-acid product. A pH of 4.6 has been selected as a dividing line between acid and low-acid food (Kumar & Sandeep, 2014). An acid food product is one with a natural pH of less than 4.6. Acid food products include apple juice, orange juice, ketchup, etc. An acidified food product is one with an equilibrium pH of less than 4.6 and a water activity (a_w) greater than 0.85. Examples of acidified foods include peppers treated in an acid brine, pickled foods (excluding foods pickled by fermentation), etc. For acid and acidified food, the application of pasteurization treatment at 90–95 °C for 30–90 sec can destroy all bacteria that are non-spore formers (usually *Lactobacillus* species) or spoilage microbes such as yeasts and molds. A low-acid food product is any food other than alcoholic beverages, with a natural equilibrium pH greater than 4.6 and a water activity greater than 0.85. These food products include butter, cheese, fresh eggs, pears, papaya, and raisins (Skudder, 1993). One food safety risk in low-acid food products, that are not a concern with

acid food, is the growth of *Clostridium botulinum* spores. *C. botulinum* is an anaerobic, gram-positive, heat-resistant spore-forming bacterium that produces a potent neurotoxin. Because certain types of *C. botulinum* spores are very heat resistant and can survive five to 10 hours in boiling water, it is necessary to apply much higher temper than pasteurization temperatures, 250 °F (121 °C), and under pressure to destroy the spores (Kumar & Sandeep, 2014).

1.1.2. Effect of thermal processing on food qualities:

Thermal processing techniques emphasize the achievement of commercial sterility while minimizing changes in nutritional value and sensory quality. However, no matter how minimal the heating method is, thermal processing can promote reactions that could affect the overall quality of foods (Awuah et al., 2007). Quality loss involves both subjective factors like taste that cannot be readily quantified and quantifiable factors such as nutrient degradation. Although pasteurized products can achieve a shelf-life of a few days or weeks, changes to the nutritional and sensory characteristics do occur from mild heat treatments (Simpson, 2009). When a high temperature is applied for an extended period of time in the autoclave (canning) process, chemical reactions occur, resulting in the loss of nutrients as well as sensory properties such as appearance, color, flavor, and texture (Kumar & Sandeep, 2014).

Vitamins:

Vitamins are one of the most susceptible food components to thermal processing. Vitamin degradation during heat treatment is not simple and dependent on other agents such as oxygen, light, and water solubility. In addition, vitamin degradation depends on pH and may be catalyzed by chemicals present, metals, other vitamins, and enzymes (Lewis & Heppell,

2000). Heat-sensitive vitamins are the fat-soluble Vitamins A, D, E, and β -carotene, and water-soluble Vitamin C (ascorbic acid), Vitamins B₁ (thiamine), and B₂ (riboflavin), nicotinic acid, pantothenic acid, and biotin C (Ryley & Kajda, 1994). In general, the largest loss of Vitamin C in non-citrus foods occurs during heating (Fennema, 1996). In canned juices, the loss of Vitamin C tends to follow consecutive first order reactions, i.e., a rapid oxygen-dependent reaction that proceeds until oxygen is depleted, followed by anaerobic degradation (Fennema, 1996).

Browning:

Even mild heat treatment from the pasteurization process can trigger Maillard reactions, which are a complex series of reactions between proteins and reducing sugars via Amadori rearrangements (Rechkemmer, 2007). The initial Maillard reaction is characterized by a colorless solution, but after several reactions, a brown or black insoluble compound called melanoidins is formed (Eliasson, 2006). Although such reactions may be desirable in generating characteristic flavors identified with some cooked products, the nutritional value of the product will be compromised by protein damage and loss of amino acids, including lysine, L-arginine, and L-histidine. The loss of lysine is important due to its essentiality in diet (Eliasson, 2006).

Proteins

The effect of thermal processing on proteins can be divided into two: those responsible for altering the secondary, tertiary, and quaternary structure of proteins and those that alter the primary structure. Breaking the secondary, tertiary, and quaternary structures unfolds the proteins and improves their bioavailability since peptide bonds become readily accessible to

digestive enzymes. However, modifications of primary protein structures by thermal treatment on the other hand may lower digestibility and produce proteins that are not biologically available as recently demonstrated by beta-lactoglobulin (Swaisgood, 1985). In cell culture model systems of Caco-2 cells and M cells, respectively, it was demonstrated that heat-denatured beta-lactoglobulin was less efficiently transported through mammalian cell membrane than the native form (Rytkönen et al., 2006).

Color

The color of processed foods plays a role in influencing consumer acceptability. Natural occurring pigments in foods are susceptible to changes or degradation from heat such as chlorophylls (in photosynthetic tissues), anthocyanins (the red and blue hues associated with many fruits and vegetables), carotenoids (found in fruits, dairy products, eggs, fish and vegetables) and betanins (present in red beetroots and meat) (Awuah et al., 2007). After heat treatment, chlorophylls are converted to pyropheophytin via pheophytin in fruits and vegetables, while carotenoids are isomerized from 5,6-epoxides to 5,8-epoxides which have less color intensity. Anthocyanins are changed by heat to brown pigments. This loss in color attributes of heat-treated food products will adversely affect the purchase decision and consumer acceptance of thermally processed foods (Fellows, 2009).

1.2. Alternative processes to thermal processing

In the last 20 years, consumer demand for high-quality, microbiologically safe, and stable foods has resulted in a growing interest in nonthermal preservation techniques capable of inactivating microorganisms and enzymes (Barbosa-Canovas & Rodriguez, 2002; Knorr et al.,

2011). This led to the development of non-thermal processing to address some key limitations of thermal treatment adversely decreases food nutrition and sensory qualities. Generally, nonthermal technologies are processes that are applied at sublethal or ambient temperature, leading to minimal or no impact on key nutritional and quality parameters of foods (Tiwari et al., 2009). The term 'nonthermal processing' is more appropriate for novel nonthermal technologies, such as high hydrostatic pressure, pulsed electric fields (PEFs), high-intensity ultrasound, ultraviolet light, and plasma treatment which are intended for application as microbe-inactivating processes (Knoerzer, 2016). The food quality preservation effect of non-thermal technologies is better than that of thermal technologies since there is a minimum presence of heat-induced formation of undesirable products/by-products in food (Van Impe et al., 2018). Some of the most extensively researched nonthermal processes are high hydrostatic pressure (HHP), pulsed electric fields (PEF), UV light irradiation, and ultrasound treatment.

1.2.1. High Hydrostatic Pressure:

High hydrostatic pressure (HHP) utilizes a very common medium, i.e., water, to apply the pressure on the product to be treated. HHP can bring about a significant decimal decrease ($\sim 5 \log$ CFU/ml) in the population of pathogenic bacteria, yeast, and mold and helps in food preservation for a longer duration (Van Impe et al., 2018). The reduction in microbial load depends on the pressure and temperature during treatment and largely depends on the type of food being processed. The pressure applied to food during treatment is in the range of 200–700 MPa (Barba et al., 2017). Food, when subjected to HHP treatment, undergoes high pressure for a short duration of time. In addition, HHP does not affect the covalent bonds that make up

most of the flavor and color compounds in fruits and vegetables (Knorr et al., 2011). As a result, the quality in terms of nutritional components, sensory, and texture of HHP-processed food is preserved better than heat treatment.

For bacterial inactivation applications, a pressure of 350–450 MPa is sufficient for the inactivation of Gram-negative bacteria, yeast, and mold at room temperature, but to inactivate Gram-positive bacteria, a pressure of more than 1,100 MPa is required (Ross et al., 2003). The high-pressure results in damage to the cell membrane of microbial cells, which changes the permeability of the microbial cell wall and membranes (Roohinejad et al., 2018). The coiled protein structure breaks and there is destruction to microbial cell enzymes, which alter the metabolic pathways; finally, the microbial cell dies, leading to a decrease in the microbial population in food (Barba et al., 2017). In contrast, the drawbacks of HPP are that this technology can also alter the noncovalent bonds that make up the structure of protein and polysaccharides, causing the undesired change in texture, physical appearance, and functionality of food (Knorr et al., 2011). Raw meat when subjected to HHP, even at a mild level of 300 MPa, for 1 min showed signs of a “cooked meat” appearance due to the denaturation of heme protein pigment of meat, thus decreasing the sensory quality of meat products (Bak et al., 2019).

Furthermore, the expensive initial capital investment and operating costs of HHP are impeding its broad use in the food business. Despite the fact that the capital cost of implementing HPP has been reduced in part by constructing larger units with a tenfold increase in vessel capacity over the last 15 years, a commercial HPP unit will still cost between US\$ 0.5 and 2.5 million, depending on the capacity and automation level (Mújica-Paz et al., 2011). This

level of capital investment is not feasible for all food producers. Furthermore, due to the difficulty of designing chambers that can sustain high-pressure processing, a technological barrier occurs at 680 MPa, and there are no vessels available for commercial uses above this pressure level. Designing a commercial system that can reach pressures above 700 MPa (sterilization level) is considerably more expensive, hence HHP is mostly used in the pasteurization process (200 - 600 MPa) (Torres & Velazquez, 2005). The cost of operating an HHP plant is determined by several factors, including the plant's operation schedule (300 days is suggested), pressure come-up time, holding time (3 min is desirable for commercial viability), and vessel filling ratio (50 % minimum recommended) (Mújica-Paz et al., 2011). The cost of operating HHP units varies depending on the level of use and vessel size, but it is estimated to be between 0.071 and 0.194 US\$/lb (Mújica-Paz et al., 2011). To be considered economically viable, HHP-treated products must generate additional profits that exceed the mentioned capital and operating costs, and this is only true for high-value food products such as high-value seafood (oysters, lobster, etc.), cold-pressed juice/cold brew coffee, and high-value meat products (Parma ham or Serrano ham) (Norton & Sun, 2008). Therefore, the use of HHP for lower-value food commodities is hindered by these cost constraints.

1.2.2. Pulsed Electric Field (PEF):

Pulsed electric field (PEF) is an emerging non-thermal technology that finds various food sector applications. In a pulsed electric field, a pulse of high field intensity is applied to food for a very short duration of time (Toepfl et al., 2006). Usually, for the treatment of food, the field intensity is from 25 to 85 kV/cm, and the exposure time is a few milliseconds or nanoseconds.

Since food is exposed to a pulsed electric field for a very short duration of time, there is no heating; thus, minimizing the undesirable changes in food (Toepfl et al., 2006). The pulsed electric field is generally used for liquid food or semi-solid food that can flow easily (Barba et al., 2017). There is damage to the cell membrane of microbes due to the high electric field intensity, causing membrane poration. Furthermore, hydrogen peroxide is observed in PEF-treated samples, causing oxidative damage to cell lipids and protein components, as well as metabolic enzymes, together with membrane damage, resulting in cell death. (Roohinejad et al., 2018). The efficiency of PEF in reducing microbial load largely depends on the intensity of the field applied, the total exposure time, temperature, and energy (Roohinejad et al., 2018). However, the following are some of the most significant drawbacks of the PEF technology: - High initial cost; little effect on bacterial spores; only appropriate for liquid particles in liquids; products of electrolysis may adversely affect foods; energy efficiency not yet certain (Knorr et al., 2011). PEF has limited applicability, which is confined to foods that can survive high electric fields. Furthermore, the particle size of liquid food restricts the use of PEF in both static and flow treatment modes. The maximum particle size in the liquid must be smaller than the gap of the treatment region in the chamber to maintain a proper processing operation (Knorr et al., 2011).

1.2.3. UV light irradiation:

Ultraviolet technology is a very economical, non-thermal technology. UV light reduces the microbial load on the surface of food materials that are indirectly exposed to radiation, which are grouped as UV-A in the electromagnetic spectrum in the range of 320–400 nm, UV-B

in the range of 280–320 nm, and UV-C in the range of 200–280 nm (Jadhav et al., 2021). When food is exposed to UV-C, with 200–280 nm, these short wavelengths are absorbed by the microbial cell nucleic acids (Popović et al., 2021). These absorbed photons cause the breakage of the bond and interlinking between thymine and pyrimidine of different strands and the formation of dimers of pyrimidine. These dimers prevent DNA transcription and translation, thus leading to the malfunctioning of the genetic material, which causes microbial cell death (Guerrero-Beltrán & Ochoa-Velasco, 2021). The photons of UV-A and UV-B result in the destruction of the cellular membranes, proteins of microbial cells, and other cellular organelles (Koutchma et al., 2021). Due to its simple operation, UV is one of the well-established non-thermal processing technologies adopted by food processing industries (Jadhav et al., 2021). The effect of UV can be more intensified if the process is coupled with antimicrobial compounds to bring about desired inactivation level (Ross et al., 2003). Some of the critical challenges with UV light irradiation include the treatment's reliance on light transmission through the treated media, so the bacterial inactivation effect is lessened when the media is cloudy or has a color that would otherwise absorb the light source wavelength. Moreover, UV-C wavelength is deemed carcinogenic that is harmful to human health (Koutchma et al., 2021). In addition, UV-A and UV-B single treatment without the use of antimicrobial compounds have a very limited bacterial inactivation effect (Barbosa-Cánovas & Rodríguez, 2002).

The aforementioned nonthermal technologies have numerous potential applications in the food sector; however, this current study focuses on ultrasound as a treatment of interest due to multiple advantages. The following section will cover the basics of ultrasonic technology,

as well as the most difficult aspects and constraints of the processes, as well as our research strategy to improve this emerging non-thermal technology.

2. Introduction to the ultrasound systems used in this study

2.1. Theory

In simple words, ultrasound is a sound wave bearing a certain frequency that is more than the normal human hearing frequency, i.e., above 20kHz (Ashokkumar, 2015). When ultrasonic waves oscillate through a medium, they generate many expansion and compression cycles in the medium. There are formations of small cavities due to the presence of air in the liquid medium. This is known as the acoustic cavitation phenomena (Rokhina et al., 2009). The cavities formed grow to a certain size and then collapse. When these cavities collapse, they generate a considerable amount of mechanical energy as well as a rise in local temperature, resulting in an increase in heat and mass transfer rates (Bhangu & Ashokkumar, 2017). Ultrasonication is used with different frequencies, which are classified as low-frequency, medium-frequency, and high-frequency ultrasonication, with frequency ranges of 20 kHz– 100 kHz, 100 kHz–1 MHz, and 1 MHz–100 MHz, respectively (Mason et al., 2015). The dominant effect of low-frequency ultrasonication is the mechanical forces in the form of the shock waves, shear forces, and micro-jets stream, released with the bursting of cavitation bubbles. In the medium frequency (100 kHz - 1MHz), the dominant effects are the formation of radical species as well as micro mixing and localized temperature rise. This frequency range is optimum for various sonochemical-assisted processes (Rokhina et al., 2009). The higher frequency range (> 1

MHz to 100 MHz) has a predominant effect on radiation forces (Duck & Leighton, 2018) and does not fall into the scope of this study.

2.1.1. Chemical and physical effects of ultrasound treatment at a different frequency

Non-thermal effects - acoustic cavitation:

According to Suslick (Suslick et al., 1999), chemical and physical effects of ultrasound occur not from direct interaction with molecular species but from the cavitation phenomenon: the formation, growth, and implosive collapse of cavities in liquids that release large amounts of highly localized energy. Cavitation can be classified into four types based on its mode of generation: acoustic, hydrodynamic, optic, and particle (Guzmán et al., 2003). Of these, only acoustic and hydrodynamic cavitation can generate the intensities required to induce chemical or physical changes in a system (Guzmán et al., 2003). The cavitation bubbles' size and the energy released when they implode are dependent on the ultrasound frequency used. The low-frequency band generates less but bigger and more powerful cavitation bubbles, and vice versa, high-frequency generates more cavitation bubbles with a smaller size and less powerful. The following section describes those relationships in detail. The cavitation bubble size is related to the resonance frequency as shown in equation 1 (Kanthale et al., 2008):

$$R_r = \frac{1}{2\pi f_r} \left(\frac{3kp}{\rho L} \right) \quad (1)$$

Where k is the polytropic coefficient - indicating a certain thermodynamic process of a system

p is the undisturbed static pressure in the liquid (Pa)

ρ is the fluid density (kg/m³)

R_r is the resonant radius of cavitation bubble (m)

f_r is the resonant frequency (Hz)

According to this equation, the radius of a cavitation bubble (R_r) is inversely related to the resonant frequency. This also means low-frequency wave leads to larger bubbles and vice versa higher frequency ultrasound will have smaller cavitation bubbles. Zhang (Zhang et al., 1989) reported that acoustic energy released during cavitation depends on bubble size according to the following relation:

$$\frac{E_{ac}}{(4/3)\pi P_h} = \frac{1}{27c} r_{max}^3 \left(\frac{2P_h}{\rho}\right)^{1/2} \left(\frac{P_h}{Q}\right)^{3/2} \quad (2)$$

Where E_{ac} is the acoustic energy (J)

r_{max} is the maximum bubble radius (m)

c is the speed of sound (m/s)

P_h is the local pressure in the flow field (Pa)

ρ is the mass density of water (kg/m³)

Q is the partial pressure of gas in the bubble for radius r_{max} (Pa)

Equation (2) shows an inverse relationship between energy (E_{ac}) released when a cavitation bubble busts and the bubble maximum radius r_{max} . When combined with equation 1, low-frequency waves create larger acoustic bubbles that release more energy when they collapse, whereas high-frequency ultrasound-induced cavitation bubbles release smaller and

less energy (Fuchs & Puskas, 2005). In addition, D'Agostino and Brennen (d'Agostino & Brennen, 1983) discovered that the number of bubbles is proportional to the square of the frequency, $N \propto \omega^2$, where N is the number of bubbles and ω is the radial frequency, which value is calculated by $2\pi f$, and f expresses the ultrasound frequency. Therefore, at higher MHz frequencies, more bubbles are formed which is due to the more cycles of compression and expansion (Chen, 2010; Fuchs & Puskas, 2005).

These characteristics in the number and size of acoustic bubble generated by different frequencies will affect chemical reactions in the medium that ultrasound is applied. The chemical reactions that happen by the effect of ultrasound treatments are known as sonochemical reactions and highly depend on ultrasound frequency (Kanthale et al., 2008). A typical sonochemical reaction happens when the energy in the form of heat from the bubble implosion hydrolyze water molecule into highly reactive hydrogen atoms ($H\bullet$) and hydroxyl radicals ($OH\bullet$). Hydroxyl radicals and hydrogen atoms then recombine to form hydrogen peroxide and molecular hydrogen, respectively. Because of this molecular environment, organic and inorganic compounds may be oxidized or reduced depending on their reactivity. As described earlier, in low-frequency ultrasound there is a more violent eruption of acoustic bubbles and with that more energy is released. This leads to a higher concentration of the free radicals generated by low-frequency ultrasound. This makes low-frequency ultrasound one of the advanced oxidation processes (AOPs) widely used in wastewater treatment (Bagal & Gogate, 2014; Mahvi, 2009; Sivakumar et al., 2002; S. Wang et al., 2008; Xiong et al., 2011). Whereas, at higher frequencies, it is proved that the rate in which the sonochemistry happens is faster according to several theoretical studies (Jun Yasuda & Shin Yoshizawa, 2015). This is

because there are more cavitation bubbles that happen at a much faster manner with a higher frequency US. This results in a higher reaction rate for sonochemical-assisted reactions (Asakura & Yasuda, 2021).

Thermal effect:

The direct effect of ultrasound that can be observed is ultrasonic heating (Humphrey, 2007). The acoustic energy removed from the wave by absorption is deposited in the medium as heat at a rate q_v per unit volume where

$$q_v = 2\alpha_a I \quad (3)$$

and I is the intensity (W/cm^2) of the wave at the measurement location. As a result of this heat deposition, the temperature T at a point in the field will initially rise at a rate given by

$$\frac{dT}{dt} = \frac{2\alpha_a I}{\rho_0 C_p} \quad (4)$$

where α_a is the total absorption coefficient associated with any absorption process and have a dependence on frequency, I is the intensity (W/cm^2), ρ_0 is the density (kg/m^3), and C_p is the specific heat capacity ($\text{J}/\text{kg}\cdot\text{K}$) of the medium at constant pressure. The quantity $2\alpha_a I/\rho_0$ has been termed acoustic dose rate and it characterizes the rate of transfer of energy from the wave to unit mass of the medium and has units W kg^{-1} (Duck & Leighton, 2018). The dependence on the frequency of the initial rate of rising of temperature is identical to the dependence of coefficient α_a on frequency (Duck & Leighton, 2018). For the simple models often used for regulatory purposes, α_a is assumed to have a linear frequency dependence at

the low MHz range (1-10 MHz). In this frequency range, the rate in which temperature rises proportionally relates to the increase of ultrasonic frequency. Draper (Draper et al., 1995) proved this relationship through measure the difference in temperature rises between 1 and 3 MHz and concluded that 3 MHz induced a much faster temperature rise at all intensities tested. Subsequent temperature rises in a media or in biological tissue depends on other factors, including the period of exposure, beam dimensions, and the dissipation of heat by thermal conduction and convection (including perfusion) (Duck & Leighton, 2018).

Biophysical effect:

It is well documented that ultrasound can produce a wide variety of biological effects in vitro and in vivo, and the acoustic mechanisms responsible for some of these bioeffects have been identified (O'Brien, 2007). The physical changes (Rokhina et al., 2009) at the molecular level are classified as thermal, including pyrolysis and combustions as well as non-thermal, including cavitation and shearing force. The thermal effects typically do not cause significant damage; however, the extent of any cell damage will depend on the absorbed energy, the maximum temperature achieved, and exposure duration (Rokhina et al., 2009). Observed cell damage can include partial and full lysis (Piyasena et al., 2003). The cavitation-induced non-thermal effects reflect on the changes to ultra-structures within cells, altering enzyme stability through the protein denaturation effect. Cavitation and shearing also alter cell growth properties, which could lead to cell lysis. Other effect includes nucleus rupture and the release of DNA as well as the breakage of extracellular polymer substances (Roohinejad et al., 2018).

Other changes include chemical and stress-induced changes. Chemical changes caused by cavitation-induced radical production include decreased cellular stability and oxidation of cellular components such as lipoprotein and nucleic acids (Van Impe et al., 2018). On the other hand, the stress-induced changes resulted from the acoustic micro streaming. This mechanical effect leads to an enhanced mass transport inside and outside of the cell including the uptake of antimicrobial compounds or the efflux of intracellular material, due to the alteration of membrane permeability (Rokhina et al., 2009). The acoustic streaming also alters cell surface charge and ruptures the cell membranes (Arroyo & Lyng, 2017).

2.2. Application of ultrasound

2.2.1. Low-frequency ultrasound (LFU)

When low-frequency ultrasound is employed, the implosive collapse of cavitation bubbles causes mechanical phenomena such as shock waves or micro-jets and micro-streaming. (Piyasena et al., 2003). Based on these mechanical phenomena, low-frequency ultrasound technology offers a wide range of applications in food processing, including defoaming, emulsification, extrusion, extraction, and waste treatment. The ultrasound frequency range from 20 to 100 kHz is used in the food industry including emulsification and extraction (Kentish & Feng, 2014; Rahimi et al., 2014). Ultrasound-assisted inactivation of foodborne pathogens and spoilage enzymes is an alternative to traditional thermal processes due to the lower processing temperatures and energy required, thus better food quality (Arroyo & Lyng, 2017; Sango et al., 2014). The application of low-frequency ultrasound for the inactivation of bacteria

in food systems has been evaluated (Arroyo & Lyng, 2017; Ashokkumar, 2015; Sango et al., 2014).

Microbial inactivation with conventional low-frequency, high-intensity ultrasound technology is mostly due to sonoporation (Meng et al., 2019). Sonoporation is the formation of pores on cellular membranes as a result of micromechanical shockwaves, shear forces, and sonochemical reactions (free radical generation) (Arroyo & Lyng, 2017; Birmpa et al., 2013; Sango et al., 2014). In addition, morphological changes, thinning or disruption of cell membranes, and altering genetic mechanisms have also been proposed as the impacts of low-frequency ultrasound treatment (Kentish & Feng, 2014). However, the key limitations of the process are limited inactivation effectiveness, only around 2 log CFU/mL, and extended treatment time from 30 min to several hours (Abdallah et al., 2014; Bang et al., 2017; Carmen et al., 2004, 2005; Dong et al., 2013). To address these limitations, ultrasound technology is often combined with other treatments such as thermal (thermosonication) or high-pressure processing (manosonication) to improve the inactivation of bacteria (Evelyn & Silva, 2015, 2018; Guzel et al., 2014; Lee et al., 2009; Paga'n et al., 1999; Palgan et al., 2012; Ross et al., 2003). Prior studies have shown that a simultaneous combination of Ultrasound with thermal treatment (thermosonication) or high-pressure (manosonication) processing can achieve 4-5 log bacterial inactivation (Coronel et al., 2011; Evelyn & Silva, 2015, 2016, 2018; Lee et al., 2009).

Despite this potential, industrial translation of these concepts has been limited due to various factors including the capital cost of combining existing ultrasound technologies with thermal or high-pressure processing, the potential deterioration of food quality attributes, or

the destruction of ultrasound devices due to the cavitation effect (Ross et al., 2003).

Additionally, thermal and high-pressure processing, even though being used at a lower level when combined with ultrasound treatment, still have an impact on the overall quality or texture of food products (Guzel et al., 2014; Lee et al., 2009).

2.2.2. High-frequency ultrasound (HFU)

It is well known that HFU generates stable cavitation in which cavitation bubbles do not implode vigorously. As a result, this type of cavitation has no sonoporation effect, hence the HFU treatment has the advantage of maintaining the structural integrity of food products. The impact of stable cavitation is the creation of free radicals and a greater rate of local temperature rise caused by volume absorption of the treated material, as stated in section 2.1.1 (Duck & Leighton, 2018; Rahimi et al., 2014). As discussed in section 2.1.1, stable cavitation also produces acoustic micro streaming, which exerts stress on biological cells due to altered membrane permeability, resulting in enhanced antimicrobial agent uptake and/or efflux of intracellular chemicals. The preservation of food structural integrity and the combined effects of free radical generation, localized temperature rise, and enhanced membrane damage make HFU a strong candidate for bacterial inactivation in food applications.

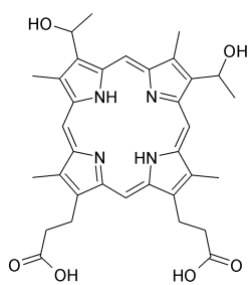
Indeed, a growing subject within high-frequency ultrasonic research is investigating the combination of HFU with antimicrobial compounds for microbial inactivation applications, known as antimicrobial sonodynamic therapy (ASDT). Because of its immense potential, the ASDT is gaining substantial traction among academic researchers and industries. Several studies have looked at ASDT applications for bacterial inactivation (Costley et al., 2017; Dadjour et al.,

2006; Drakopoulou et al., 2009; Liu et al., 2011; Nakonechny et al., 2013; Pang et al., 2019; Pourhajibagher et al., 2020; Serpe & Giuntini, 2015; Tachibana et al., 2008; X. Wang et al., 2014, 2015; Xu et al., 2016; Zhuang et al., 2014). The synergistic bacterial inactivation of the combined HFU and additional antimicrobial compounds is based on a combination of free radical augmentation (from treatment medium or from added antimicrobial compounds), mass transfer improvement, and biological membrane damage. Although SDT is conceptually similar to the well-established photodynamic therapy (PDT), which uses light instead of ultrasound to activate the sensitizer (Dougherty et al., 1998), the former still exhibits several distinct advantages. Ultrasonic irradiation is superior to light irradiation in that the applied energy can be focused precisely on the specific pathological location requiring treatment. In addition, ultrasound is a type of mechanical wave that can penetrate tissues to a greater extent than light. As a result, SDT can be used to treat deeply located diseases (Tachibana et al., 2008). Moreover, studies have shown that high-frequency and low-intensity ultrasound can alter the cell membrane, thus increasing its permeability to sonosensitizers (Harrison & Balcer-Kubiczek, 1991). The compounds that can work synergistically with ultrasound in bacterial inactivation applications are referred to as "sonosensitizers," and they are discussed in greater detail in the next section.

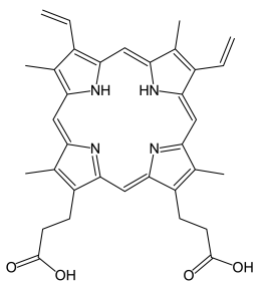
2.3. Sonosensitizer compounds

As mentioned in the previous section, the generation of free radicals or reactive oxygen species (ROS) is the mechanism underlying ASDT (Shibaguchi et al., 2011). When the sonosensitizer is exposed to a specific intensity and frequency of ultrasound, it is activated from

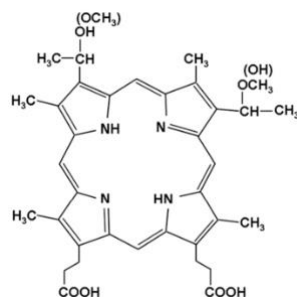
the ground to an excited state. On returning to the ground state, it releases energy, which is transferred to oxygen to produce ROS, such as singlet oxygen and free radicals. These ROS can mediate apoptosis, thereby inhibiting the growth of pathological cells (Trendowski, 2014). It is worth mentioning that these sonosensitizers have low toxicity and no inhibitory effect by themselves, and they become active only after being exposed to ultrasonic irradiation. There is a diverse spectrum of sonosensitizing chemicals available, including synthesized drugs and naturally occurring substances. However, due to their biocompatibility and potential to be introduced to the food system, naturally occurring and food-grade compounds have received a lot of attention in recent years. Examples of natural and natural-derived sonosensitizers are Porphyrins from blood (Hematoporphyrin, Protoporphyrin IX, and Hematoporphyrin monomethyl ether), Chlorophyll derivatives from green plants, and silkworm excrement (Pheophorbide a, Pyropheophorbide-a methyl ester, and Chorin a6), Hypocrellins from traditional Chinese herb *Hypocrella bambuase* (Hypocrellin B and SL-017) and lastly Curcumin from *Curcuma longa* (Curcumin and Hydroxyl-acylated curcumin) (Pang et al., 2016).



Hematoporphyrin



Protoporphyrin IX



Hematoporphyrin monomethyl ether

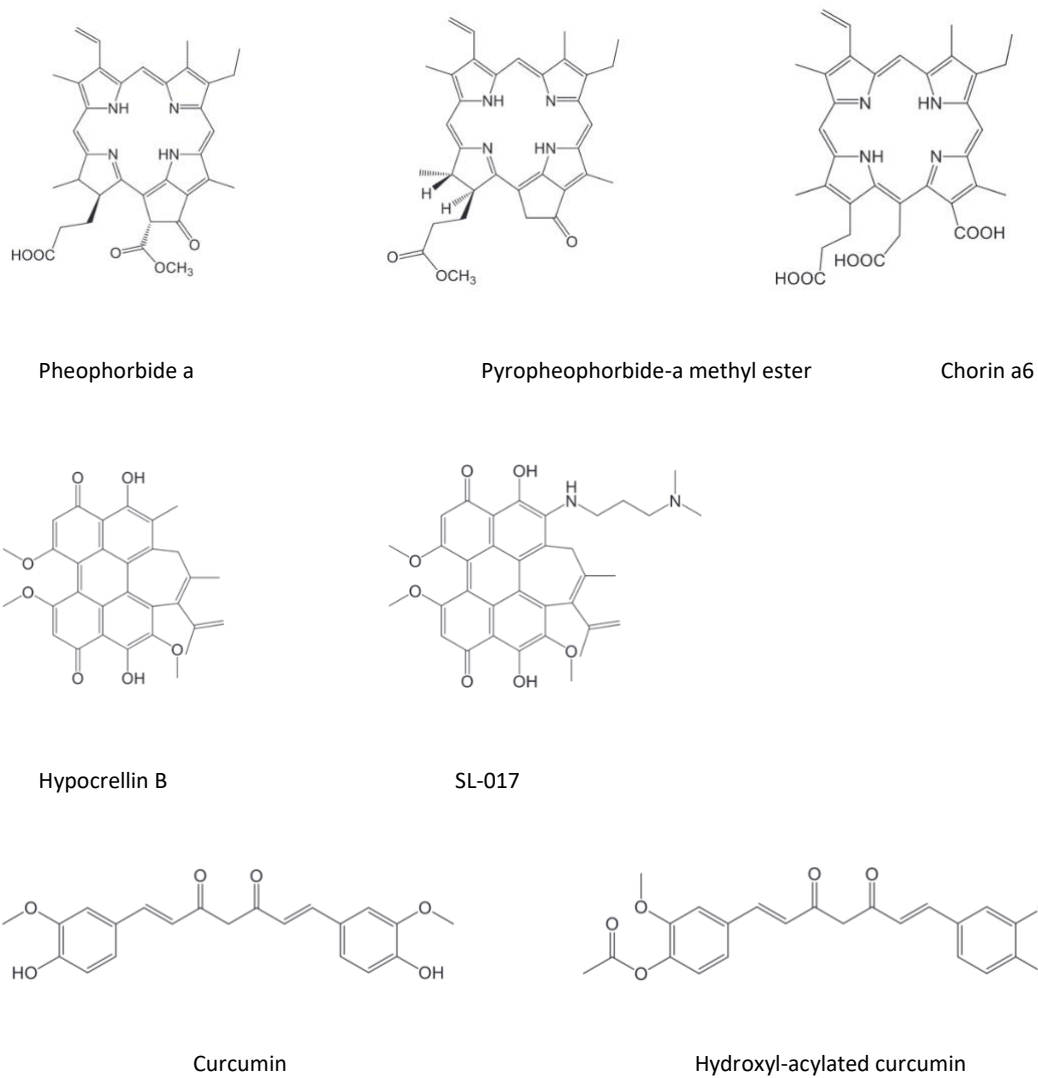


Fig.1. Chemical structures of natural and natural-derived sonosensitizers

Sonosensitizers derived from natural products play a significant role as highly potent anti-microbial, anti-infective, and anti-inflammatory agents. More importantly, natural compounds often exhibit high selectivity and specific biological activities based on their ability to modulate multiple signaling pathways (Cragg & Newman, 2013; Turrini et al., 2014). As a result, a lower dosage of natural sensitizer can be utilized to achieve the same level of inactivation as a higher concentration of chemical-based disinfection.

2.4. Microorganism target in this study

In general, both Gram-positive and Gram-negative are the target for the application of ASDT; due to a wide variation in the cellular structure and organization, the interaction of sonosensitizers with these bacterial targets are significantly different. Compared with Gram-negative species, their Gram-positive counterparts are much more susceptible to ASDT because of the thick but porous peptidoglycan layer that makes it easier for sensitizer to enter. Both bacterial species show an overall negatively charged cell surface. Such an anionic envelope acts as an electro-attractive surface for cationic sensitizers that are more efficiently bound to and internalized by bacteria (Pang et al., 2016), thus the electrostatic interaction between sonosensitizers and the bacterial membrane is critical for ASDT to work.

Due to the short lifetimes ($\sim 10^{-9}$ sec) and mobility (5 - 15 nm) of ROS (Duco et al., 2016), the sensitizers are preferable to penetrate or at least bind to bacterial cell walls for maximum oxidative damage following ASDT. The ROS generated by sensitizer molecules may interact with different cellular components based on their affinities for these targets. In general, three putative bacterial targets have been proposed, including the cell membrane phospholipids, essential proteins, and nucleic acids (Alves et al., 2021). Comparatively, membrane proteins are considered the preferred targets for photo/sonodynamic oxidation, not only due to their vital functions in bacteria but also because they are abundant on the bacterial surface and able to quickly react with ROS after binding with exogenous sensitizers (Awad et al., 2016; Dosselli et al., 2012). By damaging such targets, considerable morphological and functional changes in microbial cells are induced by APDT/ASDT. Morphological damages mainly contain the

alteration of the mesosome structure. Mesosomes are unique membranous bacterial structures that actively function in cell injury and physiological cellular processes, such as replication and separation of nucleoids and oxidative phosphorylation (Li et al., 2014). As a result, damages to this special structure will have a major impact on bacteria's capacity to carry out typical membrane operations as well as cell multiplication. Moreover, direct destruction of the bacterial cell wall and the inner membrane will break membrane integrity, resulting in the leakage of cytoplasmic contents and subsequent inactivation of the membrane transport system. Functional alterations are generally caused by a disorder of membrane potential, loss of protein and enzyme activities, and inhibition of metabolic processes (e.g., DNA replication, and glucose transport) (Alves et al., 2021; Wang et al., 2020). In most cases, those two types of changes occur simultaneously. For instance, oxidative modification of component lipids alters membrane fluidity and organization as well as membrane protein function that, when extensive enough, culminates in cell death (Alves et al., 2021).

3. Overview of the Dissertation Study

3.1. Hypothesis and specific objectives

The overall hypothesis of this study is a simultaneous combination of sub-lethal levels of ultrasound treatments and sub-lethal concentrations of sonosensitizers can lead to synergistic bacterial damages, including membrane damage and intracellular oxidation, and result in rapid and synergistic inactivation of bacteria in model aqueous and food systems. The results of this study will develop new processes for food industries based on synergistic combination of food grade sonosensitizers with ultrasound treatment to ensure microbial safety while minimizing

processing intensity on food. The study will also discover novel food grade sono-sensitizers for industrial application.

The specific objectives of the proposed research are to (a) characterize and quantify the synergism between ultrasound treatment and the selected sensitizers (i.e. benzoic acid derivatives), and (b) measure the biochemical changes in the ultrasound-treated cells with or without sonosensitizers to characterize a model of action and a potential pathway for synergistic bacterial inactivation and (c) Evaluate the translation of the synergistic inactivation between ultrasound treatment and sonosensitizers in model food model for bacterial disinfectant and compare results with other non-thermal processes. The knowledge base gained from this research project will provide a promising alternative to address some of the key limitations of both physical processing and chemical preservatives.

3.2. Study outline

3.2.1. The effect of the combination of low-frequency treatment and propyl gallate for the inactivation of target bacteria

Chapter 2 evaluated a synergistic antimicrobial treatment using a combination of low frequency and a low-intensity ultrasound (LFU) and a food-grade antioxidant, propyl gallate (PG), against a model gram-positive (*Listeria innocua*) and the gram-negative bacteria (*Escherichia coli* O157:H7). Bacterial inactivation kinetic measurements were complemented by the characterization of biophysical changes in liposomes, changes in bacterial membrane permeability, morphological changes in bacterial cells, and intracellular oxidative stress upon treatment with PG, LFU, and a combination of PG + LFU.

3.2.2. The effect of the combination of high-frequency treatment and propyl gallate for the inactivation of target bacteria

Chapter 3 evaluates a combination of high-frequency Ultrasound (HFU) and a food-grade antioxidant, propyl gallate (PG), to enhance the inactivation rates of a model Gram-positive (*Listeria innocua*) and a Gram-negative bacterium (*Escherichia coli* O157:H7) in water and a model food system. The study also evaluates potential mechanisms of synergistic interactions based on an assessment of alterations in bacterial permeability, morphology, and intracellular oxidative stress.

3.2.3. The effect of the combination of high-frequency treatment and propyl gallate for the removal and the inactivation of biofilm

Chapter 4 describes the use of high-frequency Ultrasound (HFU) and PG against a Gram-positive biofilm (*Listeria innocua*) and a multispecies biofilm model formed using raw milk. This setup included a high-frequency and low-intensity ultrasound and a food-grade antioxidant, propyl gallate (PG). The biofilm inactivation was complemented by removal efficiency, changes in enzymatic activities, and changes in morphology, in response to HFU, PG, and a combination of PG + HFU.

3.2.4. The synergistic activity of diverse class of food grade compounds combined with high frequency ultrasound for microbial inactivation

Chapter 5 describes the antimicrobial activity of the combination of either UV-A light treatment or ultrasound technology (US) and three different classes of compounds including

gallate derivatives, cinnamic acid derivatives, and others (Quercetin, Flavone, and Grape seed extract) against *Escherichia coli* O157:H7 and *Listeria innocua*. Synergistic antibacterial activity was initially screened between combinations of the UV-A light treatment and eighteen phenolic acids classified into three categories including gallates, cinnamic acid derivatives, and others. The underlying antimicrobial mechanism of the combination of UV-A and sinapic acid involved the production of intracellular reactive oxygen species (ROS), while the photodynamic treatment didn't induce enzyme inactivation in *E. coli* O157:H7. In contrast, the damage to the cell membrane was the key factor influencing the antimicrobial activity of the US and sinapic acid combination. These results may support the development and optimization of photo- and sono-antimicrobial chemotherapy for food sanitation.

Bibliography

- Ansari, J. A. Alves, F., Guimarães, G. G., Inada, N. M., Pratavieira, S., Bagnato, V. S., & Kurachi, C. (2021). Strategies to Improve the Antimicrobial Efficacy of Photodynamic, Sonodynamic, and Sonophotodynamic Therapies. *Lasers in Surgery and Medicine*, 53(8), 1113–1121. <https://doi.org/10.1002/lsm.23383>
- Arroyo, C., & Lyng, J. G. (2017). The Use of Ultrasound for the Inactivation of Microorganisms and Enzymes. In *Ultrasound in Food Processing* (pp. 255–286). John Wiley & Sons, Ltd. <https://doi.org/10.1002/9781118964156.ch9>
- Asakura, Y., & Yasuda, K. (2021). Frequency and power dependence of the sonochemical reaction. *Ultrasonics Sonochemistry*, 81, 105858. <https://doi.org/10.1016/j.ultsonch.2021.105858>

- Ashokkumar, M. (2015). Applications of ultrasound in food and bioprocessing. *Ultrasonics Sonochemistry*, 25(1), 17–23. <https://doi.org/10.1016/j.ultsonch.2014.08.012>
- Awad, M. M., Tovmasyan, A., Craik, J. D., Batinic-Haberle, I., & Benov, L. T. (2016). Important cellular targets for antimicrobial photodynamic therapy. *Applied Microbiology and Biotechnology*, 100(17), 7679–7688. <https://doi.org/10.1007/s00253-016-7632-3>
- Awuah, G. B., Ramaswamy, H. S., & Economides, A. (2007). Thermal processing and quality: Principles and overview. *Chemical Engineering and Processing: Process Intensification*, 46(6), 584–602. <https://doi.org/10.1016/j.cep.2006.08.004>
- Bak, K. H., Bolumar, T., Karlsson, A. H., Lindahl, G., & Orlien, V. (2019). Effect of high pressure treatment on the color of fresh and processed meats: A review. *Critical Reviews in Food Science and Nutrition*, 59(2), 228–252. <https://doi.org/10.1080/10408398.2017.1363712>
- Barba, F. J., Ahrné, L., Xanthakis, E., Landerslev, M. G., & Orlien, V. (2017). Chapter 2. *Innovative Technologies for Food Preservation*. <https://doi.org/10.1016/B978-0-12-811031-7.00002-9>
- Barbosa-Cánovas, G. V., & Rodríguez, J. J. (2002). Update on nonthermal food processing technologies: Pulsed electric field, high hydrostatic pressure, irradiation and ultrasound. *Food Australia*, 54(11), 513–520.
- Bhangu, S. K., & Ashokkumar, M. (2017). Theory of Sonochemistry. In J. C. Colmenares & G. Chatel (Eds.), *Sonochemistry: From Basic Principles to Innovative Applications* (pp. 1–28). Springer International Publishing. https://doi.org/10.1007/978-3-319-54271-3_1
- Dosselli, R., Million, R., Puricelli, L., Tessari, P., Arrigoni, G., Franchin, C., Segalla, A., Teardo, E., & Reddi, E. (2012). Molecular targets of antimicrobial photodynamic therapy identified

- by a proteomic approach. *Journal of Proteomics*, 77, 329–343.
<https://doi.org/10.1016/j.jprot.2012.09.007>
- Draper, D. O., Castel, J. C., & Castel, D. (1995). Rate of Temperature Increase in Human Muscle During 1 MHz and 3 MHz Continuous Ultrasound. *Journal of Orthopaedic & Sports Physical Therapy*, 22(4), 142–150. <https://doi.org/10.2519/jospt.1995.22.4.142>
- Duck, F., & Leighton, T. (2018). *Frequency bands for ultrasound, suitable for the consideration of its health effects: The Journal of the Acoustical Society of America: Vol 144, No 4*.
<https://asa.scitation.org/doi/10.1121/1.5063578>
- Duco, W., Grosso, V., Zaccari, D., & Soltermann, A. T. (2016). Generation of ROS mediated by mechanical waves (ultrasound) and its possible applications. *Methods*, 109, 141–148.
<https://www.sciencedirect.com/science/article/pii/S1046202316302274>
- Eliasson, A.-C. (Ed.). (2006). *Carbohydrates in food* (2nd ed). CRC/Taylor & Francis.
- Fellows, P. J. (2009). *Food Processing Technology: Principles and Practice*. Elsevier.
- Fennema, O. R. (1996). *Food Chemistry, Third Edition*. CRC Press.
- Guerrero-Beltrán, J. Á., & Ochoa-Velasco, C. E. (2021). 2.15—Ultraviolet-C Light Technology and Systems for Preservation of Fruit Juices and Beverages. In K. Knoerzer & K. Muthukumarappan (Eds.), *Innovative Food Processing Technologies* (pp. 210–226). Elsevier. <https://doi.org/10.1016/B978-0-08-100596-5.22937-5>
- Guzmán, H. R., McNamara, A. J., Nguyen, D. X., & Prausnitz, M. R. (2003). Bioeffects caused by changes in acoustic cavitation bubble density and cell concentration: A unified explanation based on cell-to-bubble ratio and blast radius. *Ultrasound in Medicine and Biology*, 29(8), 1211–1222. [https://doi.org/10.1016/S0301-5629\(03\)00899-8](https://doi.org/10.1016/S0301-5629(03)00899-8)

- Humphrey, V. F. (2007). Ultrasound and matter—Physical interactions. *Progress in Biophysics and Molecular Biology*, 93(1), 195–211.
<https://doi.org/10.1016/j.pbiomolbio.2006.07.024>
- Jadhav, H. B., Annapure, U. S., & Deshmukh, R. R. (2021). Non-thermal Technologies for Food Processing. *Frontiers in Nutrition*, 8, 657090. <https://doi.org/10.3389/fnut.2021.657090>
- Jun Yasuda & Shin Yoshizawa. (2015). Efficient generation of reactive oxygen species sonochemically generated by cavitation bubbles. *IEEE International Ultrasonics Symposium (IUS)*, 1–4.
<https://ieeexplore.ieee.org/stamp/stamp.jsp?tp=&arnumber=7329535>
- Kanthale, P., Ashokkumar, M., & Grieser, F. (2008). Sonoluminescence, sonochemistry (H₂O₂ yield) and bubble dynamics: Frequency and power effects. *Ultrasonics Sonochemistry*, 15(2), 143–150. <https://doi.org/10.1016/j.ultsonch.2007.03.003>
- Knoerzer, K. (2016). Nonthermal and Innovative Food Processing Technologies. In *Reference Module in Food Science* (p. 4). Elsevier. <https://doi.org/10.1016/B978-0-08-100596-5.03414-4>
- Knorr, D., Froehling, A., Jaeger, H., Reineke, K., Schlueter, O., & Schoessler, K. (2011). Emerging Technologies in Food Processing. *Annual Review of Food Science and Technology*, 2(1), 203–235. <https://doi.org/10.1146/annurev.food.102308.124129>
- Koutchma, T., Bissonnette, S., & Popović, V. (2021). 2.17—An Update on Research, Development and Implementation of UV and Pulsed Light Technologies for Nonthermal Preservation of Milk and Dairy Products. In K. Knoerzer & K. Muthukumarappan (Eds.),

- Innovative Food Processing Technologies* (pp. 256–276). Elsevier.
<https://doi.org/10.1016/B978-0-08-100596-5.22680-2>
- Kumar, P., & Sandeep, K. p. (2014). Thermal Principles and Kinetics. In *Food Processing* (pp. 17–31). John Wiley & Sons, Ltd. <https://doi.org/10.1002/9781118846315.ch2>
- Lewis, M. J., & Heppell, N. J. (2000). *Continuous thermal processing of foods: Pasteurization and UHT sterilization*. Aspen Publishers.
- Mason, T. J., Chemat, F., & Ashokkumar, M. (2015). 27—Power ultrasonics for food processing. In J. A. Gallego-Juárez & K. F. Graff (Eds.), *Power Ultrasonics* (pp. 815–843). Woodhead Publishing. <https://doi.org/10.1016/B978-1-78242-028-6.00027-2>
- O’Brien, W. D. (2007). Ultrasound-biophysics mechanisms. *Progress in Biophysics and Molecular Biology*, 93(1–3), 212–255. <https://doi.org/10.1016/j.pbiomolbio.2006.07.010>
- Pang, X., Xu, C., Jiang, Y., Xiao, Q., & Leung, A. W. (2016). Natural products in the discovery of novel sonosensitizers. *Pharmacology & Therapeutics*, 162, 144–151.
<https://doi.org/10.1016/j.pharmthera.2015.12.004>
- Piyasena, P., Mohareb, E., & McKellar, R. C. (2003). Inactivation of microbes using ultrasound: A review. *International Journal of Food Microbiology*, 87(3), 207–216.
[https://doi.org/10.1016/S0168-1605\(03\)00075-8](https://doi.org/10.1016/S0168-1605(03)00075-8)
- Popović, V., Koutchma, T., & Pagan, J. (2021). 2.22—Emerging Applications of Ultraviolet Light-Emitting Diodes for Foods and Beverages. In K. Knoerzer & K. Muthukumarappan (Eds.), *Innovative Food Processing Technologies* (pp. 335–344). Elsevier.
<https://doi.org/10.1016/B978-0-08-100596-5.22667-X>

- Rokhina, E. V., Lens, P., & Virkutyte, J. (2009). Low-frequency ultrasound in biotechnology: State of the art. *Trends in Biotechnology*, 27(5), 298–306.
<https://doi.org/10.1016/j.tibtech.2009.02.001>
- Roohinejad, S., Sant'Ana, A. S., & Greiner, R. (2018). Mechanisms of Microbial Inactivation by Emerging Technologies. *Innovative Technologies for Food Preservation*, 111–132.
<https://doi.org/10.1016/B978-0-12-811031-7.00004-2>
- Ross, A. I. V., Griffiths, M. W., Mittal, G. S., & Deeth, H. C. (2003). Combining nonthermal technologies to control foodborne microorganisms. *International Journal of Food Microbiology*. [https://doi.org/10.1016/S0168-1605\(03\)00161-2](https://doi.org/10.1016/S0168-1605(03)00161-2)
- Ryley, J., & Kajda, P. (1994). Vitamins in thermal processing. *Food Chemistry*, 49(2), 119–129.
[https://doi.org/10.1016/0308-8146\(94\)90148-1](https://doi.org/10.1016/0308-8146(94)90148-1)
- Rytkönen, J., Valkonen, K. H., Virtanen, V., Foxwell, R. A., Kyd, J. M., Cripps, A. W., & Karttunen, T. J. (2006). Enterocyte and M-cell Transport of Native and Heat-Denatured Bovine β -Lactoglobulin: Significance of Heat Denaturation. *Journal of Agricultural and Food Chemistry*, 54(4), 1500–1507. <https://doi.org/10.1021/jf052309d>
- Simpson, R. (Ed.). (2009). Principles of Thermal Processing: Pasteurization. In *Engineering Aspects of Thermal Food Processing*. CRC Press.
- Skudder, P. J. (1993). Ohmic heating. In E. M. A. Willhoft (Ed.), *Aseptic Processing and Packaging of Particulate Foods* (pp. 74–89). Springer US. https://doi.org/10.1007/978-1-4615-3112-8_4

- Suslick, K. S., Didenko, Y., Fang, M., H Y E O N, T., Kolbeck, K. J., M C N A M A R A lii, W. B., & Mdleleni A N D M I K E W O N G, M. M. (1999). *Acoustic cavitation and its chemical consequences*.
- Swaisgood, H. E. (1985). *Characteristics of edible fluids of animal origin: Milk*.
- Toepfl, S., Mathys, A., Heinz, V., & Knorr, D. (2006). Review: Potential of high hydrostatic pressure and pulsed electric fields for energy efficient and environmentally friendly food processing. *Food Reviews International*, 22(4), 405–423.
<https://doi.org/10.1080/87559120600865164>
- Van Impe, J., Smet, C., Tiwari, B., Greiner, R., Ojha, S., Stulić, V., Vukušić, T., & Režek Jambrak, A. (2018). State of the art of nonthermal and thermal processing for inactivation of microorganisms. *Journal of Applied Microbiology*, 125(1), 16–35.
<https://doi.org/10.1111/jam.13751>
- Wang, X., Zhong, X., Gong, F., Chao, Y., & Cheng, L. (2020). Newly developed strategies for improving sonodynamic therapy. *Materials Horizons*, 7(8), 2028–2046.
<https://doi.org/10.1039/d0mh00613k>
- , Ismail, M., & Farid, M. (2017). Investigation of the use of ultrasonication followed by heat for spore inactivation. *Food and Bioproducts Processing*, 104, 32–39.
<https://doi.org/10.1016/J.FBP.2017.04.005>
- Arroyo, C., & Lyng, J. G. (2017). The Use of Ultrasound for the Inactivation of Microorganisms and Enzymes. In *Ultrasound in Food Processing* (pp. 255–286). John Wiley & Sons, Ltd.
<https://doi.org/10.1002/9781118964156.ch9>
- Ashokkumar, M. (2015). Applications of Ultrasound in food and bioprocessing. *Ultrasonics*

- Sonochemistry*, 25(1), 17–23. <https://doi.org/10.1016/j.ultsonch.2014.08.012>
- Bagal, M. V., & Gogate, P. R. (2014). Wastewater treatment using hybrid treatment schemes based on cavitation and Fenton chemistry: A review. *Ultrasonics Sonochemistry*, 21(1), 1–14. <https://doi.org/10.1016/j.ultsonch.2013.07.009>
- Barbosa-Canovas, G. V., & Rodriguez, J. J. (2002). Update on nonthermal food processing technologies: Pulsed electric field, high hydrostatic pressure, irradiation and Ultrasound. *Food Australia*, 54(11), 513–520.
- Bermudez-Aguirre, D., & Barbosa-Cánovas, G. V. (2012). *Inactivation of Saccharomyces cerevisiae in pineapple, grape and cranberry juices under pulsed and continuous thermo-sonication treatments—ScienceDirect*.
<https://www.sciencedirect.com/science/article/pii/S0260877411004948>
- Birmipa, A., Sfika, V., & Vantarakis, A. (2013). Ultraviolet light and Ultrasound as nonthermal treatments for the inactivation of microorganisms in fresh ready-to-eat foods. *International Journal of Food Microbiology*, 167(1), 96–102.
<https://doi.org/10.1016/J.IJFOODMICRO.2013.06.005>
- Boyd, L., & Beveridge, E. G. (1981). Antimicrobial activity of some alkyl esters of gallic acid (3,4,5,-trihydroxybenzoic acid) against *Escherichia coli* NCTC 5933 with particular reference to n-propyl gallate. *Microbios*, 30(120), 73–85.
<http://www.ncbi.nlm.nih.gov/pubmed/6272069>
- Chen, X. (2010). *Multiple Scattering from Bubble Clouds*. University of Miami.
<https://scholarship.miami.edu/esploro/outputs/graduate/Multiple-Scattering-from-Bubble-Clouds/991031447256702976>

- Chung, K.-T., Jr, S. E. S., Lin, W.-F., & Wei, C. I. (1993). Growth inhibition of selected food-borne bacteria by tannic acid, propyl gallate and related compounds. *Letters in Applied Microbiology*, *17*(1), 29–32. <https://doi.org/10.1111/j.1472-765X.1993.tb01428.x>
- Coronel, C. P., Jiménez, M. T., López-Malo, A., & Palou, E. (2011). Modelling thermosonication inactivation of *Aspergillus flavus* combining natural antimicrobial at different pH. *Procedia Food Science*, *1*, 1007–1014. <https://doi.org/10.1016/J.PROFOO.2011.09.151>
- Costley, D., Nesbitt, H., Ternan, N., Dooley, J., Huang, Y.-Y. Y., Hamblin, M. R., McHale, A. P., & Callan, J. F. (2017). Sonodynamic inactivation of Gram-positive and Gram-negative bacteria using a Rose Bengal–antimicrobial peptide conjugate. *International Journal of Antimicrobial Agents*, *49*(1), 31–36. <https://doi.org/10.1016/j.ijantimicag.2016.09.034>
- d’Agostino, L., & Brennen, C. E. (1983). *On the Acoustical Dynamics of Bubble Clouds: Vol. FED-2* (J. W. Hoyt, Ed.; No. 2; Issue 2, pp. 72–75). American Society of Mechanical Engineers. <https://resolver.caltech.edu/CaltechAUTHORS:DAGasmecmff83>
- Dadjour, M. F., Ogino, C., Matsumura, S., Nakamura, S., & Shimizu, N. (2006). Disinfection of *Legionella pneumophila* by ultrasonic treatment with TiO₂. *Water Research*, *40*(6), 1137–1142. <https://doi.org/10.1016/j.watres.2005.12.047>
- del Valle, P., García-Armesto, M. R., de Arriaga, D., González-Donquiles, C., Rodríguez-Fernández, P., & Rúa, J. (2016). Antimicrobial activity of kaempferol and resveratrol in binary combinations with parabens or propyl gallate against *Enterococcus faecalis*. *Food Control*, *61*, 213–220. <https://doi.org/10.1016/j.foodcont.2015.10.001>
- Drakopoulou, S., Terzakis, S., Fountoulakis, M. S., Mantzavinos, D., & Manios, T. (2009). Ultrasound-induced inactivation of gram-negative and gram-positive bacteria in

- secondary treated municipal wastewater. *Ultrasonics Sonochemistry*, 16(5), 629–634.
<https://doi.org/10.1016/J.ULTSONCH.2008.11.011>
- Duck, F., & Leighton, T. (2018). *Frequency bands for Ultrasound, suitable for the consideration of its health effects: The Journal of the Acoustical Society of America: Vol 144, No 4*.
<https://asa.scitation.org/doi/10.1121/1.5063578>
- Evelyn, E., & Silva, F. V. M. (2015). Thermosonication versus thermal processing of skim milk and beef slurry: Modeling the inactivation kinetics of psychrotrophic *Bacillus cereus* spores. *Food Research International*, 67, 67–74.
<https://doi.org/10.1016/J.FOODRES.2014.10.028>
- Evelyn, Milani, E., & Silva, F. V. M. (2017). Comparing high pressure thermal processing and thermosonication with thermal processing for the inactivation of bacteria, moulds, and yeasts spores in foods. *Journal of Food Engineering*, 214, 90–96.
<https://doi.org/10.1016/J.JFOODENG.2017.06.027>
- Evelyn, & Silva, F. V. M. (2016). High pressure processing pretreatment enhanced the thermosonication inactivation of *Alicyclobacillus acidoterrestris* spores in orange juice. *Food Control*, 62, 365–372. <https://doi.org/10.1016/J.FOODCONT.2015.11.007>
- Evelyn, & Silva, F. V. M. (2018). Differences in the resistance of microbial spores to thermosonication, high pressure thermal processing and thermal treatment alone. *Journal of Food Engineering*, 222, 292–297.
<https://doi.org/10.1016/J.JFOODENG.2017.11.037>
- Fuchs, J. F., & Puskas, W. L. (2005). *Application of Multiple Frequency Ultrasonics*.
<https://www.ctgclean.com/application-of-multiple-frequency-ultrasonics>

Gomez-Gomez, A., Brito-de la Fuente, E., Gallegos, C., Garcia-Perez, J. V., & Benedito, J. (2021).

Combined pulsed electric field and high-power ultrasound treatments for microbial inactivation in oil-in-water emulsions. *Food Control*, 130, 108348.

<https://doi.org/10.1016/j.foodcont.2021.108348>

Guzel, B. H., Arroyo, C., Condón, S., Pagán, R., Bayindirli, A., & Alpas, H. (2014). Inactivation of *Listeria monocytogenes* and *Escherichia coli* by Ultrasonic Waves Under Pressure at Nonlethal (Manosonication) and Lethal Temperatures (Manothermosonication) in Acidic Fruit Juices. *Food and Bioprocess Technology*, 7(6), 1701–1712.

<https://doi.org/10.1007/s11947-013-1205-6>

Hagenson, L. C., & Doraiswamy, L. K. (1998). Comparison of the effects of Ultrasound and mechanical agitation on a reacting solid-liquid system. *Chemical Engineering Science*, 53(1), 131–148. [https://doi.org/10.1016/S0009-2509\(97\)00193-0](https://doi.org/10.1016/S0009-2509(97)00193-0)

Kentish, S., & Feng, H. (2014). Applications of Power Ultrasound in Food Processing. *Annual Review of Food Science and Technology*, 5(1), 263–284.

<https://doi.org/10.1146/annurev-food-030212-182537>

Knoerzer, K. (2016). Nonthermal and Innovative Food Processing Technologies. In *Reference Module in Food Science* (p. 4). Elsevier. <https://doi.org/10.1016/B978-0-08-100596-5.03414-4>

Knorr, D., Froehling, A., Jaeger, H., Reineke, K., Schlueter, O., & Schoessler, K. (2011). Emerging Technologies in Food Processing. *Annual Review of Food Science and Technology*, 2(1), 203–235. <https://doi.org/10.1146/annurev.food.102308.124129>

Lee, H., Zhou, B., Liang, W., Feng, H., & Martin, S. E. (2009). Inactivation of *Escherichia coli* cells

- with sonication, manosonication, thermosonication, and manothermosonication: Microbial responses and kinetics modeling. *Journal of Food Engineering*, 93(3), 354–364. <https://www.sciencedirect.com/science/article/pii/S0260877409000636>
- Lighthill, S. J. (1978). Acoustic streaming. *Journal of Sound and Vibration*, 61(3), 391–418. Scopus. [https://doi.org/10.1016/0022-460X\(78\)90388-7](https://doi.org/10.1016/0022-460X(78)90388-7)
- Liu, B., Wang, D.-J., Liu, B.-M., Wang, X., He, L.-L., Wang, J., & Xu, S.-K. (2011). *The influence of Ultrasound on the fluoroquinolones antibacterial activity*. <https://doi.org/10.1016/j.ultsonch.2011.02.001>
- Mahvi, A. H. (2009). Application of ultrasonic technology for water and wastewater treatment. *Iranian Journal of Public Health*, 38(2), 1–17. Scopus.
- Marchand, S., De Block, J., De Jonghe, V., Coorevits, A., Heyndrickx, M., & Herman, L. (2012). Biofilm Formation in Milk Production and Processing Environments; Influence on Milk Quality and Safety. *Comprehensive Reviews in Food Science and Food Safety*, 11(2), 133–147. <https://doi.org/10.1111/j.1541-4337.2011.00183.x>
- Mason, T. J. (2003). Sonochemistry and sonoprocessing: The link, the trends and (probably) the future. *Ultrasonics Sonochemistry*, 10(4), 175–179. [https://doi.org/10.1016/S1350-4177\(03\)00086-5](https://doi.org/10.1016/S1350-4177(03)00086-5)
- McClements, D. J. (1995). Advances in the application of Ultrasound in food analysis and processing. *Trends in Food Science & Technology*, 6(9), 293–299. [https://doi.org/10.1016/S0924-2244\(00\)89139-6](https://doi.org/10.1016/S0924-2244(00)89139-6)
- Meng, L., Liu, X., Wang, Y., Zhang, W., Zhou, W., Cai, F., Li, F., Wu, J., Xu, L., Niu, L., & Zheng, H. (2019). Sonoporation of Cells by a Parallel Stable Cavitation Microbubble Array.

- Advanced Science*, 6(17), 1900557. <https://doi.org/10.1002/advs.201900557>
- Nakonechny, F., Nisnevitch, M., Nitzan, Y., & Nisnevitch, M. (2013). Sonodynamic Excitation of Rose Bengal for Eradication of Gram-Positive and Gram-Negative Bacteria. *BioMed Research International*, 2013. <https://doi.org/10.1155/2013/684930>
- Nakonieczna, J., Wolnikowska, K., Ogonowska, P., Neubauer, D., Bernat, A., & Kamysz, W. (2018). Rose bengal-mediated photoinactivation of multidrug resistant pseudomonas aeruginosa is enhanced in the presence of antimicrobial peptides. *Frontiers in Microbiology*, 9(AUG). <https://doi.org/10.3389/fmicb.2018.01949>
- Nyborg, W. L. (1958). Acoustic Streaming near a Boundary. *The Journal of the Acoustical Society of America*, 30(4), 329–339. <https://doi.org/10.1121/1.1909587>
- Oliveira, G. S., Lopes, D. R. G., Andre, C., Silva, C. C., Baglinière, F., & Vanetti, M. C. D. (2019). Multispecies biofilm formation by the contaminating microbiota in raw milk. *Biofouling*, 35(8), 819–831. <https://doi.org/10.1080/08927014.2019.1666267>
- Paga'n, R., Paga'n, P., Man~as, P., Man~as, M., Raso, J., Condo'n, S., & Condo'n, C. (1999). Bacterial Resistance to Ultrasonic Waves under Pressure at Nonlethal (Manosonication) and Lethal (Manothermosonication) Temperatures. In *APPLIED AND ENVIRONMENTAL MICROBIOLOGY* (Vol. 65, Issue 1, pp. 297–300). <https://www.ncbi.nlm.nih.gov/pmc/articles/PMC91018/pdf/am000297.pdf>
- Palgan, I., Muñoz, A., Noci, F., Whyte, P., Morgan, D. J., Cronin, D. A., & Lyng, J. G. (2012). Effectiveness of combined Pulsed Electric Field (PEF) and Manothermosonication (MTS) for the control of *Listeria innocua* in a smoothie type beverage. *Food Control*, 25(2), 621–625. <https://doi.org/10.1016/j.foodcont.2011.11.009>

- Pang, X., Xiao, Q., Cheng, Y., Ren, E., Lian, L., Zhang, Y., Gao, H., Wang, X., Leung, W., Chen, X., Liu, G., & Xu, C. (2019). Bacteria-Responsive Nanoliposomes as Smart Sonotheranostics for Multidrug Resistant Bacterial Infections. *ACS Nano*, *13*(2), 2427–2438.
<https://doi.org/10.1021/acsnano.8b09336>
- Pang, X., Xu, C., Jiang, Y., Xiao, Q., & Leung, A. W. (2016). Natural products in the discovery of novel sonosensitizers. *Pharmacology & Therapeutics*, *162*, 144–151.
<https://doi.org/10.1016/j.pharmthera.2015.12.004>
- Patist, A., & Bates, D. (2008). Ultrasonic innovations in the food industry: From the laboratory to commercial production. *Innovative Food Science & Emerging Technologies - INNOV FOOD SCI EMERG TECHNOL*, *9*, 147–154. <https://doi.org/10.1016/j.ifset.2007.07.004>
- Pourhajibagher, M., Rahimi esboei, B., Hodjat, M., & Bahador, A. (2020). Sonodynamic excitation of nanomicelle curcumin for eradication of *Streptococcus mutans* under sonodynamic antimicrobial chemotherapy: Enhanced anti-caries activity of nanomicelle curcumin. *Photodiagnosis and Photodynamic Therapy*, *30*, 101780.
<https://doi.org/10.1016/j.pdpdt.2020.101780>
- Rahimi, M., Azimi, N., & Parvizian, F. (2013). Using microparticles to enhance micromixing in a high frequency continuous flow sonoreactor. *Chemical Engineering and Processing: Process Intensification*, *70*, 250–258. <https://doi.org/10.1016/j.cep.2013.03.013>
- Rahimi, M., Safari, S., Faryadi, M., & Moradi, N. (2014). Experimental investigation on proper use of dual high-low frequency ultrasound waves—Advantage and disadvantage. *Chemical Engineering and Processing: Process Intensification*, *78*, 17–26.
<https://doi.org/10.1016/j.cep.2014.02.003>

- Ross, A. I. V., Griffiths, M. W., Mittal, G. S., & Deeth, H. C. (2003). Combining nonthermal technologies to control foodborne microorganisms. *International Journal of Food Microbiology*. [https://doi.org/10.1016/S0168-1605\(03\)00161-2](https://doi.org/10.1016/S0168-1605(03)00161-2)
- Sango, D. M., Abela, D., Mcelhatton, A., & Valdramidis, V. P. (2014). Assisted ultrasound applications for the production of safe foods. *Journal of Applied Microbiology*, *116*(5), 1067–1083. <https://doi.org/10.1111/jam.12468>
- Serpe, L., & Giuntini, F. (2015). Sonodynamic antimicrobial chemotherapy: First steps towards a sound approach for microbe inactivation. *Journal of Photochemistry and Photobiology B: Biology*, *150*, 44–49. <https://doi.org/10.1016/J.JPHOTOBIO.2015.05.012>
- Sivakumar, M., Tatake, P. A., & Pandit, A. B. (2002). Kinetics of p-nitrophenol degradation: Effect of reaction conditions and cavitation parameters for a multiple frequency system. *Chemical Engineering Journal*, *85*(2), 327–338. [https://doi.org/10.1016/S1385-8947\(01\)00179-6](https://doi.org/10.1016/S1385-8947(01)00179-6)
- Strippoli, V., D'auria, F. D., Tecca, M., Callari, A., & Simonetti, G. (2000). Propyl gallate increases in vitro antifungal imidazole activity against *Candida albicans*. In *International Journal of Antimicrobial Agents* (No. 09248579/00; Vol. 16, pp. 73–76). www.ischemo.org
- Tachibana, K., Feril, L. B., & Ikeda-Dantsuji, Y. (2008). Sonodynamic therapy. *Ultrasonics*, *48*(4), 253–259. <https://doi.org/10.1016/j.ultras.2008.02.003>
- Tiwari, B. K., Patras, A., Bruntonb, N., Cullen, P. J., & O'Donnella, C. P. (2009). *Effect of ultrasound processing on anthocyanins and color of red grape juice | Elsevier Enhanced Reader*. <https://doi.org/10.1016/j.ultsonch.2009.10.009>
- Wang, Q., De Oliveira, E. F., Alborzi, S., Bastarrachea, L. J., & Tikekar, R. V. (2017). On

- mechanism behind UV-A light enhanced antibacterial activity of gallic acid and propyl gallate against *Escherichia coli* O157:H7. *Scientific Reports*, 7(1), 1–11.
<https://doi.org/10.1038/s41598-017-08449-1>
- Wang, S., Wu, X., Wang, Y., Li, Q., & Tao, M. (2008). Removal of organic matter and ammonia nitrogen from landfill leachate by Ultrasound. *Ultrasonics Sonochemistry*, 15(6), 933–937. <https://doi.org/10.1016/j.ultsonch.2008.04.006>
- Wang, X., Ip, M., Leung, A. W., Wang, P., Zhang, H., Hua, H., & Xu, C. (2016). Sonodynamic action of hypocrellin B on methicillin-resistant *Staphylococcus aureus*. *Ultrasonics*, 65, 137–144. <https://doi.org/10.1016/j.ultras.2015.10.008>
- Wang, X., Ip, M., Leung, A. W., & Xu, C. (2014). Sonodynamic inactivation of methicillin-resistant *Staphylococcus aureus* in planktonic condition by curcumin under ultrasound sonication. *Ultrasonics*, 54(8), 2109–2114. <https://doi.org/10.1016/j.ultras.2014.06.017>
- Wang, X., Ip, M., Leung, A. W., Yang, Z., Wang, P., Zhang, B., Ip, S., & Xu, C. (2015). Sonodynamic action of curcumin on foodborne bacteria *Bacillus cereus* and *Escherichia coli*. *Ultrasonics*, 62, 75–79. <https://doi.org/10.1016/j.ultras.2015.05.003>
- Weber, M., Liedtke, J., Plattes, S., & Lipski, A. (2019). Bacterial community composition of biofilms in milking machines of two dairy farms assessed by a combination of culture-dependent and –independent methods. *PLOS ONE*, 14(9), e0222238.
<https://doi.org/10.1371/journal.pone.0222238>
- Weiler, C., Ifland, A., Naumann, A., Kleta, S., & Noll, M. (2013). Incorporation of *Listeria monocytogenes* strains in raw milk biofilms. *International Journal of Food Microbiology*, 161(2), 61–68. <https://doi.org/10.1016/j.ijfoodmicro.2012.11.027>

- Xiong, Z., Cheng, X., & Sun, D. (2011). Pretreatment of heterocyclic pesticide wastewater using ultrasonic/ozone combined process. *Journal of Environmental Sciences*, 23(5), 725–730.
[https://doi.org/10.1016/S1001-0742\(10\)60465-2](https://doi.org/10.1016/S1001-0742(10)60465-2)
- Xu, C., Dong, J., Ip, M., Wang, X., & Leung, A. W. (2016). Sonodynamic action of chlorin e6 on *Staphylococcus aureus* and *Escherichia coli*. *Ultrasonics*, 64, 54–57.
<https://doi.org/10.1016/j.ultras.2015.07.010>
- Zhang, Y. J., Li, S. C., & Hammitt, S. G. (1989). *Statistical investigation of bubble collapse and cavitation erosion effect—ScienceDirect*.
<https://www.sciencedirect.com/science/article/pii/0043164889900409>
- Zhuang, D., Hou, C., Bi, L., Han, J., Hao, Y., Cao, W., & Zhou, Q. (2014). Sonodynamic effects of hematoporphyrin monomethyl ether on *Staphylococcus aureus* in vitro. *FEMS Microbiology Letters*, 361(2), 174–180. <https://doi.org/10.1111/1574-6968.12628>

Chapter 2

Synergistic inactivation of bacteria based on a combination of low frequency, low-intensity ultrasound and a food-grade antioxidant

Cuong Nguyen Huu^a, Rewa Rai^a, Xu Yang^{a,1}, Rohan Tikekar^b, Nitin Nitin^{a, c}

^a Department of Food Science and Technology, University of California, Davis, CA, USA.

^b Department of Nutrition and Food Science, University of Maryland, College Park, MD, USA.

^c Department of Biological and Agricultural Engineering, University of California, Davis, CA, USA.

Address correspondence to Nitin Nitin, nnitin@ucdavis.edu, Robert Mondavi Institute South, Room 2221, Hilgard Ln, Davis, CA 95616

¹ Present Address: Nutrition and Food Science Department, California State Polytechnic University Pomona, 3801 West Temple Ave, Pomona, CA, 91768 USA

Abstract

This study evaluated a synergistic antimicrobial treatment using a combination of low frequency and a low-intensity ultrasound (LFU) and a food-grade antioxidant, propyl gallate (PG), against a model gram-positive (*Listeria innocua*) and the gram-negative bacteria (*Escherichia coli* O157:H7). Bacterial inactivation kinetic measurements were complemented by characterization of biophysical changes in liposomes, changes in bacterial membrane permeability, morphological changes in bacterial cells, and intracellular oxidative stress upon treatment with PG, LFU, and a combination of PG + LFU. The combination of PG+ LFU significantly (more than 4 log CFU/mL, $P < 0.05$) enhanced the inactivation of both *L. innocua* and *E. coli* O157:H7 compared to PG or LFU treatment. As expected, *L. innocua* had a significantly higher resistance to inactivation compared to *E. coli* using a combination of PG + LFU. Biophysical measurements in liposomes, bacterial permeability measurements, and SEM-based morphological measurements show rapid interactions of PG with membranes. Upon extended treatment of cells with PG + LFU, a significant increase in membrane damage was observed compared to PG or LFU alone. A lack of change in the intracellular thiol content following the combined treatment and limited effectiveness of exogenously added antioxidants in attenuating the synergistic antimicrobial action demonstrated that oxidative stress was not a leading mechanism responsible for the synergistic inactivation by PG+ LFU. Overall, the study illustrates synergistic inactivation of bacteria using a combination of PG+LFU based on enhanced membrane damage and its potential for applications in the food and environmental systems.

1. Introduction

Low-frequency ultrasound is used in the food industry for diverse applications including homogenization, extraction of bioactive compounds from complex food materials, and cleaning of equipment and surfaces [1]. The key advantage of ultrasound processing is its ability to simultaneously create micro and macroscale mass transport effects [2]. These effects manifest in the form of mechanical impacts including microstreaming, bubble collapse, turbulence, and localized thermal effects. In addition, bubble collapse during ultrasound processing can generate free radicals that may facilitate chemical reactions [3]. Based on these mechanical effects and chemical impacts, the application of ultrasound for inactivation of bacteria in food systems has been evaluated [2,4,5]. The results of these prior studies suggest that even though low-frequency ultrasound may disrupt cell membranes, the overall effectiveness of ultrasound-induced inactivation of bacteria is limited to 1-2 log in model food systems. To address these limitations, ultrasound technology is often combined with other treatments such as thermal or high-pressure processing to improve inactivation of bacteria [6]. Prior studies have shown that simultaneous combination of ultrasound with thermal treatment or high-pressure processing can achieve 4-5 log bacterial inactivation (4-5 log CFU) [6]. Despite this potential, industrial translation of these concepts has been limited due to various factors including the capital cost of combining existing ultrasound technologies with high pressure or thermal processing. In addition, the negative impact of thermal and high-pressure processing on the overall quality or texture of food products is also a significant limitation. Therefore, there is an unmet need to improve effectiveness of ultrasound processing for enhancing inactivation of pathogens and spoilage microbes in food systems.

Sonodynamic therapy (SDT) is one of the emerging approaches that is based on a combination of a chemical compound and an ultrasound process to enhance inactivation of diverse types of cells including cancer and bacterial cells [7]. In this concept, a synergistic combination of a chemical compound with the US may result in enhanced chemical and mechanical damage to cells [7–10]. This

enhanced cellular damage and inactivation may be a result due to generation of oxidative stress and membrane damage induced by a combination of US and selected chemical compounds [7,10–13]. Despite these working hypotheses, there are significant gaps in mechanistic understanding of sonodynamic processes that may result in bacterial inactivation. Overall, the sonodynamic inactivation of bacterial cells has a significant potential for the food industry, as the cytotoxic effects of the selected compounds are only limited to ultrasound processing time, unlike other chemical preservatives and additives currently used in the industry. However, most of the currently used compounds for the sonodynamic applications in biomedical systems are not food grade [9]. Thus, the overall goal of this study was to evaluate the synergistic combination of a food-grade compound with a low frequency (40 kHz) and a low power density (0.092 W/mL) ultrasound process to achieve inactivation of bacteria and characterize the role of mechanical damage and oxidative stress for synergistic bacterial inactivation.

In this study, propyl gallate (PG), a derivative of gallic acid (Gallate acid propyl ester) was selected as a model food-grade sonosensitizer. Propyl gallate is a well-known antioxidant used in diverse food products, cosmetics, and food packaging materials to prevent rancidity and spoilage. Besides the antioxidant effect, alkyl gallates including PG are reported to have a mild antimicrobial effect against a wide variety of planktonic bacteria, biofilm, and fungi [14–21]. In this study, PG was selected based on its reported membrane activity [22] as well as its ability to generate oxidative stress [17,23] when combined with light irradiation.

In this study, bacterial strains of both the gram-positive (*Listeria innocua*) and the gram-negative bacteria (a non-Shiga toxin-producing *Escherichia coli* O157:H7) representing key foodborne pathogens were selected. Furthermore, the biological changes to cellular membranes and intracellular thiol content were measured in treated bacterial cells to evaluate potential pathways for bacterial inactivation. In summary, this study will illustrate the potential of food-grade compounds with a low frequency and a

low-intensity US system (LFU) to achieve synergistic inactivation of target bacteria and characterize the possible mechanisms for this synergistic interaction.

2. Materials and Methods

2.1. Reagents

Propyl gallate (PG), L- α -phosphatidylcholine from egg yolk (egg PC), reduced L-glutathione (GSH), sodium chloride (NaCl), sodium dodecyl sulfate (SDS), chloroform, methanol, ethylenediaminetetraacetic acid (EDTA), and Triton X-100 were all obtained from Sigma-Aldrich (St. Louis, MO, USA). Measure-iT™ Thiol Assay Kit, a thiol-reactive fluorescence probe, was purchased from Molecular Probes (Eugene, OR, USA). 1-Hexadecanoyl-2-(1-pyrenedecanoyl)-sn-glycero-3-phosphocholine (β -Py-C10-HPC) was purchased from Invitrogen by Thermo Fisher Scientific (Waltham, MA, USA). Zirconia-silica beads (0.1 mm diameter) were acquired from Biospec Products (Bartlesville, OK, USA). Luria-Bertani (LB) broth, tryptic soy broth (TSB), tryptic soy agar (TSA), phosphate-buffered saline (PBS), and tris-hydrochloride (1M; Tris-HCl) were purchased from Fisher BioReagents (Pittsburgh, PA, USA). Ultrapure water was obtained using a Milli-Q filtration system (EDM Millipore; Billerica, MA, USA).

2.2. Microbial strains, culture methods, and enumeration of bacteria

Escherichia coli O157:H7 (ATCC 700728, Manassas, VA, USA) and *Listeria innocua* (ATCC 33090, Manassas, VA, USA) were provided by Dr. Linda Harris and Dr. Trevor Suslow, respectively, at the University of California, Davis. These strains were selected as models for the gram-negative and gram-positive bacteria respectively. Both bacterial strains have been modified with a Rifampicin resistance plasmid, enabling a selective culture of these strains in the Rifampicin-containing growth media. Antibacterial experiments were performed against the stationary phase bacteria, at an initial bacterial concentration of 10^6 CFU/mL. Inactivation of bacteria following treatments were assessed based on the standard plate counting method, where treated bacterial samples were serially diluted in a phosphate-

buffered saline (PBS) followed by overnight culturing of bacteria on the Rifampicin modified tryptic soy agar (TSA) plates.

2.3. Study Design

To investigate synergistic effect of the combined LFU and PG treatment for inactivation of *E. coli* O157:H7 and *L. innocua*, sample size was determined using a balanced one-way analysis of variance power analysis. For this analysis, the following parameters were selected: number of treatment groups = 4, significance level = 0.05, a power level = 0.8 and f value = 1.2. Based on the power analysis, a sample size of n = 3 for each treatment group was determined.

Briefly, 200 µL of bacterial suspension with a concentration of 1.0×10^7 CFU/mL was added to each well of a round-bottom 12-well plate (Corning, Falcon™, USA) and randomly assigned into four treatment groups.

Group 1. Control without any treatment.

Group 2. PG 10 mM; 200 µL of the bacterial suspension was added to wells containing 2 mL of PG solution at 10 mM concentration and then incubated at room temperature for 30 min for *E. coli* O157:H7 and 45 min for *L. innocua* in the dark.

Group 3. LFU; The wells containing bacterial suspension were exposed to ultrasound waves at a frequency of 40 kHz and treatment time ranging from 5 to 30 minutes for *E. coli*, and from 10 to 45 minutes for *L. innocua*.

Group 4. LFU+PG; To evaluate the influence of combined treatments based on PG @10 mM and low frequency ultrasound energy. The bacteria suspension was added to the PG solution and immediately exposed to ultrasound.

The detailed experimental design is also illustrated in Fig. 1. The PG concentration was selected based on the solubility limit of the PG in aqueous solution and similar order of magnitude to the allowable limits approved by the FDA for food applications [24].

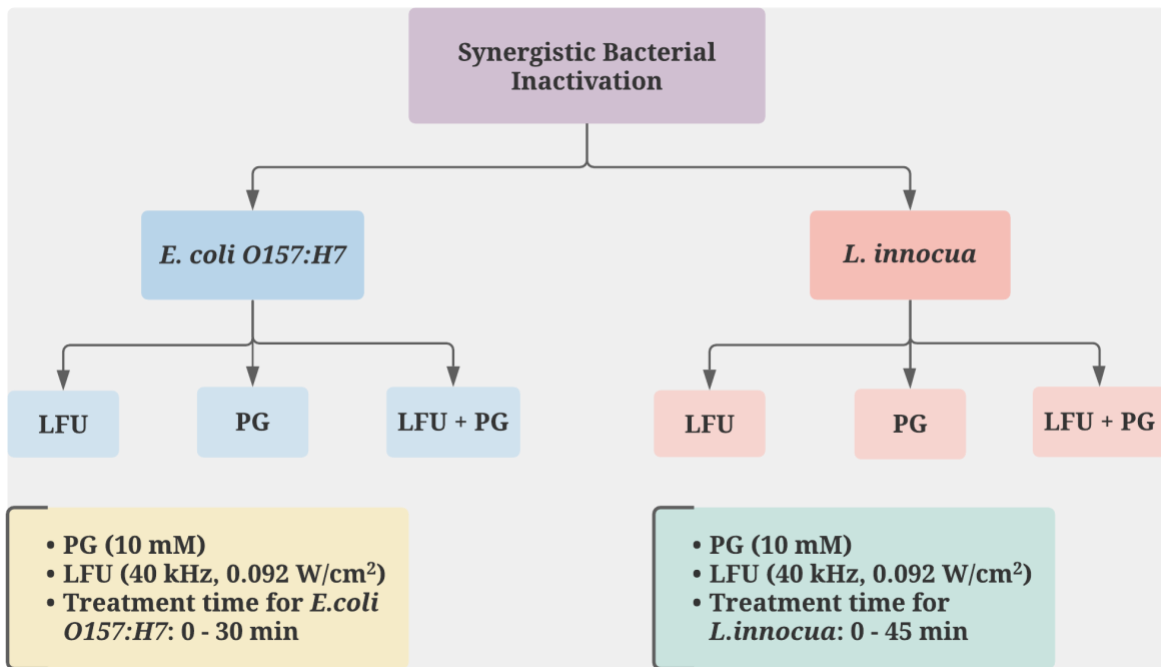


Fig. 2.1 Experimental design of this current study where LFU – Low-frequency ultrasound treatment, PG – Propyl gallate treatment, LFU+PG – combined Low-frequency ultrasound and PG treatment.

2.4. Low-frequency and low power density ultrasound treatment (LFU)

A bath sonicator model FB505 (Fisher Scientific, Pittsburgh, PA) was selected as a low-intensity ultrasound process with a frequency of 40 kHz and a power density of (0.092 W/mL) for this study. This system was selected as it can be easily scaled up compared to probe-based US systems. During the process, the temperature of the water was monitored and kept at room temperature by continuously adding cold water. Samples (100 μ L) were aseptically collected as a function of treatment time and serial dilutions (1:100 and 1:1000) were prepared using PBS (Fluka Analytical, St. Louis, MO). A volume of 100 μ L of each dilution was inoculated onto antibiotic modified TSA plates in triplicates. In order to reduce the detection limit to 1 CFU/mL, the entire volume of the first dilution (1 mL) was also inoculated onto

TSA plates (333 μ L per plate). TSA plates were incubated at 37 °C for 24 hours, and the viable bacterial count was determined.

2.5. Microbial Inactivation Kinetics

Microbial inactivation kinetics was determined by log-linear regression analysis using GlnaFit, an add-in Excel component that was released by Geeraerd et al. [25]. The log-linear equation is a first-order inactivation kinetics that is commonly used to describe inactivation of the bacteria [26].

$$\ln N = \ln N_0 - kt$$

where N and N_0 are respectively cell count over time and the initial cell count; t is the time (minutes) and k is the inactivation rate constant.

2.6. Membrane Damage

2.6.1. Preparation of model lipid membrane with and without pyrene labeled lipid

To understand the influence of PG, LFU, and their combination on bacterial membranes, biophysical changes in liposomes, a model system for the bacterial membrane, were evaluated. These biophysical changes were measured based on changes in the particle size, ξ potential, and lateral membrane mobility in liposomes. Changes in the particle size and ξ potential of liposomes can suggest lysis of the liposomes and the surface interactions of the liposomes with PG and LFU. Lateral mobility measurements can assess changes in the membrane fluidity induced by interactions of PG and LFU with liposomes. Briefly, Egg PC (2.5 mg/ml) with and without 1 mol % of pyrene labeled lipid [1-hexadecanoyl-2-(1-pyrenedecanoyl)-sn-glycero-3-phosphocholine (β -Py-C10-HPC)] was dissolved in a mixture of chloroform and methanol (4:1 v/v). The solvent was evaporated under vacuum and dried lipid film was resuspended in an autoclaved water to prepare multilamellar vesicles. Lipid solution

underwent extrusion for 15 cycles through 400 nm polycarbonate track-etched membranes to obtain unilamellar vesicles with and without pyrene label.

Size distributions (nm) and ξ potentials (mV) of the liposomal model cell membranes were measured after treatment with PG (10 mM), LFU (30 min), and a combination of PG and LFU using a dynamic light scattering system (Malvern Zetasizer Nano, Westborough, MA). Both treated and untreated samples were diluted 10-fold in 1× PBS. Polystyrene cuvette with a standard path length of 10 mm and reusable capillary zeta cells was used for size distribution and ξ potential measurements, respectively. Solutions were equilibrated at 25 °C for 2 min before data acquisition. The scattered light was detected at 90° relative to the incident laser (633-nm He-Ne laser) light for 15 to 20 runs of 10 to 20 s each, with a medium viscosity of 0.89 Pa.s and a refractive index of 1.33.

2.6.2. Measurement of lateral mobility using pyrene labeled liposomes

Pyrene labeled probes have been used to measure the lateral mobility of lipid membranes based on the ratio of fluorescence intensity of excimer (470 nm) to monomer (390 nm) peak. Fluorescence emission spectra of liposome model cell membranes labeled with β -Py-C10-HPC ($\lambda_{ex} = 340$ nm; $\lambda_{em} = 350 - 600$ nm) were acquired using SpectraMax® M5 Multi-Mode Microplate Reader. The instrument was equipped with a Xenon flash lamp (1 joule/flash) as an excitation source with two holographic diffraction grating monochromators as wavelength selection devices and a photomultiplier tube as the detector. Emission spectra of β -Py-C10-HPC were acquired using pyrene labeled liposomes after treatment with PG (10 mM), ultrasound (30 min), and a combination of both LFU+PG. Treated and untreated control samples were 5-fold diluted with 1× PBS before fluorescence measurements. Spectral response from appropriate control samples was subtracted before the data analysis. The ratio of the intensity of excimer (470 nm) to monomer (390 nm) peak were calculated to evaluate the change in lateral mobility of liposomal membrane induced by interactions of PG, LFU, and PG + LFU with the membrane.

2.6.3. Propidium iodide dye assay

To measure the magnitude of membrane damage after ultrasound treatment, Propidium Iodide (PI) dye was used for staining the DNA of membrane compromised bacteria as previously described [23]. PI is a red-fluorescent nuclear and chromosome counterstain that can only permeate bacteria with damaged membranes and is frequently used to detect cell membrane damage [27,28]. Test solutions consisting of bacteria ($\sim 1 \times 10^9$ CFU/mL) suspended in PG solution (10 mM), were treated with ultrasound as described previously. Bacteria in DI water alone in the dark was used as a control. After treatment, samples were washed with DI water and centrifuged for 2 min at 10,000 g. Then, a volume of 50 μ L of PI was added to each sample to reach a final concentration of 5 μ M, following incubation in the dark at room temperature for 15 min. Subsequently, the incubated samples were washed and suspended in 500 μ L 1 \times PBS. A volume of 100 μ L of this sample was transferred to a 96-well plate, and the fluorescence intensity was measured using a plate reader (Tecan SPECTRAFluor Plus) with an excitation and emission wavelength of 488/520 nm respectively.

2.6.4. Scanning Electron Microscope (SEM)

Bacterial cells before and after treatment were fixed in 4% glutaraldehyde solution in PBS (pH 7.4) at 4 $^{\circ}$ C for 2 h and washed twice using Milli-Q water. Ten microliters of samples were then dropped onto aluminum stubs with a carbon conductive adhesive tape, air-dried for 30 min, and sputter-coated with 10 nm of gold. Microscopy was performed on a Philips XL-30 electron microscope with a 10 kV accelerating voltage.

2.7. Oxidative damage

2.7.1. Total intracellular thiol oxidation

Reduction in the intracellular thiol content of *E. coli* O157:H7 and *L. innocua* cells upon individual and combined treatments was evaluated according to the method proposed by Wang et al. [23]. The intracellular thiol-containing compounds were extracted by lysing the bacterial cells through bead

beating. First, 1 mL of each sample containing 1×10^9 CFU mL⁻¹ of *E. coli* O157:H7 or *L. innocua* were exposed to low-frequency ultrasound treatment, as previously described. Following treatments, the samples were centrifuged (10,000 × g; 10 min) and the bacterial pellet was resuspended in 500 µL of a sterile lysis buffer (Tris-HCl 50 mM, NaCl 25 mM, EDTA 25 mM, SDS 2%, Triton X-100 1%) and transferred into a sterile 1.5 mL tube containing 400 µL of zirconia-silica beads (0.1 mm). The bacterial suspension was vortexed for 10 minutes and then centrifuged (16,000 × g; 10 min) before recovering the supernatant. This supernatant was used for the total thiol content measurement. The total thiol content was quantified through fluorescence spectroscopy using the Measure-iT™ Thiol Assay Kit from Molecular Probes (Eugene, OR, USA). The fluorescence intensity was measured using a fluorescence plate reader (Tecan SPECTRAFluor Plus) using an excitation filter of 488 nm and an emission filter of 520 nm. The total thiol content (µM) was determined using a standard curve based on the known concentration levels of reduced glutathione (GSH). The results were expressed in terms of remaining thiol concentration (%) compared to the untreated bacterial sample (Control).

2.7.2. Antioxidant assay

To further confirm the contributions of ROS for the antimicrobial synergistic interaction between PG and ultrasound treatment, two different antioxidants, glutathione and thiourea were exogenously added to the bacterial sample solutions before ultrasound treatment at a concentration of 10 and 100 ppm respectively. These concentration levels were selected based on the previous studies evaluating the role of reactive oxygen species in cell death [28–32]. Both glutathione and thiourea are known scavengers of ROS and potent antioxidants. These compounds can prevent damage to important cellular components caused by reactive oxygen species such as free radicals, peroxides, lipid peroxides, and heavy metals by directly scavenging free radicals through the donation of hydrogen atoms mechanism.

2.8. Data analysis

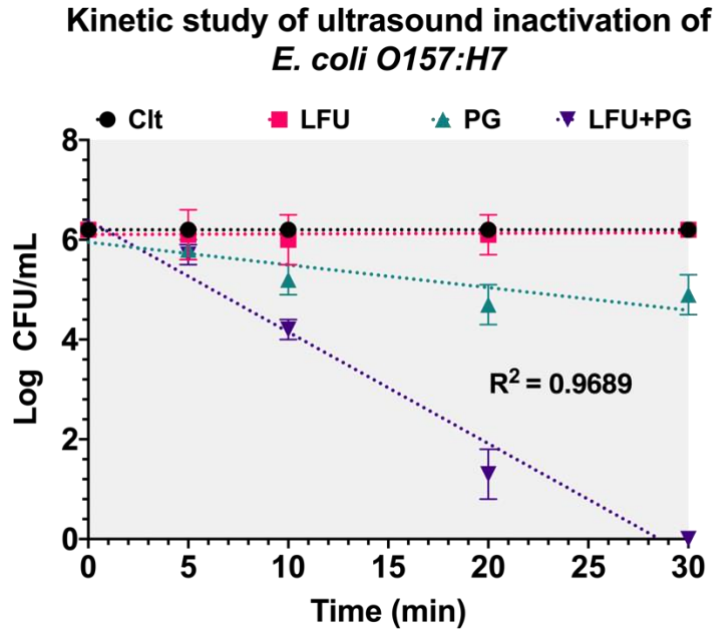
All data were presented as mean \pm standard deviation and all experiments were performed in triplicates. Statistical analysis was conducted using a one-way ANOVA and the pairwise differences were evaluated using the Tukey's range test to identify significant differences between each sample group. The difference between the results was considered significant if the P-value was less than 0.05.

3. Results and Discussion

3.1. Inactivation Kinetics of *E. coli O157:H7* and *L. innocua* by low-frequency ultrasound (LFU)

Figure 2 shows inactivation of the selected gram-negative (*E. coli O157:H7*) and the gram-positive (*L. innocua*) bacteria as a function of treatment time in the presence of PG or LFU alone and their combined treatment (PG + LFU). The combined treatment of PG and LFU led to an enhanced bacterial inactivation compared to the individual treatments of PG or LFU ($P < 0.05$). Combined LFU+PG treatment achieved a 6-log reduction in both *E. coli O157:H7* and *L. innocua* within 30 and 45 minutes respectively. Meanwhile, the LFU by itself caused no significant reduction in both bacteria. Incubation of *E. coli O157:H7* cells with PG by itself resulted in about 2-log inactivation of bacteria after 30 min of incubation, while no antimicrobial activity against *L. innocua* was observed after 45 min of incubation. Based on the first-order kinetic model, the kinetic rate constant, k values of 0.51 ± 0.015 and $0.34 \pm 0.011 \text{ min}^{-1}$ were obtained for the *E. coli O157:H7* and *L. innocua*, respectively, using the combined treatment. D-values, calculated from these rate constants, were $4.6 \pm 0.2 \text{ min}$ and $6.88 \pm 0.4 \text{ min}$ for the *E. coli O157:H7* and *L. innocua*, respectively ($P < 0.05$). These bacterial inactivation parameters confirmed higher susceptibility of the gram-negative *E. coli O157:H7* to the combined LFU + PG treatment than the gram-positive *L. innocua*. The difference in susceptibility of *E. coli O157:H7* and *L. innocua* to the combined treatment could be attributed to differences in the bacterial membrane/cell wall properties and potential differences in interactions between the PG and the bacterial membrane.

A.



B.

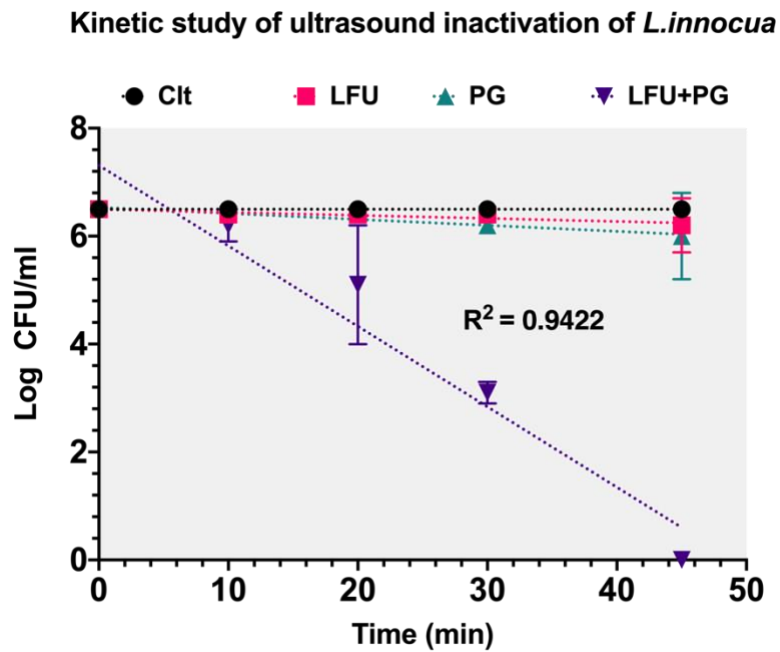


Fig. 2.2 Inactivation kinetics of *E. coli* O157:H7 (A) and *L. innocua* (B) upon treatment with LFU – Low-frequency ultrasound treatment, PG – Propyl gallate treatment, LFU+PG – combined Low-frequency ultrasound and PG treatment.

The lethal effect caused by conventional LFU treatments in bacterial and mammalian cells has been attributed to a cavitation process [33]. Cavitation can generate mechanical stress on the cell membrane during bubble expansion and contraction and a collapse of bubbles can create a localized shock effect that propels a high-velocity jet of liquid towards the surface. This set of mechanical forces can perforate the bacterial membrane [34] and result in a release of the intracellular components including nucleic acid.

Among possible synergies between PG and LFU, interactions of PG with membranes can further enhance the extent of damage caused by the LFU treatment. PG is known to interact with the bacterial cell membrane [23]. Thus, PG can alter the permeation and fluidity properties of the bacterial membrane.

3.2. Membrane damage

3.2.1. Analysis of membrane damage using model liposomes

To identify the role of membrane damage in the synergistic antimicrobial activity both model liposomes and bacterial cells were evaluated. The use of model liposomes enabled assessment of the influence of PG, LFU, and LFU+PG treatments on the biophysical aspects of the model membrane structure. Previously, we have demonstrated the application of model liposomes to study the synergistic antimicrobial activity of a food-grade peptide with light and mild heat [35]. The structural changes in liposomes cell model membranes induced by PG, LFU, and their combined treatment were evaluated using a combination of particle size and ξ potential measurements, as well as changes in the lateral mobility of model liposomes. The average volume means diameter, polydispersity indices (PDI), and ξ potential of liposomes with and without treatments are shown in Table 1. A low PDI (0.152) and a high zeta potential (-32.7 mV) demonstrated stable monodisperse uni-lamellar vesicles with an average particle size of ~ 230 nm. After treatment with PG, LFU, and LFU+PG, the average diameter of liposomes

did not change significantly ($P > 0.05$), and PDI was in the range of 0.15 – 0.2 (Table 1), demonstrating no lysis or flocculation of the liposomes. However, a statistically significant but relatively small reduction in zeta potential was observed ($P < 0.05$) after treatment of liposomes with PG, LFU, and LFU+PG.

Statistical analysis also showed no significant change ($P > 0.2$) in ξ potential between liposomes treated with LFU+PG and liposomes with PG or LFU alone.

Table 2.1 Size distributions, polydispersity indices (PDI), and ξ potentials of model liposomes in the presence of propyl gallate (PG), after low-frequency ultrasound treatment (LFU), and after the combined treatment of propyl gallate and ultrasound (LFU+PG).

Samples	Avg Size (nm)	PDI	ξ Potential (mV)
Liposome	229.6 \pm 57.04	0.152	– 32.7 \pm 1.1
Liposome + PG (10 ppm)	225.7 \pm 73.6	0.222	– 28.7 \pm 0.3
Liposome + LFU (30 min)	178.6 \pm 83.6	0.205	– 25.8 \pm 1.1
Liposome + PG (10 ppm) + LFU (30 min)	196.9 \pm 64.2	0.192	– 27.6 \pm 1.2

Emission spectra of β -Py-C10-HPC in liposome displays the pyrene monomer peak at 390 nm and a broad excimer peak at 470 nm [36]. Based on this spectral measurement (supplementary Fig. S.1), the excimer to monomer ratio (I_E/I_M) was calculated (Fig. 3). The results show an increase in the lateral mobility of the membrane illustrated by an increase in the excimer to monomer ratio upon treatment with PG, LFU, and a combination of PG+ LFU compared to the control liposomes.

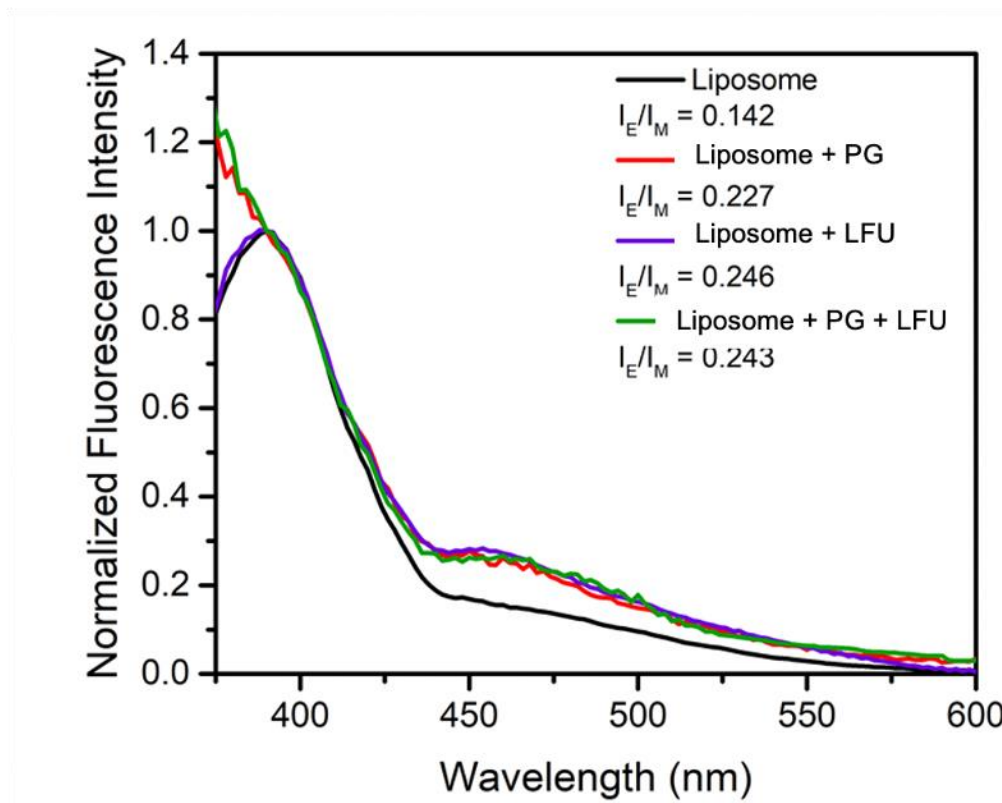


Fig. 2.3 Normalized fluorescence intensities and the excimer to monomer intensity ratios (I_E/I_M) of β -Py-C10-HPC in liposomes with and without treatments with propyl gallate (PG, 10 mM), low-frequency ultrasound (LFU, 30 min), and combination of LFU+PG.

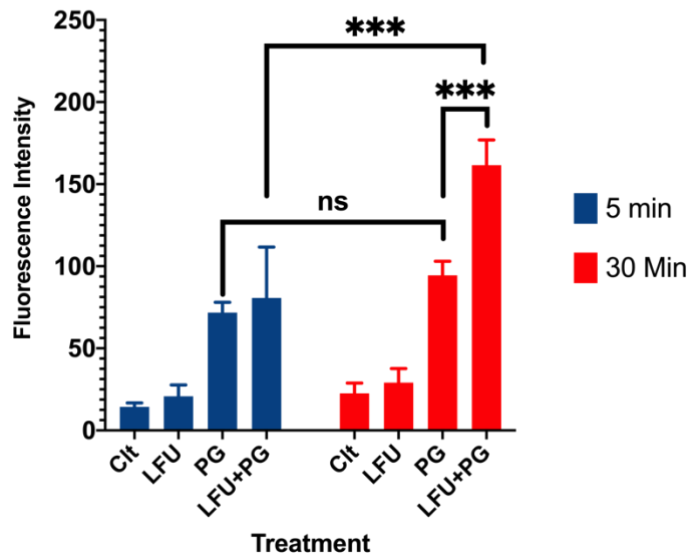
Similar to particle size distribution and ξ potential values, combined treatment of PG and LFU did not show significant changes in the β -Py-C10-HPC labeled fluorescence response in comparison to PG or LFU treatment alone. In addition to changes in excimer to monomer ratio, significant fluorescence quenching was also observed in the liposome samples (Supplementary Fig. S.1) treated with PG and LFU+PG, illustrating significant interactions of PG with the membrane-associated fluorescence dye and therefore support the plausibility of permeation of PG into the membrane. Overall, these results suggest rapid interactions between PG and model liposomes, however, these interactions did not induce significant lysis of the membrane as observed in our prior study with lauric arginate (LAE) [35].

3.2.2. Analysis of bacterial membrane permeability using PI dye

To complement measurements using liposomes, changes in the bacterial cell membrane upon interactions of LFU and PG were measured using propidium iodide as a membrane permeability indicator. Figure 3 illustrates changes in the membrane permeability of bacteria upon treatment with PG, LFU, and PG + LFU. For the gram-negative *E. coli O157:H7*, the combined LFU+PG treatments significantly increased the membrane permeability with an increase in treatment time ($P < 0.05$). Meanwhile, treatments with PG alone also generated substantial damage compared to US treatment alone and the control cells. The damage caused by PG was independent of the incubation time. It did not change significantly with an increase in incubation time ($P > 0.05$). In contrast, limited changes in cell permeability were detected for the gram-positive *L. innocua* within the first 10 min of treatment. However, a significant increase in PI permeability was observed after treating for 45 minutes using a combined LFU+PG treatment ($P < 0.05$).

A.

E. coli O157:H7 PI dye result



B.

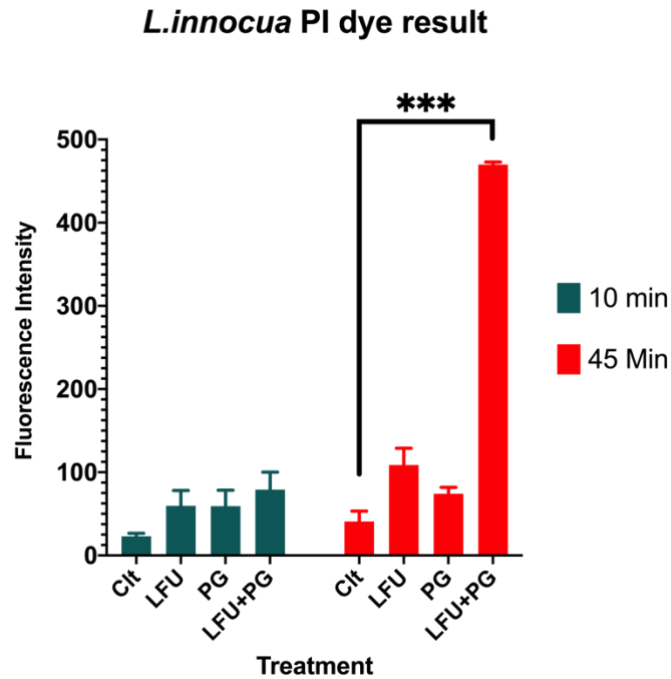


Fig. 2.4 Relative intracellular PI uptake by bacterial cells as a measure of bacterial membrane integrity after PG, LFU, and LFU+PG treatments of *E. coli* O157:H7 (A) and *L. innocua* (B) for 10 and 45 minutes.

Using both liposomes and the gram-negative bacterial cells, the results illustrate significant interactions of PG with the membrane. Similar to the results with liposomes, the bacterial cell permeability measurements showed no synergistic increase in membrane permeability with combined treatment of PG and LFU during the first five minutes. The results in Fig. 4-A also show a synergistic increase in the membrane permeability with extended treatment (LFU+PG treatment) for 30 min. Together the results using both liposomal model system and bacterial cells show rapid interactions of PG with lipid membranes based on changes in membrane fluidity and permeability respectively. However, with extended LFU treatment, the PG incubated bacterial cells accumulate a significant increase in the membrane permeability.

A similar trend was also observed in the case of gram-positive *L. innocua* cells. In this case, no synergistic increase in the membrane permeability with PG and LFU was achieved with 10 min of treatment. After a combined treatment of 45 min, an increase in the membrane permeability was observed ($P < 0.001$) as illustrated in Fig. 4-B. Comparison between the gram-negative and the gram-positive results in Fig. 4, also illustrate significant differences in the sensitivity of bacterial cells to the synergistic antimicrobial activity of LFU and the food-grade compound. These differences in susceptibility of bacterial cells can be attributed to the presence of a thicker and a rigid cell wall in the gram-positive bacteria that can reduce susceptibility of the bacteria to PG and its combination with LFU.

3.2.3. SEM figures compare *E. coli* O157:H7 and *L. innocua* cellular morphology change under individual and combined treatment of PG and LFU

Figure 5 reveals the morphological changes of *E. coli* O157:H7 and *L. innocua* cells after LFU treatment with and without the presence of PG using the SEM technique. In addition, the influence of PG only treatment on cellular morphology was also assessed. After LFU treatment in the presence of PG for 30 minutes, most *E. coli* O157:H7 cells were severely deformed and notable morphological changes were observed (Figure 5-E). Ruptured and distorted cell envelopes were also observed. Moreover, it appears that *E. coli* O157:H7 cells were reduced in size probably due to leakage of the intracellular components as a result of the membrane damage. The untreated *E. coli* O157:H7 cells retained the rod-shaped cell morphology with a smooth surface (Figure 5-A). The images of *E. coli* O157:H7 cells after incubation for 5 and 30 minutes with PG alone were similar to the images of cells obtained after treatment with the combined LFU+PG treatment for 5 minutes (Figures 5-B, C, D). These features include pore formation and localized rupture as highlighted in the Figures 5-B, C, D. During these treatment conditions, only a fraction of the bacterial cells was influenced, while several cells retained their structure and morphology, similar to the controls. This further highlights the increased membrane damage induced by the combination of LFU+ PG is only achieved after extended treatment. These

results also support the observations in Figs 3 and 4 that PG rapidly interacts with lipid membranes. In contrast, cells treated with the combined LFU+PG for an extended period had extensive changes in cellular morphology across the majority of the bacterial cells and these changes were distinct from the results observed in Figs. 5 B-D including fusion of cellular mass.

Figure 6 describes the morphological changes of *L. innocua* cells after LFU treatment with and without the presence of PG. In contrast to the results with the *E. coli O157:H7*, the combined LFU+PG treatments caused minor changes to the *L. innocua* cell morphology. After LFU+PG treatment for 10 minutes, most *L. innocua* cells maintained similar cell morphology, but part of the cells showed minor damage (Figure 6-B). In Figure 6-C, after 45 minutes of LFU+PG treatment, concave cell envelopes were observed although the shape of *L.innocua* cells did not change. The pore formation and localized rupture were not observed in *L.innocua* after the treatment. These results in combination with membrane permeability measurements further confirm the higher susceptibility of the gram-negative *E. coli O157:H7* to the PG and to the combined LFU+PG treatments than the gram-positive *L. innocua*.

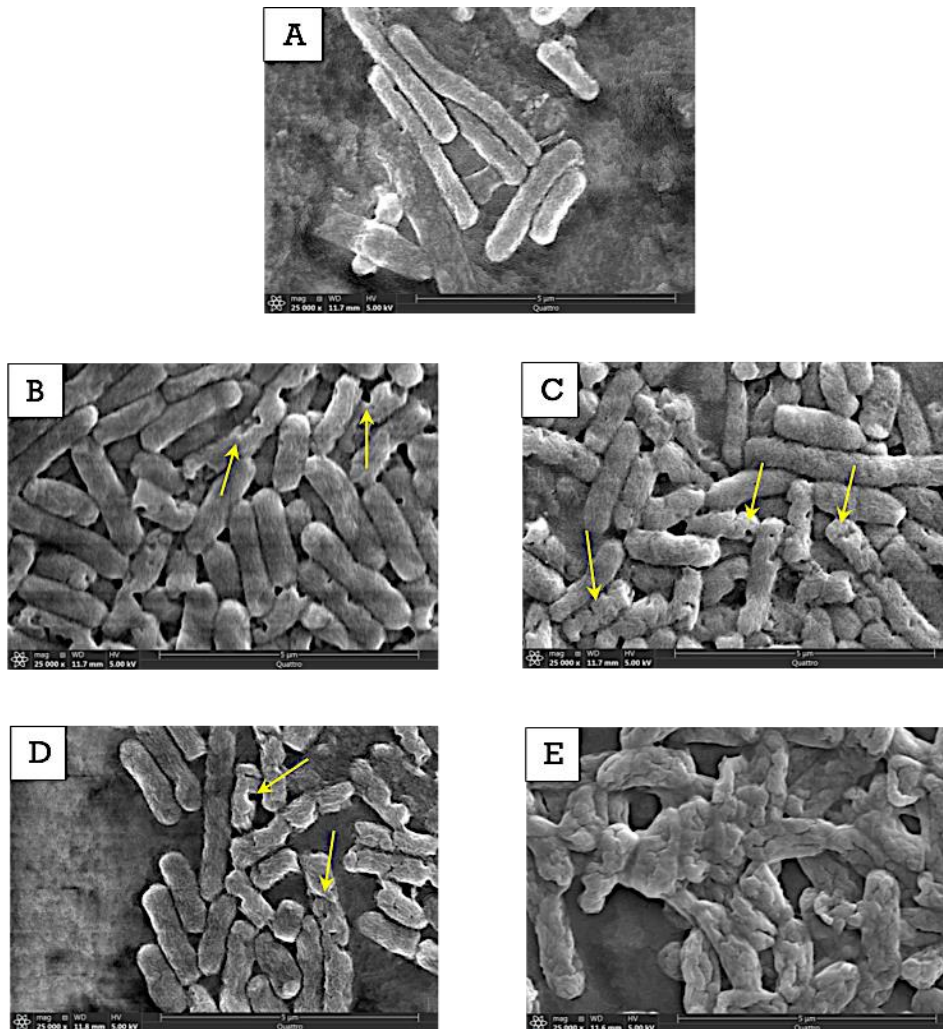


Fig. 2.5 Scanning electron microscope (SEM) images of ultrasound treated *E. coli* O157:H7 cells: control sample (A), sample which was incubated in PG for 5 minutes (B), sample which was incubated in PG for 30 minutes (C), combined LFU+PG treatment for 5 minutes (D), combined LFU+PG treatment for 30 minutes (E)

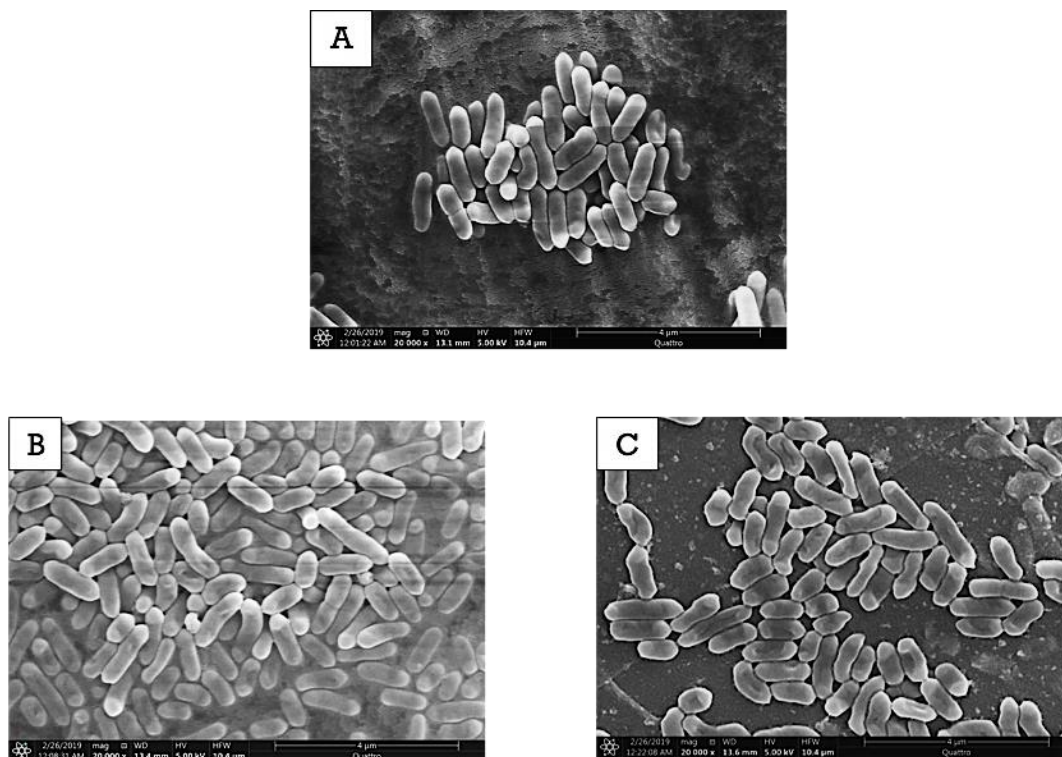


Fig. 2.6 Scanning electron microscope (SEM) images of ultrasound treated *L.innocua* cells: control sample (A), combined LFU+PG treatment for 10 minutes (B), combined US+PG treatment for 45 minutes (C)

3.3. Oxidative damage

3.3.1. Total Intracellular thiol reduction of *E. coli O157:H7*

To evaluate influence of the combined LFU and PG treatment to generate ROS, an endogenous intracellular oxidative stress indicator was utilized. Within the cell cytoplasm, thiol content is a reliable indicator of oxidative stress levels as changes in the thiol content has been correlated with the intracellular ROS formation [23,37–39]. Figure 7 demonstrates the reduction in the intracellular thiol content of *E. coli O157:H7* after treatment with LFU in the presence of PG. *E. coli O157:H7* cells were selected for this assay based on the fact that the intracellular thiol content in *L. innocua* is inherently low [40–42], which may limit detection of further reduction in its level after the treatment. There were no significant differences ($P>0.05$) in the total thiol content among all selected treatments except for the

positive controls which were treated with sodium hypochlorite. The results indicate that under the selected conditions, LFU, PG treatment, and the combined LFU+PG treatment did not generate oxidative stress in the cytoplasm, and thus the oxidative damage may not play a significant role in the synergistic bacterial inactivation.

***E. coli* O157:H7 Intracellular thiol reduction**

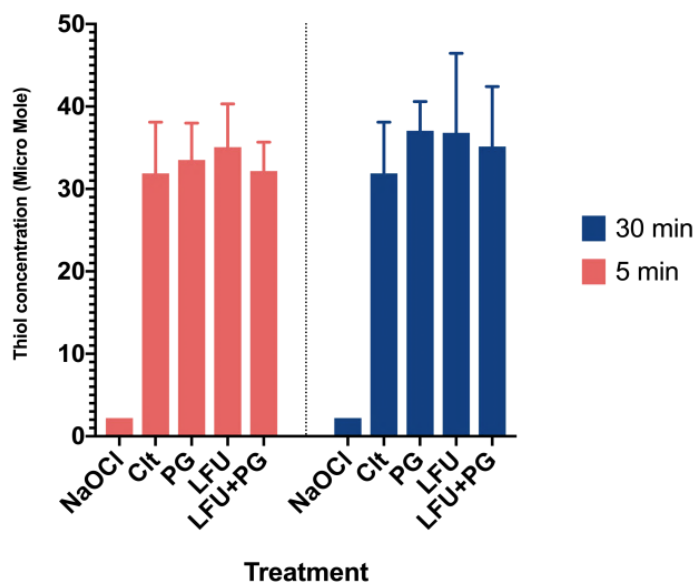


Fig. 2.7 Intracellular thiol content in *E. coli* O157:H7 cells following treatment with PG, LFU, or LFU+PG for 5 or 30 minutes. Untreated cells were used as a negative control and sodium hypochlorite (100 ppm) treated cells were used as a positive control.

The oxidative stress generation as a result of the sonochemical reactions has been suggested as one of the inactivation mechanisms for the ultrasound treatment [43–47]. The ROS can be generated by the transient cavitation processes or it can result from the excitation of exogenous or endogenous cellular components by the ultrasound as well as the localized thermal effects of ultrasound. Cavitation induced ROS generation is one of the most frequently described bactericidal mechanism of ultrasound in

the literature [34,48–50]. In this study, the intracellular ROS generation could not be confirmed (Figure 7). The reason can be attributed to the low energy density of the selected ultrasound treatment. The device used in this study only provides an energy density of 0.092 W/mL, which is low compared to the other high-intensity ultrasound devices that generate more vigorous cavitation.

3.3.2. Evaluation of the role of oxidation in combined LFU + PG synergy by supplementing Antioxidants

To further validate the lack of ROS generation by the combined LFU+PG treatment, exogenous antioxidants were added to the solution during treatment as ROS quenchers. It was hypothesized that the addition of ROS quenchers would reduce the bactericidal effect and protect the treated bacteria from the combined treatment. Figure 8 describes the antimicrobial effect of the combined treatment in the presence of glutathione and thiourea. There was a 5 to 6 log reduction in samples with added exogenous antioxidants. This number of log reduction was equivalent to the LFU+PG treated sample without the presence of ROS quenchers. There was no significant difference ($P > 0.05$) between samples with and without glutathione. There was a small but significant difference between samples with and without thiourea ($P < 0.05$); however, this difference is attributed to the fact that the concentration of thiourea was ten times higher than that of glutathione. In general, the protective effect from the addition of antioxidants was not observed. This observation together with the data from the total intracellular thiol reduction confirms the lack of significant role of ROS in the observed synergistic inactivation of bacteria.

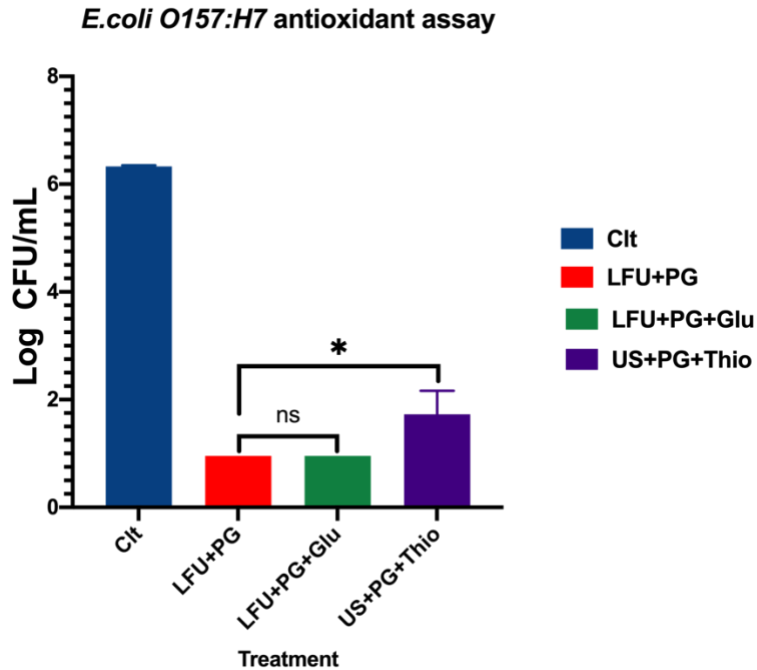


Fig. 2.8 The effect of antioxidant addition to the combined LFU and PG treatment at 30 minutes of treatment time where Glu is glutathione and Thio is thiourea

4. Conclusions

Low-frequency ultrasound (LFU) and Propyl Gallate (PG) act synergistically to enhance the inactivation rates of the gram-negative *E. coli* O157:H7 and the gram-positive *L. innocua*. Based on the measurements using both liposomes and bacteria cells, rapid interaction of PG with lipid membranes is one of the key factors for the observed accelerated inactivation of bacteria. This interaction increases lateral mobility in the membrane of liposomes and enhances permeability in the bacterial membrane. In bacterial cells, the combination of LFU with PG increased the membrane permeability with extended treatment time. SEM imaging corroborated with the results obtained from the bacterial membrane damage assay. A lack of significant change in the intracellular thiol content as well as a lack of protective effect from exogenous antioxidants to the antibacterial effect indicate that oxidative stress generation was not a leading mechanism responsible for the enhanced antimicrobial effect. Overall, these results

illustrate a novel approach to achieve more than 5 log inactivation of bacteria using a synergistic combination of PG with a low intensity and a low-frequency ultrasound process.

Acknowledgments

This project was supported by the Agriculture and Food Research Initiative by grant no. 2014-67017-21642 from the USDA National Institute of Food and Agriculture (USDA-NIFA) Program in Improving Food Quality (A1361) and by grant no. 2015-68003- 23411 from the USDA-NIFA Program Enhancing Food Safety through Improved Processing Technologies (A4131).

References

- [1] M. Ashokkumar, Applications of ultrasound in food and bioprocessing, *Ultrason. Sonochem.* 25 (2015) 17–23. doi:10.1016/j.ultsonch.2014.08.012.
- [2] F.J. Barba, L. Ahrné, E. Xanthakis, M.G. Landerslev, V. Orlien, Chapter 2. Innovative Technologies for Food Preservation, (2017). doi:10.1016/B978-0-12-811031-7.00002-9.
- [3] S. Kentish, H. Feng, Applications of Power Ultrasound in Food Processing, *Annu. Rev. Food Sci. Technol.* 5 (2014) 263–284. doi:10.1146/annurev-food-030212-182537.
- [4] A. Moody, G. Marx, B.G. Swanson, D. Bermúdez-Aguirre, A comprehensive study on the inactivation of *Escherichia coli* under nonthermal technologies: High hydrostatic pressure, pulsed electric fields and ultrasound, *Food Control.* 37 (2014) 305–314. doi:10.1016/J.FOODCONT.2013.09.052.
- [5] A.M. Rediske, B.L. Roeder, M.K. Brown, J.L. Nelson, R.L. Robison, D.O. Draper, G.B. Schaalje, R.A. Robison, W.G. Pitt, Ultrasonic enhancement of antibiotic action on *Escherichia coli* biofilms: An in vivo model, *Antimicrob. Agents Chemother.* 43 (1999) 1211–1214. doi:10.1128/aac.43.5.1211.
- [6] A.I. V Ross, M.W. Griffiths, G.S. Mittal, H.C. Deeth, Combining nonthermal technologies to control

- foodborne microorganisms, *Int. J. Food Microbiol.* (2003). doi:10.1016/S0168-1605(03)00161-2.
- [7] H. Hirschberg, S.J. Madsen, Synergistic efficacy of ultrasound, sonosensitizers and chemotherapy: A review, *Ther. Deliv.* 8 (2017) 331–342. doi:10.4155/tde-2016-0080.
- [8] F. Harris, S.R. Dennison, D.A. Phoenix, Using sound for microbial eradication - light at the end of the tunnel?, *FEMS Microbiol. Lett.* 356 (2014) 20–22. doi:10.1111/1574-6968.12484.
- [9] X. Pang, C. Xu, Y. Jiang, Q. Xiao, A.W. Leung, Natural products in the discovery of novel sonosensitizers, *Pharmacol. Ther.* 162 (2016) 144–151. doi:10.1016/J.PHARMTHERA.2015.12.004.
- [10] F. Giuntini, F. Foglietta, A.M. Marucco, A. Troia, N. V. Dezhkunov, A. Pozzoli, G. Durando, I. Fenoglio, L. Serpe, R. Canaparo, Insight into ultrasound-mediated reactive oxygen species generation by various metal-porphyrin complexes, *Free Radic. Biol. Med.* 121 (2018) 190–201. doi:10.1016/j.freeradbiomed.2018.05.002.
- [11] M.M. Rahman, K. Ninomiya, C. Ogino, N. Shimizu, Ultrasound-induced membrane lipid peroxidation and cell damage of *Escherichia coli* in the presence of non-woven TiO₂ fabrics, *Ultrason. Sonochem.* 17 (2010) 738–743. doi:10.1016/j.ultsonch.2009.12.001.
- [12] X. Wang, A.W. Leung, H. Hua, C. Xu, M. Ip, Sonodynamic action of hypocrellin B on biofilm-producing *Staphylococcus epidermidis* in planktonic condition, *J. Acoust. Soc. Am.* 138 (2015) 2548–2553. doi:10.1121/1.4932014.
- [13] X. Wang, M. Ip, A.W. Leung, C. Xu, Sonodynamic inactivation of methicillin-resistant *Staphylococcus aureus* in planktonic condition by curcumin under ultrasound sonication, *Ultrasonics.* 54 (2014) 2109–2114. doi:10.1016/j.ultras.2014.06.017.
- [14] K. Kajiyama, H. Hojo, M. Suzuki, F. Nanjo, S. Kumazawa, T. Nakayama, Relationship between

- Antibacterial Activity of (+)-Catechin Derivatives and Their Interaction with a Model Membrane, (2004). doi:10.1021/jf0350111.
- [15] L.J. Nohynek, H.-L. Alakomi, M.P. Kähkönen, M. Heinonen, I.M. Helander, K.-M. Oksman-Caldentey, R.H. Puupponen-Pimiä, Berry Phenolics: Antimicrobial Properties and Mechanisms of Action Against Severe Human Pathogens, *Nutr. Cancer*. 54 (2006) 18–32. doi:10.1207/s15327914nc5401_4.
- [16] E.F. De Oliveira, A. Cossu, R. V. Tikekar, N. Nitin, J. Björkroth, E.F. de Oliveira, A. Cossu, R. V. Tikekar, N. Nitin, Enhanced Antimicrobial Activity Based on a Synergistic Combination of Sublethal Levels of Stresses Induced by UV-A Light and Organic Acids, *Appl. Environ. Microbiol.* 83 (2017) AEM.00383-17. doi:10.1128/AEM.00383-17.
- [17] E.F. De Oliveira, A. Cossu, R. V. Tikekar, N. Nitin, J. Björkroth, Enhanced Antimicrobial Activity Based on a Synergistic Combination of Sublethal Levels of Stresses Induced by UV-A Light and Organic Acids, (2017). doi:10.1128/AEM.
- [18] K. Nakamura, K. Ishiyama, H. Sheng, H. Ikai, T. Kanno, Y. Niwano, Bactericidal Activity and Mechanism of Photoirradiated Polyphenols against Gram-Positive and-Negative Bacteria, (2015). doi:10.1021/jf5058588.
- [19] A. Borges, C. Ferreira, M.J. Saavedra, M. Simões, Antibacterial Activity and Mode of Action of Ferulic and Gallic Acids Against Pathogenic Bacteria, *Microb. Drug Resist.* 19 (2013) 256–265. doi:10.1089/mdr.2012.0244.
- [20] K. Nakamura, Y. Yamada, H. Ikai, T. Kanno, K. Sasaki, Y. Niwano, Bactericidal Action of Photoirradiated Gallic Acid via Reactive Oxygen Species Formation, *J. Agric. Food Chem.* 60 (2012) 10048–10054. doi:10.1021/jf303177p.
- [21] L. Boyd, E.G. Beveridge, Antimicrobial activity of some alkyl esters of gallic acid (3,4,5,-

- trihydroxybenzoic acid) against *Escherichia coli* NCTC 5933 with particular reference to n-propyl gallate., *Microbios.* 30 (1981) 73–85. <http://www.ncbi.nlm.nih.gov/pubmed/6272069> (accessed March 7, 2019).
- [22] P. Tammela, L. Laitinen, A. Galkin, T. Wennberg, R. Heczko, H. Vuorela, J.P. Slotte, P. Vuorela, Permeability characteristics and membrane affinity of flavonoids and alkyl gallates in Caco-2 cells and in phospholipid vesicles, *Arch. Biochem. Biophys.* 425 (2004) 193–199. doi:10.1016/j.abb.2004.03.023.
- [23] Q. Wang, E.F. De Oliveira, S. Alborzi, L.J. Bastarrachea, R. V. Tikekar, On mechanism behind UV-A light enhanced antibacterial activity of gallic acid and propyl gallate against *Escherichia coli* O157:H7, *Sci. Rep.* 7 (2017) 1–11. doi:10.1038/s41598-017-08449-1.
- [24] Scientific Opinion on the re-evaluation of propyl gallate (E 310) as a food additive, *EFSA J.* 12 (2014) 3642. <https://doi.org/10.2903/j.efsa.2014.3642>.
- [25] A.H. Geeraerd, V.P. Valdramidis, J.F. Van Impe, GlnaFIT, a freeware tool to assess non- log-linear microbial survivor curves, *Int. J. Food Microbiol.* 102 (2005) 95–105. doi:10.1016/j.ijfoodmicro.2004.11.038.
- [26] T.A. Bigelow, T. Northagen, T.M. Hill, F.C. Sailer, The Destruction of *Escherichia Coli* Biofilms Using High-Intensity Focused Ultrasound, *Ultrasound Med. Biol.* 35 (2009) 1026–1031. doi:10.1016/j.ultrasmedbio.2008.12.001.
- [27] H.M. Davey, P. Hexley, Red but not dead? Membranes of stressed *Saccharomyces cerevisiae* are permeable to propidium iodide, *Environ. Microbiol.* 13 (2011) 163–171. doi:10.1111/j.1462-2920.2010.02317.x.
- [28] R. Virto, P. Mañas, I. Álvarez, S. Condon, J. Raso, Membrane damage and microbial inactivation by chlorine in the absence and presence of a chlorine-demanding substrate, *Appl. Environ.*

- Microbiol. 71 (2005) 5022–5028. doi:10.1128/AEM.71.9.5022-5028.2005.
- [29] M.A. Kohanski, M.A. DePristo, J.J. Collins, Sublethal Antibiotic Treatment Leads to Multidrug Resistance via Radical-Induced Mutagenesis, *Mol. Cell.* 37 (2010) 311–320. doi:10.1016/j.molcel.2010.01.003.
- [30] D. Farmer, P. Burcham, P. Marin, The ability of thiourea to scavenge hydrogen peroxide and hydroxyl radicals during the intra-coronal bleaching of bloodstained root-filled teeth, *Aust. Dent. J.* 51 (2006) 146–152. doi:10.1111/j.1834-7819.2006.tb00418.x.
- [31] B.W. Davies, M.A. Kohanski, L.A. Simmons, J.A. Winkler, J.J. Collins, G.C. Walker, Hydroxyurea Induces Hydroxyl Radical-Mediated Cell Death in *Escherichia coli*, *Mol. Cell.* 36 (2009) 845–860. doi:10.1016/j.molcel.2009.11.024.
- [32] J.J. Foti, B. Devadoss, J. Winkler, J. Collins, G. Walker, Oxidation of the Guanine Nucleotide Pool Underlies Cell Death by Bactericidal Antibiotics, *Science* (80-.). 336 (2012) 315–319.
- [33] J.E. Repine, R.B. Fox, E.M. Berger, Hydrogen peroxide kills *Staphylococcus aureus* by reacting with staphylococcal iron to form hydroxyl radical, *J. Biol. Chem.* 256 (1981) 7094–7096.
- [34] P. Piyasena, E. Mohareb, R.C. McKellar, Inactivation of microbes using ultrasound: A review, *Int. J. Food Microbiol.* 87 (2003) 207–216. doi:10.1016/S0168-1605(03)00075-8.
- [35] M. Erriu, C. Blus, S. Szmukler-Moncler, S. Buogo, R. Levi, G. Barbato, D. Madonnaripa, G. Denotti, V. Piras, G. Orrù, Microbial biofilm modulation by ultrasound: Current concepts and controversies, *Ultrason. Sonochem.* 21 (2014) 15–22. doi:10.1016/j.ultsonch.2013.05.011.
- [36] X. Yang, R. Rai, C.N. Huu, N. Nitin, Synergistic antimicrobial activity by light or thermal treatment and lauric arginate: Membrane damage and oxidative stress, *Appl. Environ. Microbiol.* 85 (2019). doi:10.1128/AEM.01033-19.

- [37] Q. Zhang, S.P. Morgan, P. O'Shea, M.L. Mather, Ultrasound induced fluorescence of nanoscale liposome contrast agents, *PLoS One*. 11 (2016). doi:10.1371/journal.pone.0159742.
- [38] J.R. Terrill, H.G. Radley-Crabb, T. Iwasaki, F.A. Lemckert, P.G. Arthur, M.D. Grounds, Oxidative stress and pathology in muscular dystrophies: Focus on protein thiol oxidation and dysferlinopathies, *FEBS J*. 280 (2013) 4149–4164. doi:10.1111/febs.12142.
- [39] H. Kundi, I. Ates, E. Kiziltunc, M. Cetin, H. Cicekcioglu, S. Neselioglu, O. Erel, E. Ornek, A novel oxidative stress marker in acute myocardial infarction; Thiol/disulphide homeostasis, *Am. J. Emerg. Med.* 33 (2015) 1567–1571. doi:10.1016/j.ajem.2015.06.016.
- [40] Z. Lou, P. Li, X. Sun, S. Yang, B. Wang, K. Han, A fluorescent probe for rapid detection of thiols and imaging of thiols reducing repair and H₂O₂ oxidative stress cycles in living cells, *Chem. Commun.* 49 (2013) 391–393. doi:10.1039/c2cc36839k.
- [41] J. Sun, Y. Hang, Y. Han, X. Zhang, L. Gan, C. Cai, Z. Chen, Y. Yang, Q. Song, C. Shao, Y. Yang, Y. Zhou, X. Wang, C. Cheng, H. Song, Deletion of glutaredoxin promotes oxidative tolerance and intracellular infection in *Listeria monocytogenes*, (2019). doi:10.1080/21505594.2019.1685640.
- [42] M. Erriu, C. Blus, S. Szmukler-Moncler, S. Buogo, R. Levi, G. Barbato, D. Madonnaripa, G. Denotti, V. Piras, G. Orrù, Microbial biofilm modulation by ultrasound: Current concepts and controversies, *Ultrason. Sonochem.* 21 (2014) 15–22. doi:10.1016/j.ultsonch.2013.05.011.
- [43] S. Subhra Chatterjee, H. Hossain, S. Otten, C. Kuenne, K. Kuchmina, S. Machata, E. Domann, T. Chakraborty, T. Hain, Intracellular Gene Expression Profile of *Listeria monocytogenes* †, *Infect. Immun.* 74 (2006) 1323–1338. doi:10.1128/IAI.74.2.1323-1338.2006.
- [44] A. Demirdöven, T. Baysal, The Use of Ultrasound and Combined Technologies in Food Preservation, *Food Rev. Int.* 25 (2008) 1–11. doi:10.1080/87559120802306157.

- [45] P. Piyasena, E. Mohareb, R.C. McKellar, Inactivation of microbes using ultrasound: A review, *Int. J. Food Microbiol.* 87 (2003) 207–216. doi:10.1016/S0168-1605(03)00075-8.
- [46] H. Lee, B. Zhou, W. Liang, H. Feng, S.E. Martin, Inactivation of *Escherichia coli* cells with sonication, manosonication, thermosonication, and manothermosonication: Microbial responses and kinetics modeling, *J. Food Eng.* 93 (2009) 354–364.
<https://www.sciencedirect.com/science/article/pii/S0260877409000636> (accessed February 18, 2019).
- [47] S. Gao, G. Lewis, Y. Hemar, Ultrasonic Inactivation of Microorganisms, (n.d.). doi:10.1007/978-981-287-278-4_69.
- [48] P. Singh, A. Kumar, N.K. Dubey, R. Gupta, Ultrasound enhanced sanitizer efficacy in reduction of *Escherichia coli* O157:H7 population on spinach leaves, *J. Food Sci.* 74 (2009) 308–313.
doi:10.1111/j.1750-3841.2009.01223.x.
- [49] B. Liu, D.-J. Wang, B.-M. Liu, X. Wang, L.-L. He, J. Wang, S.-K. Xu, The influence of ultrasound on the fluoroquinolones antibacterial activity, (2011). doi:10.1016/j.ultsonch.2011.02.001.
- [50] F. Nakonechny, M. Nisnevitch, Y. Nitzan, M. Nisnevitch, Sonodynamic excitation of rose bengal for eradication of gram-positive and gram-negative bacteria, *Biomed Res. Int.* 2013 (2013).
doi:10.1155/2013/684930.
- [51] H.L. Dolan, L.J. Bastarrachea, R. V. Tikekar, Inactivation of *Listeria innocua* by a combined treatment of low-frequency ultrasound and zinc oxide, *LWT.* 88 (2018) 146–151.
doi:10.1016/j.lwt.2017.10.008.

Chapter 3

Combination of high-frequency ultrasound with a food-grade antioxidant for enhancing the inactivation of bacteria in water and a model food system

Cuong Nguyen Huu^a, Rohan Tikekar^b, Nitin Nitin^{a, c}

^a Department of Food Science and Technology, University of California, Davis, CA, USA.

^b Department of Nutrition and Food Science, University of Maryland, College Park, MD, USA.

^c Department of Biological and Agricultural Engineering, University of California, Davis, CA, USA.

Address correspondence to Nitin Nitin, nnitin@ucdavis.edu, Robert Mondavi Institute South, Room 2221, Hilgard Ln, Davis, CA 95616

Keywords: High-frequency ultrasound, propyl gallate, sonodynamic antimicrobial treatment, synergistic antimicrobial treatment, *E. coli* O157:H7, *L. innocua*

Abstract

This study evaluates a combination of high-frequency ultrasound (HFU, 1 MHz, 1.6 W/cm²) and a food-grade antioxidant, propyl gallate (PG, 10 mM), to enhance inactivation rates of a model Gram-positive (*Listeria innocua*) and a Gram-negative bacterium (*Escherichia coli* O157:H7) in water and a model beverage (apple juice). Treatment times ranged from 5 to 20 minutes. The study also assesses the potential mechanisms of synergistic interactions based on an evaluation of changes in bacterial permeability, morphology, and intracellular oxidative stress. HFU+PG significantly (5.5 log CFU/mL, P < 0.05) enhanced the inactivation of both *L. innocua* and *E. coli* O157:H7 compared to the individual PG or HFU treatments in both water and apple juice within 15 min of treatment time. Overall, *L. innocua* demonstrated significantly higher resistance to inactivation than *E. coli* O157:H7 using a combination of HFU+PG. The synergistic antimicrobial activity of HFU+ PG resulted in enhanced membrane damage and oxidative stress induction in bacteria compared to the individual treatments of HFU or PG alone.

Industrial relevance

The technologies used for food processing should be capable of destroying food-borne pathogens within minutes (~few minutes) as well as significantly (~5 log) to retain food nutritional and sensory quality attributes. Additionally, any additives used in food processing should have a food-grade status, preferably a generally recognized as safe or GRAS designation. The synergistic oxidative stress induction by HFU+PG treatment demonstrates the unique potential of this approach to inactivate bacteria beyond the membrane damage observed by conventional ultrasound treatments. As a result, the treatment time was reduced significantly. Moreover, the antioxidant compound PG used in this study to combine with HFU can be used in food products due to its GRAS status. This study illustrates the effectiveness of combining HFU with PG in reducing microbial populations in food and water systems as an alternative to thermal processing.

1. Introduction

Ultrasound (US) technology has been used for food processing applications including extraction of bioactive compounds, enhancing the rate of drying processes, and improving cleaning and sanitation in food process industries (Ashokkumar, 2015). In addition, US technology has also demonstrated moderate efficacy for the inactivation of bacteria in food systems (Arroyo & Lyng, 2017; Demirdöven & Baysal, 2008). Among various innovations in US technology, the development and application of sonodynamic antimicrobial treatment (SAT) have the potential to improve the inactivation of bacteria and associated biofilms (Bai et al., 2012; Chen et al., 2014; Costley et al., 2017). The SAT approach is analogous to a more established photodynamic therapy (PDT) (Alves et al., 2018). Typically, SAT uses high-frequency ultrasound (HFU), greater than 1 MHz, to excite sonosensitive agents called sonosensitizers to generate reactive oxygen species (ROS) in biological systems and promote inactivation of bacteria (Alves et al., 2018; Wang et al., 2015; Zhuang et al., 2014). Despite its potential, there is limited application of SAT for inactivation of bacteria in food and environmental application since there are only a limited food-grade compounds that can be used synergistically with HFU (Nguyen et al., 2021; Pang et al., 2016; X. Wang et al., 2015). In addition, there is a lack of comprehensive understanding of the potential of SAT approaches for the inactivation of both Gram-positive and Gram-negative bacteria. Based on these considerations, there is an unmet need to develop and deploy SAT in the food industry. These applications will require the use of food-grade compounds for the synergistic inactivation of target bacteria and provide a novel non-thermal technology for food processing industries.

For applications in food processing, rapid (~few min) and significant (~5 log) inactivation of contaminating bacteria in food are some of the key requirements for the processing technologies. In addition, any additives used for food processing need to have a food-grade status and preferably a GRAS status. Thus, to translate the applications of SAT technology for food applications, there is a need to

evaluate the kinetics of inactivation of both the Gram-positive and Gram-negative bacteria using food-grade sonosensitizers in model systems, including food products and evaluate the possible mechanisms for the inactivation of both types of bacteria.

Therefore, to address these gaps in knowledge, this study evaluated a synergistic antimicrobial treatment using a combination of high-frequency (HFU) and a food-grade antioxidant, propyl gallate (PG), against a model Gram-positive (*Listeria innocua*) and a Gram-negative bacterium (*Escherichia coli* O157:H7). These selected bacteria represent both the Gram-negative pathogenic bacteria and a surrogate of a Gram-positive pathogen (*Listeria monocytogenes*). The selected compound for this study was Propyl gallate (PG). PG is a derivative of gallic acid (Gallate acid propyl ester) and is used as an antioxidant in processed foods, cosmetics, and food packaging materials to prevent rancidity and spoilage (del Valle et al., 2016; Hirofumi Shibata, 2016; Shibata et al., 2009; Strippoli et al., 2000; Takai et al., 2011). PG was selected based on its antimicrobial efficacy in a low frequency (40 kHz) and a low-intensity US system to inactivate bacteria, as demonstrated in our previous study (Nguyen et al., 2021). However, in this study, the process required a relatively long incubation time, such as approximately 45 min for the inactivation of *Listeria innocua* in an aqueous environment. The mechanism of inactivation of bacteria was predominantly associated with membrane damage of bacterial cells.

The overall goal of this study was to evaluate the synergistic inactivation of bacteria in model systems, including a liquid food, based on a combination of high-frequency ultrasound (1 MHz, 1.6 W/cm²) and food-grade antioxidant PG. The synergistic activity of HFU+ PG was characterized based on enhancement in the inactivation of bacteria using the standard plate counting assays. Isobologram analysis was used to quantitatively assess the degree of antimicrobial synergism achieved by the combination of HFU and PG compared to individual treatments. To identify the potential mechanisms for the synergistic inactivation of bacteria using the combined treatment, the physiological changes in

the bacterial cell membrane permeability and intracellular thiol content were measured. In summary, this study illustrates the potential of low-energy and high-frequency ultrasound treatment in combination with a model food grade compound to achieve synergistic inactivation of bacteria. These synergistic processes can improve both the safety and quality of food products.

2. Materials and methods

2.1. Reagent

Propyl Gallate, Propidium Iodide, Thiourea, Sodium Chloride (NaCl), Sodium Dodecyl Sulfate (SDS), EDTA, N, N-dimethyl-4-nitrosoaniline (RNO), and Triton X-100 were obtained from Sigma-Aldrich. A Thiol-reactive fluorescent probe, Measure-iT™ Thiol Assay Kit, was purchased from Molecular Probes (Eugene, OR, USA). Beads of zirconia-silica (0.1 mm diameter) were obtained from Biospec Products (Bartlesville, OK, USA). Luria-Bertani (LB) broth, Tryptic Soy Broth (TSB), Tryptic Soy Agar (TSA), Phosphate-buffered Saline (PBS), and Tris-hydrochloride (1M; Tris-HCl) were purchased from Fisher BioReagents (Pittsburgh, PA, USA). Ultra-purified water was obtained using a Milli-Q filtration system (EDM Millipore; Billerica, MA, USA). Apple juice sample was obtained from Signature SELECT Apple Juice brand with 12 °Bx and pH value of 3.6 ± 0.2 .

2.2. Cultivation and enumeration of model bacteria

Escherichia coli O157: H7 (ATCC 700728, Manassas, VA, USA) and *Listeria innocua* (ATCC 33090, Manassas, VA, USA) were selected as models of Gram-positive and Gram-negative bacteria. As discussed in a previous study, *L. innocua* was selected as a surrogate for the pathogenic strain *L. monocytogenes* (Huang et al., 2018). Two bacterial strains were modified with Rifampicin resistance plasmids, enabling them to be selectively cultivated in a Rifampicin-containing culture medium. Antibacterial experiments were conducted against stationary phase bacteria as described in a previous study (de Oliveira et al., 2018). Changes in bacterial counts following treatments with HFU, PG, and HFU + PG and control

samples were assessed based on the standard plate counting method. The treated and control bacterial samples were serially diluted using Phosphate-Buffered Saline (PBS) followed by overnight cultivation on Rifampicin modified Tryptic Soy Agar (TSA) plates.

2.3. Experimental design

Four experimental groups were designed to investigate the combined effect of HFU and PG treatment on the inactivation of *E. coli* O157:H7 and *L. innocua* namely HFU+PG, HFU, PG, and control without any treatment. These experiments were conducted using sterilized DI water. Briefly, an aliquot of 200 μL of overnight bacterial culture with a concentration of 1.0×10^7 CFU/mL was added to each well of a round-bottom 12-well plate (Corning, Falcon™, USA) and randomly assigned into four experimental groups. For the PG treatment group, PG at 10 mM concentration was added to the aqueous solution inoculated with bacteria and incubated in the dark at room temperature for 15 min and 20 min for *E. coli* O157:H7 and *L. innocua*, respectively. For the HFU treatment, bacterial suspension was treated at a frequency of 1 MHz for up to 15 minutes in the case of *E. coli* O157:H7 suspension and for up to 20 minutes for *L. innocua*. For the HFU+PG treatment, bacterial suspension was treated with a combination of PG and HFU using the same conditions as described for the individual HFU and PG treatments.

An experiment was conducted with clarified apple juice to illustrate the potential application of synergistic processing of apple juice. In both the control and treatment groups, 10^6 CFU/mL of the selected bacteria were inoculated. Similar experimental parameters and sample groups as designed for the treatment of bacteria inoculated water samples were used. The inoculated apple juice samples were transferred to 1.5 mL centrifuge tubes and assigned to different treatments: high-frequency ultrasound alone (HFU), 10 mM propyl gallate alone (PG), and high-frequency ultrasound plus propyl gallate 10 mM (HFU+PG). The treatment times ranged from 2.5 to 10 minutes. Three independent replicates of each experiment were performed.

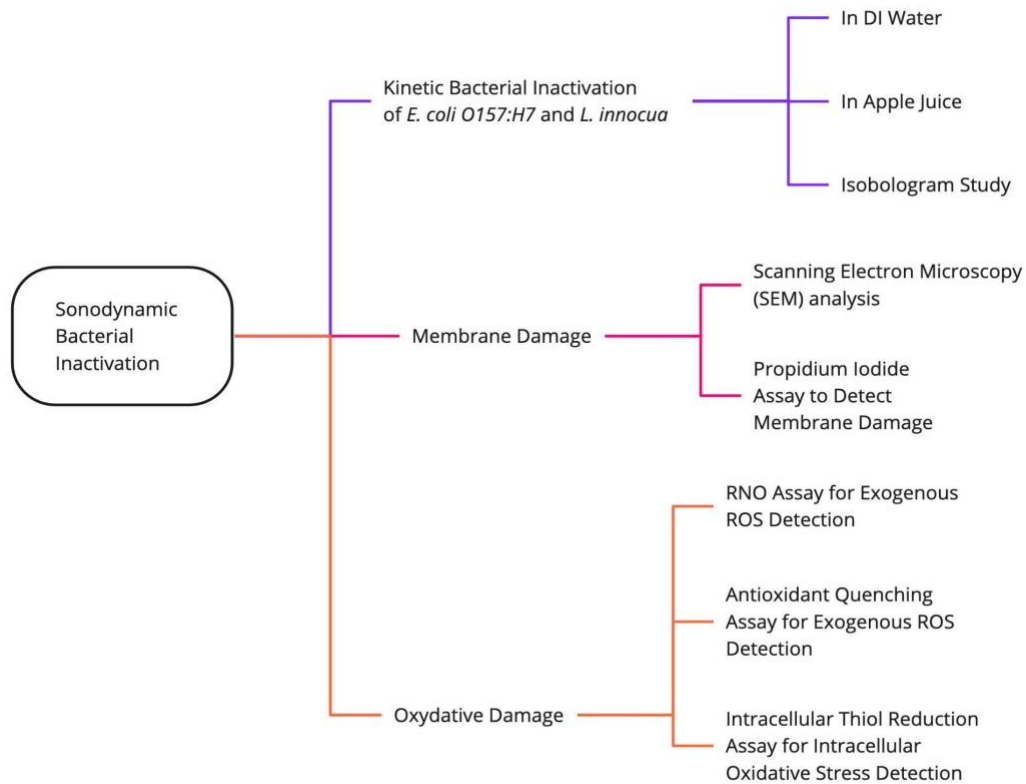


Fig. 3.1 Schematic representation of the experimental design for this study

2.4. High-frequency ultrasound treatment

A high-frequency ultrasound probe (Chattanooga medical supply, TN, USA) with an ultrasound intensity range between 1 to 2.5 W/cm² and a frequency between 1 to 3 MHz, respectively, was used. Based on our preliminary experiments and literature related to SAT topics, a frequency value of 1 MHz and an intensity level of 1.6 W/cm² were selected. Any frequency above 2.5 MHz cuts off acoustic cavitation and reduces the effect of HFU. Any level of intensity higher than 1.6 W/cm² will be lethal to the tested cells, making it difficult to measure the level of synergism between HFU and PG. The bacterial sample was inoculated in a 12 well- plate, and the HFU probe was fixed at a distance of 2 cm from the plate bottom. The 12 well-plates floated above the probe sonicator, which was submerged in water. Deionized and degassed water was used as the ultrasonic transmitting medium.

2.5. Evaluating synergy between PG and HFU using isobologram analysis

Isobologram is a graphical representation approach to characterize synergy generated by a combination of treatments such as a combination of drug compounds (Holland-Letz et al., 2018). In this study, we extend this approach to characterize synergy between HFU and PG treatments. Since the synergistic antimicrobial activity was expected to significantly improve the kinetics of bacterial inactivation, the conventional isobologram approach was adapted to represent synergism based on the treatment time.

The synergistic combination between the selected concentration of PG and HFU was evaluated based on the isobologram analysis. The methods developed in previous studies were adopted (Markovsky et al., 2014; Yang et al., 2019), with some minor modifications. For this analysis, the inactivation of bacteria was measured by varying the incubation time of PG solution (fixed concentration of 10 mM) incubated with bacterial cells without HFU treatment. Similarly, the inactivation of bacterial cells was evaluated with the variation in the time exposure of cells to HFU without the presence of PG. Then, each synergistic combination was selected and tested for a bactericidal activity, where PG was fixed at 10 mM and HFU treatment time varied between 5 and 15 minutes.

2.6. Microbial inactivation kinetics

Microbial inactivation kinetics was modeled using a first-order inactivation kinetic model (Bigelow & Esty, 1920), and the rate constant was determined based on the slope of the inactivation curve on a semi-log plot using GlnaFit, an add-in for Excel (Geeraerd et al., 2005).

$$\text{Log}_{10} N = \text{Log}_{10} N_0 - kt$$

Where N and N_0 are, respectively the cell count over time and the initial cell count; t is the time (minutes), and k is the inactivation rate constant.

2.7. Membrane damage

2.7.1. Propidium Iodide (PI) dye assay

Propidium Iodide (PI) dye was used to stain the DNA of membrane-damaged bacterial populations as a function of treatments as described previously (De Oliveira et al., 2017). This stain is commonly used to identify the extent of cell membrane damage (Borges et al., 2013; Nakamura et al., 2015). A suspension of bacteria ($\sim 1.0 \times 10^9$ CFU/mL) in PG (10 mM) was exposed to the ultrasound as described previously. Bacteria in DI water incubated in the dark was the control for this experiment. The detailed experimental protocol is described in the supplemental materials and methods section.

2.7.2. Scanning Electron Microscope (SEM)

After treatment, the bacteria were fixed with 4% glutaraldehyde solution in PBS (pH 7.4) for 2 h and washed twice with Milli-Q water. After chemically fixing the samples, ten microliters of the sample were added onto aluminum stubs with carbon conductive adhesive tape, air-dried for 30 minutes, and sputter-coated with gold. The scanning electron microscope used for this study was the Philips XL-30, which was operated at 10 kV accelerating voltage. Images were acquired at a 25,000x magnification level.

2.8. Oxidative damage

2.8.1. Exogenous ROS generation measurement

2.8.1.1. RNO bleaching assay

The generation of hydroxyl radical ($\text{HO} \cdot$) with HFU, PG, and HFU+PG treatments was measured based on the loss of color of *N,N*-dimethyl-4-nitrosoaniline (RNO) upon reaction with hydroxyl radicals (Pedraza-Chaverrí et al., 2004). In an aqueous solution, RNO gives a strong yellow color based on the electron configuration of the molecule including conjugated double bonds. However, this organic dye reacts with the hydroxyl radical generated by the sonochemistry reactions, and the loss of color was

measured based on UV-Vis measurement at 440 nm. RNO has been primarily used as a spin trap for the detection of hydroxyl radicals, as it does not react with singlet oxygen ($^1\text{O}_2$), superoxide anions (O_2^-), or other peroxy compounds (Simonsen et al., 2010).

2.8.1.2. Antioxidant quenching assay

To validate the role of ROS in the synergistic antimicrobial activity of PG and HFU treatment, an antioxidant, thiourea, was exogenously added to the bacterial sample solutions before HFU or HFU+PG or PG treatments at a concentration of 100 ppm. The solutions were then incubated for 2 min. This concentration level was selected based on previous studies (Davies et al., 2009; Farmer et al., 2006; Foti et al., 2012; Kohanski et al., 2010; Repine et al., 1981) evaluating the role of reactive oxygen species for the inactivation of bacteria-induced by diverse antimicrobial treatments. These studies have demonstrated quenching of diverse oxidative stresses induced by free radicals, peroxides, lipid peroxides, and heavy metals using thiourea.

2.8.2. Intracellular oxidative stress measurement

The intracellular oxidative stress was measured by reduction in the intracellular thiol content of *E. coli* O157:H7 and *L. innocua* cells as a function of treatments (HFU (15 min), PG (10 mM), and HFU (15 min) +PG (10 mM)) based on a method described by previous studies (Kundi et al., 2015; Lou et al., 2013; Q. Wang et al., 2017). The detailed protocol is described in the supplemental section of this manuscript.

2.9. Data analysis

Statistical analysis was performed using GraphPad Prism software V.9.3.1 (Graphpad Software, Inc., La Jolla, CA). To analyze differences between multiple experimental groups, a one-way analysis of variance ($P < 0.05$) was conducted to evaluate the statistical significance of the results. This statistical approach was used for the analysis of bacterial inactivation kinetics, PI measurement of membrane damage, extra- and intracellular ROS generation measurement, and antioxidant assay.

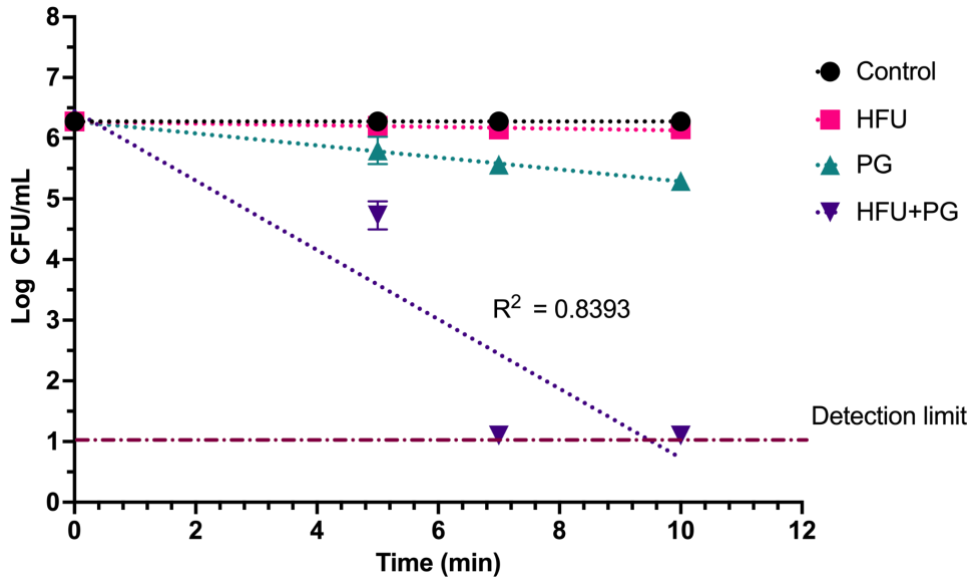
3. Results

3.1. Inactivation of *E. coli* O157:H7 and *L. innocua* by high-frequency ultrasound (HFU) and propyl gallate (PG)

3.1.1. Kinetics of bacterial inactivation in DI water

The inactivation kinetics of the target bacteria in an aqueous solution were evaluated to determine the synergistic activity of a combination of PG and HFU. For this evaluation, both the individual treatments (PG, HFU) and combined treatment (PG + HFU) were used to assess the inactivation of Gram-negative (*E. coli* O157:H7) and Gram-positive (*L. innocua*) bacteria suspended in an aqueous solution. The results in Fig. 2 indicate an enhanced bacterial inactivation by the SAT treatments compared to the individual treatment of PG or HFU. The combined HFU+PG treatment inactivated 5 log CFU/mL of both *E. coli* O157:H7 and *L. innocua* within 15 minutes. The *E. coli* O157:H7 was more susceptible to the combined treatment than *L. innocua*. The first-order kinetic model was selected to fit the inactivation data for the synergistic treatments. Based on the first-order kinetic model fit, the inactivation rate constant, k values of 0.54 ± 0.1 and 0.27 ± 0.028 per min for *E. coli* O157:H7 and *L. innocua*, respectively were calculated. In contrast to the synergistic inactivation, HFU by itself caused no significant reduction in both the selected bacteria. PG single treatment only showed a mild antimicrobial activity against *E. coli* O157:H7 with nearly one log inactivation after 10 minutes of treatment time. Furthermore, PG treatment alone had no significant antimicrobial activity against *L. innocua* during 20 minutes of incubation.

A.



B.

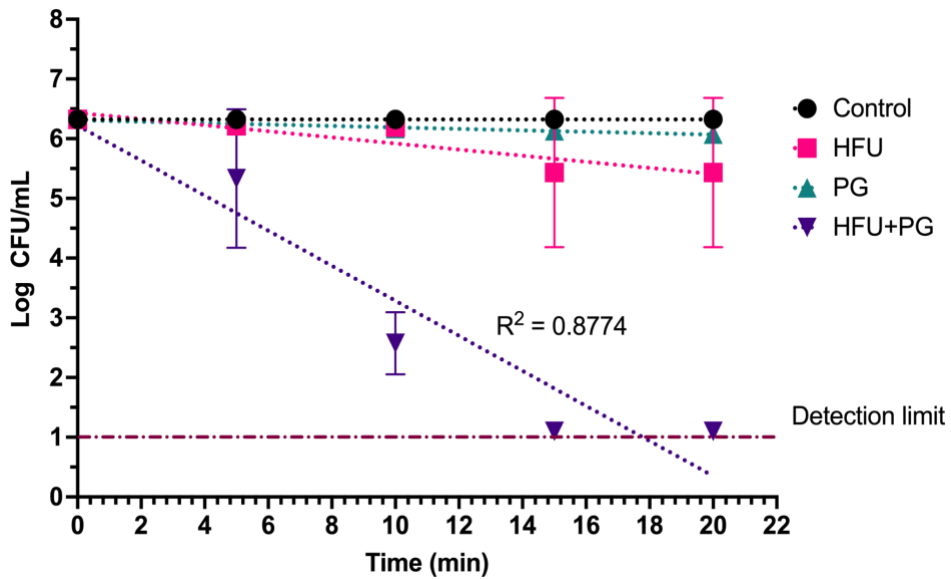
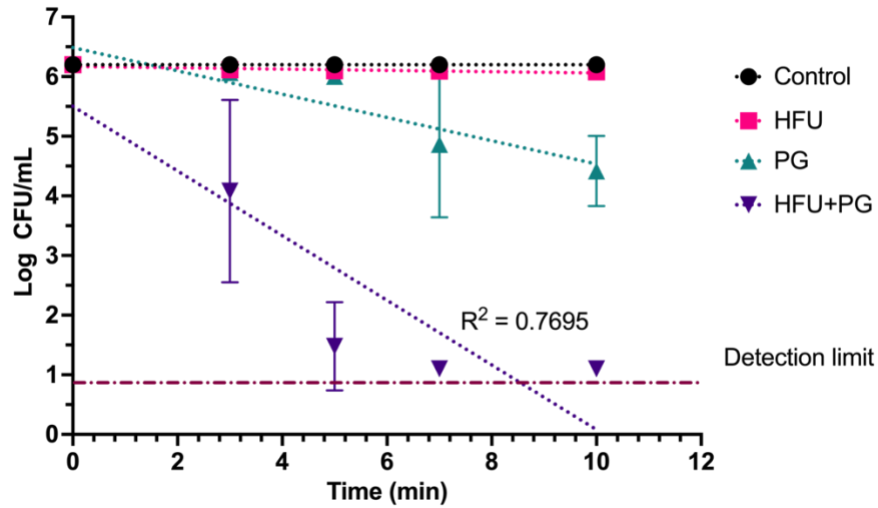


Fig. 3.2 Inactivation of *E. coli* O157: H7 (A) and *L. innocua* (B) in aqueous solution as a function of time with the following treatments: HFU – High-frequency ultrasound treatment, PG – Propyl gallate treatment, HFU+PG – Combined high-frequency ultrasound, and PG treatment.

3.1.2. Kinetics of bacterial inactivation in model apple juice

The inactivation kinetics of the target bacteria in an apple juice model were evaluated in Fig. 3. The pH of the apple juice sample was 3.6. The antibacterial effect of the combined HFU+PG treatment was slightly enhanced compared to inactivation in DI water. Based on the first-order kinetic model fit, the inactivation rate constant, k values of 0.5714 ± 0.079 and 0.2935 ± 0.03 per min for *E. coli* O157:H7 and *L. innocua*, respectively were calculated. These k values were slightly higher than those of *E. coli* O157:H7 and *L. innocua* treated with the combination of HFU+PG in DI water. Relatively higher k values indicate a faster inactivation rate. The Gram-negative *E. coli* O157:H7 also was more susceptible to the combined HFU+PG treatment than Gram-positive *L. innocua* as the inactivation rate of *E. coli* O157:H7 was almost twice that of *L. innocua*.

A.



B.

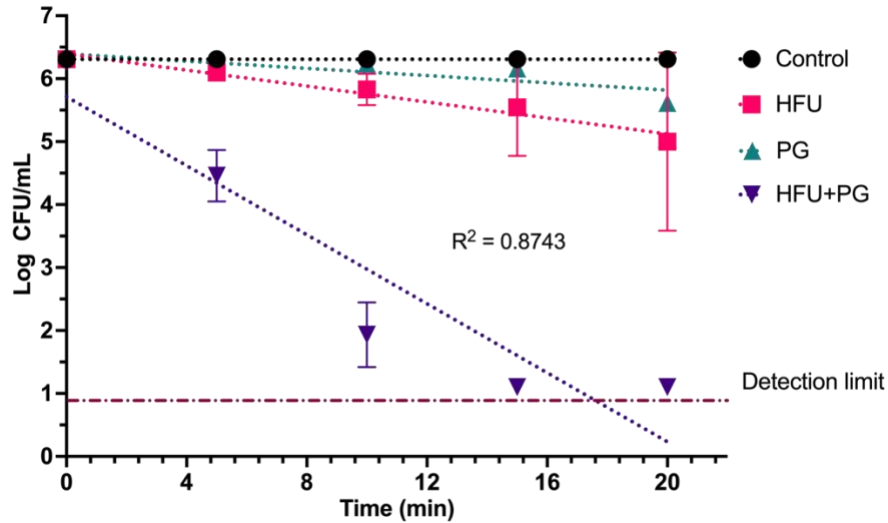


Fig. 3.3 Kinetic inactivation of *E. coli* O157:H7 (A) and *L. innocua* (B) in apple juice model with a pH value of 3.6: HFU – High-frequency ultrasound treatment, PG – Propyl gallate treatment, HFU+PG – Combined high-frequency ultrasound and PG treatment.

3.1.3. Synergistic effect measurement using isobologram

Based on isobologram analysis, the synergistic interaction between HFU and PG was evaluated. The *E. coli* O157:H7 was selected as a representative bacterium for the isobologram analysis. For the isobologram analysis (Fig. 4), the Y and X axes represent the treatment time required for 1, 2, and 5 log inactivation of inoculated bacteria using HFU treatment and PG (10 mM) incubation alone, respectively. The straight lines connecting the intercepts on the Y and X axes represent the additive effect of the treatments (theoretical prediction) for the same level of bacterial inactivation. The triangle and square dots represent the experimentally observed time required for achieving 1 log, 2 log, and 5 log inactivation of *E. coli* O157:H7 using the combined HFU+PG treatments. Results indicate that the HFU and PG combination was synergistic compared to individual treatments as the observed time was significantly lower than the theoretically predicted time for the additive effect of the treatments. Compared to the individual treatments, the combined treatments were ~ 16 times (250 minutes divided

by 15 minutes) faster than HFU alone and four times (60 minutes divided by 15 minutes) faster than PG alone.

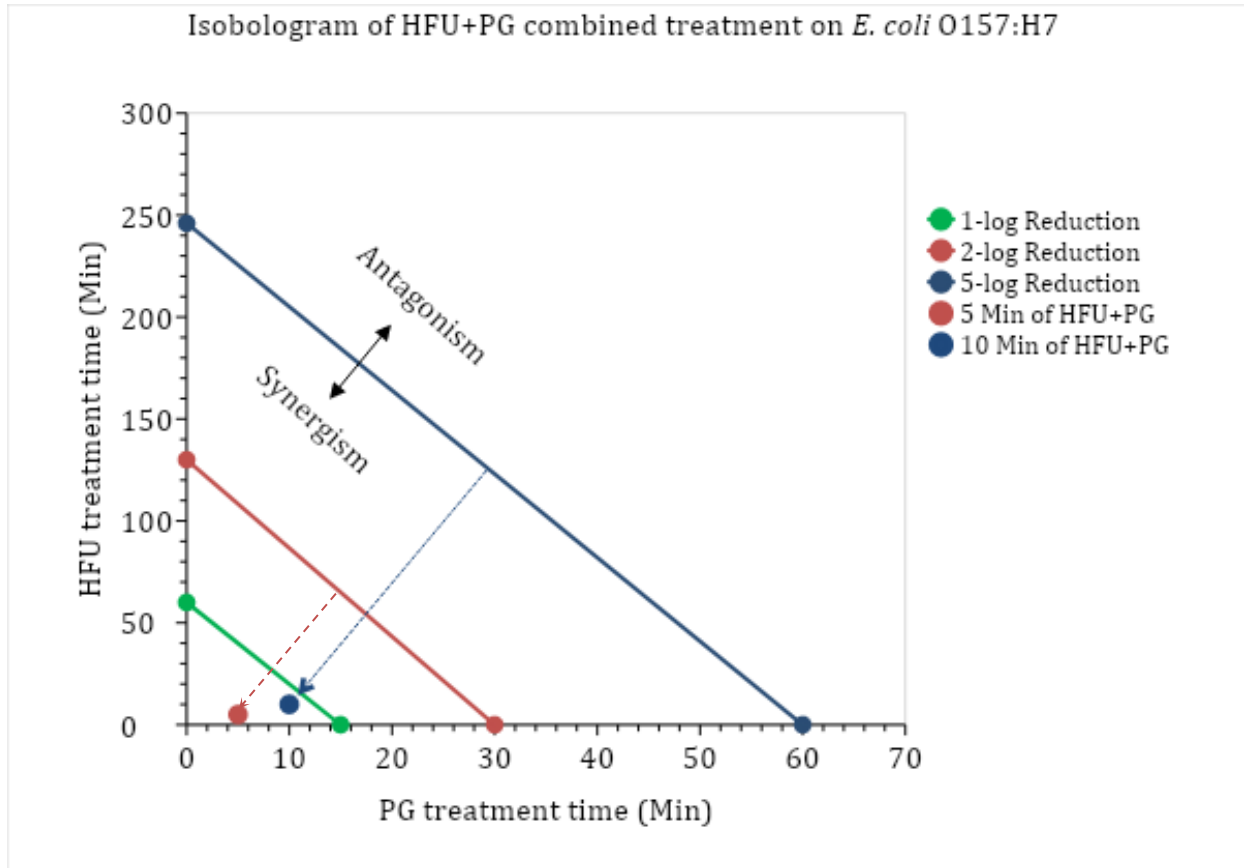


Fig. 3.4 Isobologram to demonstrate the synergistic effects of HFU and PG on *E. coli* O157:H7

inactivation. Color-coded lines were used to connect the treatment times of individual treatments of both HFU and PG, i.e., 1-log reduction - green line, 2-log reduction - red line, and 5-log inactivation - blue line. A synergistic treatment time of 5 minutes was adequate to generate at least 2 log inactivation. Thus, 5 min synergistic treatment time point was coded red and compared with the results of a 2-log reduction line. Similarly, a synergistic treatment time point of 10 min achieved 5 log inactivation and was coded blue to compare it with a 5-log reduction line. When the combined treatment point is below the desired log reduction line, it is a synergistic effect; otherwise, it is an antagonism effect.

3.2. Membrane damage of HFU treated bacteria

3.2.1. SEM observation of treated bacteria after SAT treatment

Fig. 5 and Fig. 6 reveal the morphological changes in *E. coli* O157:H7 and *L. innocua* cells after the ultrasound treatment using SEM imaging. After sonication treatment in the presence of PG for 10 minutes, most *E. coli* O157:H7 cells were physically damaged into fragments (Fig. 5-D). Heavily deformed cell envelopes and the effect of sonoporation were also observed. Moreover, the surface of *E. coli* O157:H7 cells shrank and retracted, likely caused by the leakage of intracellular material as a result of severe membrane damage. The untreated *E. coli* O157:H7 cells were rod-shaped with a smooth surface (Fig. 5-A). The *E. coli* O157:H7 cells, after incubation for 10 minutes with PG without the HFU (Fig. 5-C) and the HFU by itself showed some level of bacterial cell damage, but a significant part of the bacterial population retained its original shape.

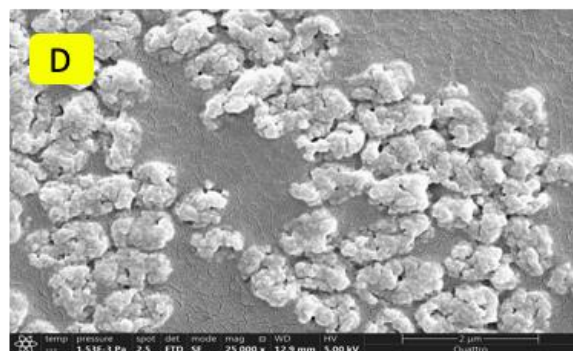
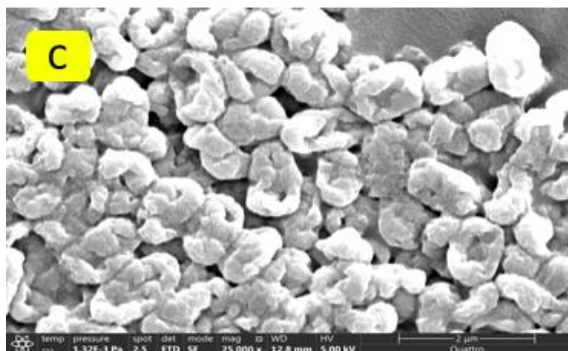
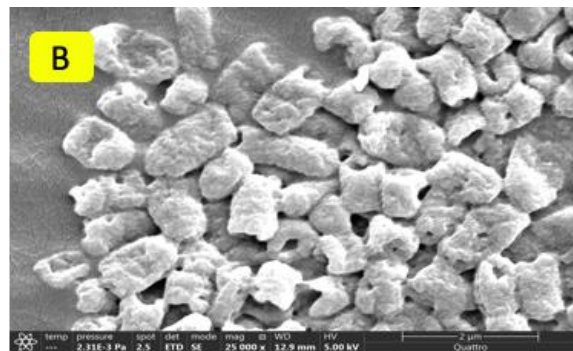
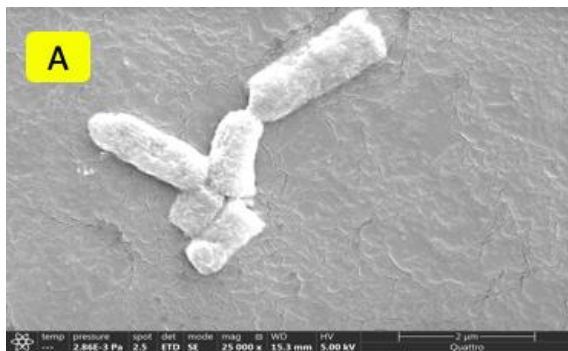


Fig. 3.5 Scanning electron microscope (SEM) images of *E. coli* O157:H7 cells as a function of selected treatments: the control sample (A), cells treated with the HFU for 10 minutes (B), cells incubated with PG for 10 minutes (C), cells treated with a combination of HFU+PG for 10 minutes (D).

In contrast, the combined HFU+PG treatments caused only a minor change in the morphology of *L. innocua* cells. After sonication in the presence of PG for 10 minutes, most *L. innocua* cells maintained the original cell morphology, but some damage on the cell surface was also visible (Fig. 6-D). After 20 minutes of the combined HFU+PG treatment, concave cell envelopes were observed, although the cell shape of *L. innocua* did not change (Fig. 6-D). The pore formation and localized rupture were not observed in *L. innocua* after the combined treatments in contrast to the results with *E. coli* O157:H7 cells after the combined treatment. Taken together, the results in Fig. 5 and 6 further confirm the higher susceptibility of the Gram-negative *E. coli* O157:H7 to the combined HFU+PG treatments than the Gram-positive *L. innocua*.

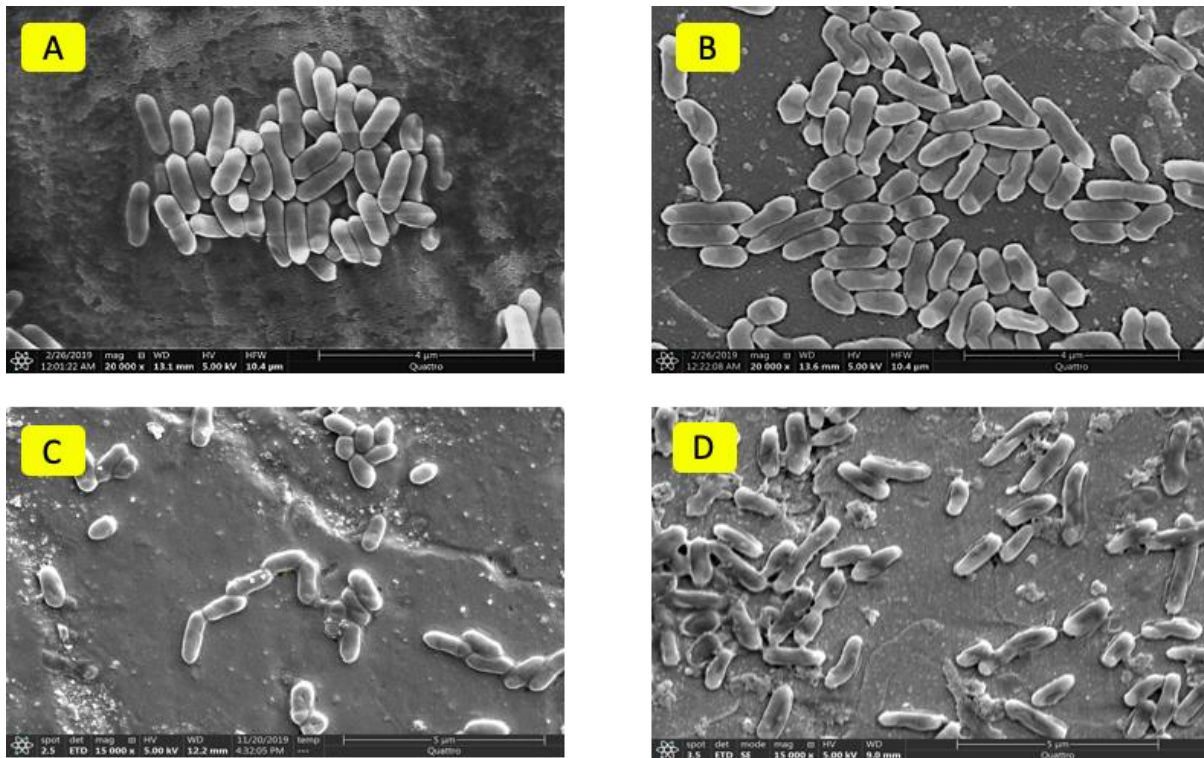


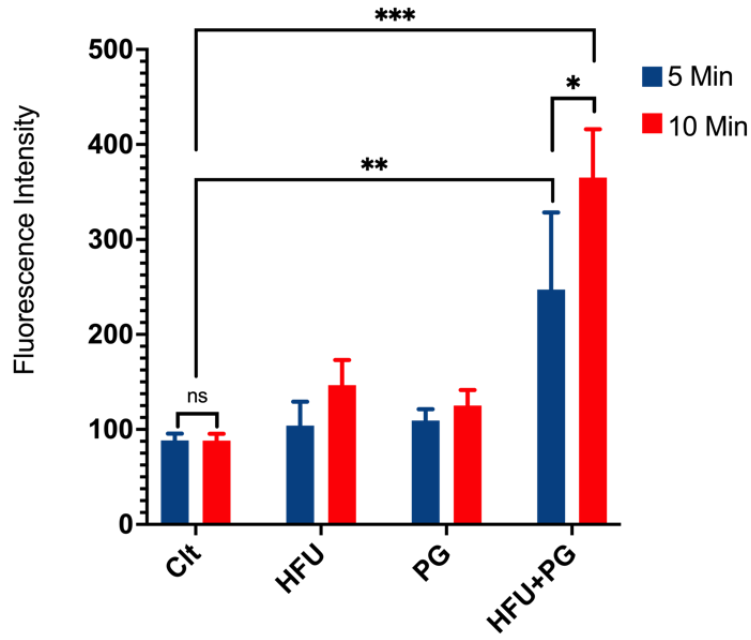
Fig. 3.6 Scanning electron microscope (SEM) images of *L. innocua* cells as a function of selected treatments: the control sample (A), cells treated with HFU for 20 minutes (B), cells incubated with PG for 20 minutes (C), cells treated with a combination of HFU+PG for 20 minutes (D).

3.2.2. PI measurement of membrane damage

To elucidate the role of bacterial membrane damage by the SAT, bacterial membrane damage was investigated using the membrane-impermeable nucleic acid binding PI dye. The results in Fig. 7 show changes in the PI dye fluorescence intensity as a result of increased permeation of the PI dye in bacterial cells with compromised membranes after the selected treatments. In the case of Gram-negative *E. coli* O157:H7, the combined HFU+PG treatment resulted in a significant increase in fluorescence intensity of PI labeled cells suggesting increased membrane permeability with the combined treatment. With an increase in treatment time, the combined HFU+PG treatment demonstrated a significant increase in membrane damage ($P < 0.05$). Meanwhile, PG or HFU *per se* did not show any significant differences between treatment times ($P > 0.05$). Treatment times of 5 and 10 min for this assay were selected based on the inactivation kinetics measurements in Fig. 2.

By contrast, in Gram-positive *L. innocua*, a significant change in PI signal was only detected after 20 minutes of the combined HFU+PG treatment ($P < 0.001$). The increase in the fluorescence signal of PI dye could be a result of inactivated cells, which have permeabilized membranes. These results also illustrate a significant difference between the membrane damage response of the Gram-positive and Gram-negative bacteria to the combined treatment.

A.



B.

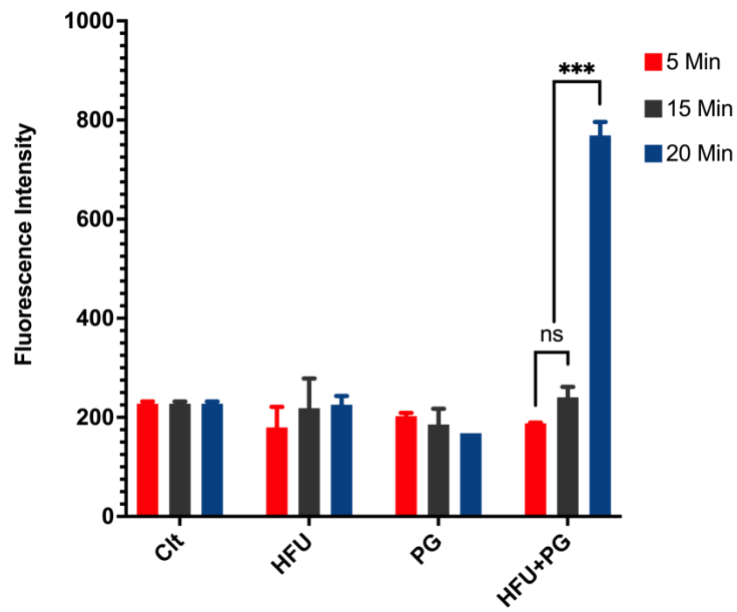


Fig. 3.7 PI dye assay to assess changes in the permeability of cell membrane for (a) *E. coli* O157:H7 and (b) *Listeria innocua* cells as a function of selected treatments: the control sample, cells treated with the

HFU, cells incubated with PG, cells treated with a combination of HFU+PG. Changes in the membrane permeability were assessed after 5 and 10 min of treatment for *E.coli* O157: H7 and after 5, 15, and 20 min of treatment for *L. innocua* cell membrane as a function of the following treatments (a) control cells; (b) HFU; (c) PG; treatment of *E. coli* O157:H7 (A) and *L. innocua* (B). Note: P values greater than 0.05 are reported as not significant, P values less than 0.05 are reported as one asterisk, P values less than 0.005 are reported as two asterisks and P values less than 0.001 are reported as three asterisks.

3.3. Oxidative damage measurement of the SAT treated bacteria

3.3.1. Extracellular ROS generation measurements

Fig. 8 demonstrates the generation of hydroxyl radical ($\text{HO}\cdot$) in an aqueous solution induced by HFU, PG, and HFU+PG treatments, respectively. The generation of hydroxyl radicals in the combined treatment of HFU+PG was significantly higher than either single treatment of HFU or PG. The HFU single treatment-induced hydroxyl radical generation while no hydroxyl radicals were generated by the addition of PG to an aqueous solution. The difference between the combined HFU+PG and HFU single treatment can be seen after 10 minutes of treatment time. After 45 minutes of treatment time, the levels of hydroxyl radicals generated by HFU+PG were 40% more than the level generated by the HFU treatment alone. These results indicate the sonosensitizing properties of PG.

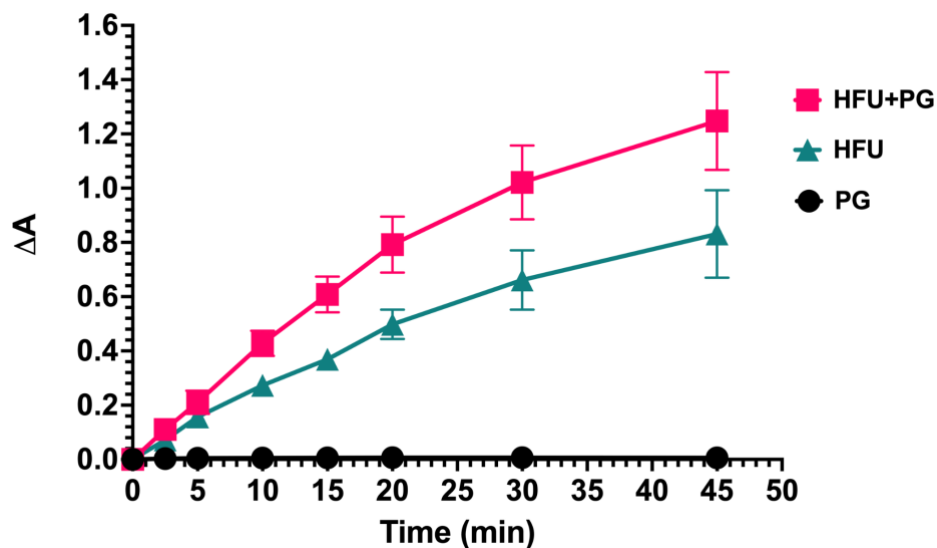


Fig. 3.8 RNO beaching assay to measure the production of extracellular hydroxyl radical $\text{HO}\cdot$ in aqueous solution as a function of time (0 - 45 min) with the following treatments: HFU – High-frequency ultrasound treatment, PG: Propyl gallate treatment, HFU+PG: Combined high-frequency ultrasound and PG treatment.

3.3.2. Antioxidant assay

To examine the role of ROS generation in the synergistic inactivation of bacteria, thiourea was selected as a radical scavenger (Fig. 9). Thiourea can quench both singlet oxygen and hydroxyl radicals (Davies et al., 2009; Farmer et al., 2006; Foti et al., 2012; Kohanski et al., 2010; Repine et al., 1981). Bacterial cells were incubated with thiourea before the treatments, as described in the materials and methods section. The bactericidal effect of sono-activated propyl gallate was impaired in the presence of thiourea. After 10 minutes of combined treatment, only 2 log CFU/mL reduction was observed with the synergistic treatment in the presence of thiourea. Meanwhile, the SAT treatment without thiourea resulted in a 5 log CFU reduction ($p < 0.01$). These results suggest a significant role of ROS in the synergistic inactivation of bacteria using a combination of HFU and PG treatments.

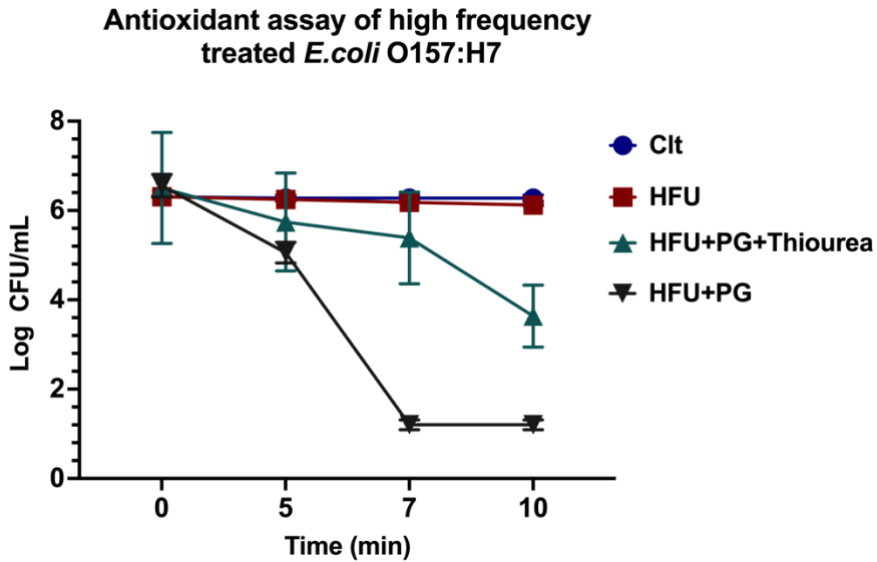


Fig. 3.9 The effect of the addition of thiourea (quencher of ROS) on the inactivation of *E. coli* O157:H7 with the selected treatments of HFU, PG, and HFU+PG, respectively. The total treatment time was 10 min.

3.3.3. Intracellular ROS generation measurements

Fig. 10 demonstrates reduction in the intracellular thiol content of *E. coli* O157:H7 as a result of intracellular oxidative stress. The combined HFU+PG treatment induced a 50% reduction in the initial intracellular thiol concentration after 5 minutes of treatment time. When the treatment time reached 10 minutes, a combined treatment of HFU+PG reduced 80% of the initial intracellular thiol concentration indicating a significant role of intracellular oxidative stress in bacterial inactivation. In addition, following treatment of HFU for 10 minutes, the intracellular thiol levels decreased by more than 50%, showing oxidative stress in HFU treated cells, while no significant change was observed in the intracellular thiol content with the PG treatment for both 5 and 10 minutes.

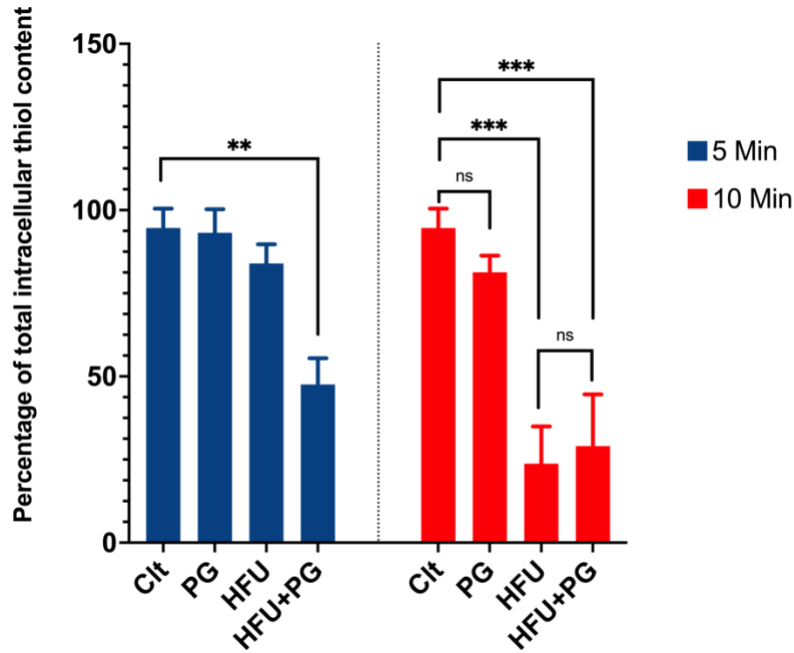


Fig. 3.10 Changes in the total intracellular thiol content of *E. coli* O157:H7 after 5 and 10 min of the selected treatments: control; cells treated with HFU; cells incubated with PG; and cells treated with a combined treatment of HFU+PG, respectively.

4. Discussion

4.1. The bacterial inactivation effectiveness of the combined HFU and PG

4.1.1. In DI water model

Results from Fig. 2 demonstrate the effectiveness of the combined HFU and PG treatment in reducing bacterial counts in water. The combination of a high frequency (1 MHz) and a low intensity (1.6 W/cm²) ultrasound with a water-soluble, colorless food grade antioxidant achieved more than 5 log inactivation of both the Gram-positive and the Gram-negative bacteria within 15 minutes of treatment time. This new approach provides several advantages over the conventional US processing, using low-frequency and high-intensity US for the inactivation of bacterial cells (Arroyo & Lyng, 2017; Ashokkumar, 2015). The level of inactivation of bacterial cells using these conventional approaches is relatively low

(less than 2 log inactivation), and often long treatment times are required for this activation (Barbosa-Cánovas & Rodríguez, 2002). Complementary to this conventional approach, several studies have evaluated the combination of chemical compounds with the high-frequency US to enhance the rate of inactivation of bacteria (Costley et al., 2017; Dadjour et al., 2006; Drakopoulou et al., 2009; Liu et al., 2011; Nakonechny et al., 2013; Pang et al., 2019; Pourhajibagher et al., 2020; Serpe & Giuntini, 2015; Tachibana et al., 2008; H. Wang et al., 2014; X. Wang et al., 2015, 2016; Xu et al., 2016; Zhuang et al., 2014). Most of the prior studies observed only an additive effect based on the combination of ultrasound and chemical compounds or inorganic nanoparticles, and many of these studies reported less than 3 log inactivation of target bacteria. Some of these studies also reported more than 5 log inactivation using a combination of HFU with a hydrophobic compound, curcumin, or a combination of HFU with peptide conjugated rose bengal to specifically target the delivery of the compound to the bacteria (Costley et al., 2017; Nakonechny et al., 2013; Nakonieczna et al., 2010; Pourhajibagher et al., 2020; H. Wang et al., 2014; X. Wang et al., 2015). In contrast to these prior studies (Costley et al., 2017; Nakonechny et al., 2013; Pourhajibagher et al., 2020; X. Wang et al., 2015), this current study is based on a high frequency (1 MHz) and low intensity (1.6 W/cm²) ultrasound in combination with a water-soluble, colorless food grade antioxidant achieved 5.5 log inactivation of both the Gram-positive and the Gram-negative bacteria within 15 minutes of treatment time. Using the culture-based methods, the limit of detection of bacteria in the aqueous solution was 10 CFU/mL. Thus, it is a relatively simple approach that can be adapted for diverse applications in food systems without significant constraints on the solubility and color properties of food products.

In clarified apple juice model

Pasteurization and sterilization are common thermal food processing technologies used in fruit juice processing, but the combination of time and temperature in these processes leads to the loss of

phytonutrients, organoleptic properties, and development of some other undesirable modifications in fruit juices (Aneja et al., 2014; Khandpur & Gogate, 2016; Vasantha Rupasinghe & Juan, 2012). Thus, there is a significant unmet need to develop non-thermal processing technologies in the beverage industry.

The results of this study illustrate the potential of ultrasound treatment to enhance the rate of inactivation of target bacteria in a model juice (commercial apple juice) and achieve more than 5-log inactivation of target *E. coli* O157:H7 and *L. innocua* cells within 15 min. These results highlight the significant improvement in inactivation efficiency compared to conventional US processing. For example, previous studies demonstrated the application of low frequency (20 – 25 kHz) and high-power density (500 - 100W/cm²) for an extended treatment time from 30 to 90 minutes to achieve less than 2 log bacterial inactivation (Abid et al., 2013; Jingfei & H. P. Vasantha, 2012; Khandpur & Gogate, 2016; Martínez-Flores et al., 2015; Zou et al., 2016). Moreover, the acidic condition of apple juice, pH 3.6 could result in a faster inactivation rate compared to the inactivation in DI water. In this case, the acidic pH could work additively with ultrasound treatment to inactivate target bacteria as described by Guerrero et al. (Guerrero et al., 2017). In brief, the synergistic combination of HFU and a food-grade antioxidant has the potential to achieve the targeted 5 log inactivation of the bacteria required for pasteurization of a juice product (FDA, 2021).

This approach can significantly improve both the quality of the fruit juices as well as reduce the energy required for processing. Further studies are required to characterize the scale-up of these synergistic processes, including uniformity of treatment, evaluate the role of diverse food matrices in influencing both uniformity and efficacy of the process, as well as the cost of developing ultrasonic reactors for synergistic food processing.

4.2. Membrane damage and ROS discussion

4.2.1. Membrane damage

Both the SEM and PI permeation studies illustrate the key role of membrane damage in the synergistic antimicrobial activity of a combination of HFU+PG for both the selected Gram-negative and the Gram-positive bacteria. In the SEM and PI permeation results, *E. coli* O157:H7 showed higher susceptibility to membrane damage and deformation compared to *L. innocua*. This result agrees with the higher rates of inactivation of *E. coli* O157:H7 cells compared to *L. innocua*. In contrast to these results, many of the previous studies have reported higher levels of inactivation of Gram-positive bacteria compared to Gram-negative cells (Nakonechny et al., 2013; Pang et al., 2020; Piyasena et al., 2003; Serpe & Giuntini, 2015; X. Wang et al., 2015). This has been attributed to the unique membrane structure of the gram-negative cells that may reduce the permeability of sonochemical agents and thus reduce the synergistic interactions between sonosensitizers and ultrasound treatment (Pang et al., 2020). However, in this study, the results suggest that PG by itself can induce changes in the membrane structure of *E. coli* O157:H7 cells, as observed in the SEM images. These structural changes introduced by PG in the lipid membranes have been recently characterized in our previous study (Nguyen et al., 2021) using liposomes. The results from this previous study suggest rapid partitioning of PG in the model lipid membranes. Upon interaction with a lipid membrane, PG can modify membrane properties by increasing permeation, membrane polarity, and fluidity (Boyd & Beveridge, 1981; del Valle et al., 2016; Strippoli et al., 2000; Q. Wang et al., 2017).

It is important to note that the membrane deformation induced by PG alone was not adequate for more than 2 log inactivation of bacteria, and the treated bacteria may recover from this damage occurred during culturing. These changes in the membrane structure can be further enhanced when PG treatment is combined with HFU, as observed in the SEM images (Fig. 5D). Thus, the enhanced

partitioning properties of PG in membranes may provide a unique advantage in increasing the susceptibility of the Gram-negative bacteria based on the synergistic interaction with the HFU.

4.3. ROS generation

The role of ROS for the inactivation of bacteria using a combination of sonosensitizers such as porphyrin, chlorin-e6, and rose bengal derivatives and the US has been suggested by previous studies (Costley et al., 2017; Dadjour et al., 2006; Giuntini et al., 2018; Guo et al., 2013; Nakonechny et al., 2013; Nakonieczna et al., 2010; Pang et al., 2016; Xu et al., 2016; Yumita et al., 2007). Among the diversity of ROS species, singlet oxygen ($^1\text{O}_2$) generation has been well documented for a combination of sonosensitizers such as porphyrin and rose bengal with ultrasound (Guo et al., 2013; Nakonieczna et al., 2018). In addition, Komori reported the generation of hydroxyl free radicals ($\text{HO}\cdot$) based on a combination of high-frequency ultrasound (2 MHz, 0.24 W/m²) and methylene blue (Komori et al., 2009). The results of this study illustrate that the combination of PG with HFU enhanced the generation of hydroxyl radicals (Fig. 8) that can induce oxidative stress in bacterial cells. To further confirm this hypothesis, the results outlined in Fig. 9 demonstrate the role of exogenous antioxidants in quenching the synergistic antimicrobial activity of HFU and PG. Thus, suggesting the role of ROS generation in the synergistic antimicrobial activity of the HFU and PG. These results were also supported by changes in the content of the intracellular thiol of bacterial cells following HFU and PG treatments, as shown in Fig. 10. In contrast to these results, our previous study demonstrated no significant contributions of oxidative stress in bacterial inactivation using a combination of low-frequency ultrasound (LFU) and PG (Nguyen et al., 2021). These findings are in agreement with other theoretical and experimental studies that indicate increased generation of ROS species with HFU processing compared to LFU (Ashokkumar, 2011; Ji et al., 2018). This increase in ROS with HFU has been attributed to a much stronger vibrational excitation of chemical species and enhanced cavitation at a higher frequency of US processing compared to low-frequency US (Ji et al., 2018; Pang et al., 2016). Furthermore, initial membrane damage/deformation

induced by PG can further enhance the rate of ROS generation upon exposure to HFU based on microbial response to exogenous stress. In our previous study, we observed that the membrane damage induced by LAE in combination with UV-A light irradiation significantly enhanced the level of oxidative stress generated in bacterial cells compared to UV-A treatment alone (Yang et al., 2019). This evidence supports the combined role of PG-induced membrane damage and HFU treatment in enhancing oxidative stress in cells. Further gene expression studies are required to understand the molecular response of cells under the cotreatment of HFU and PG.

Based on the aforementioned results, we summarize the overall mechanism of the enhanced bacterial inactivation of HFU+PG in figure 11. PG by itself is a membrane active compound that can easily penetrate a bacterial membrane bilayer structure. Upon exposure to HFU, PG generates both extra- and intracellular ROS, leading to oxidative damage. The combined membrane damage and oxidative stress resulted in enhanced bacterial inactivation compared to a single treatment of either HFU or PG.

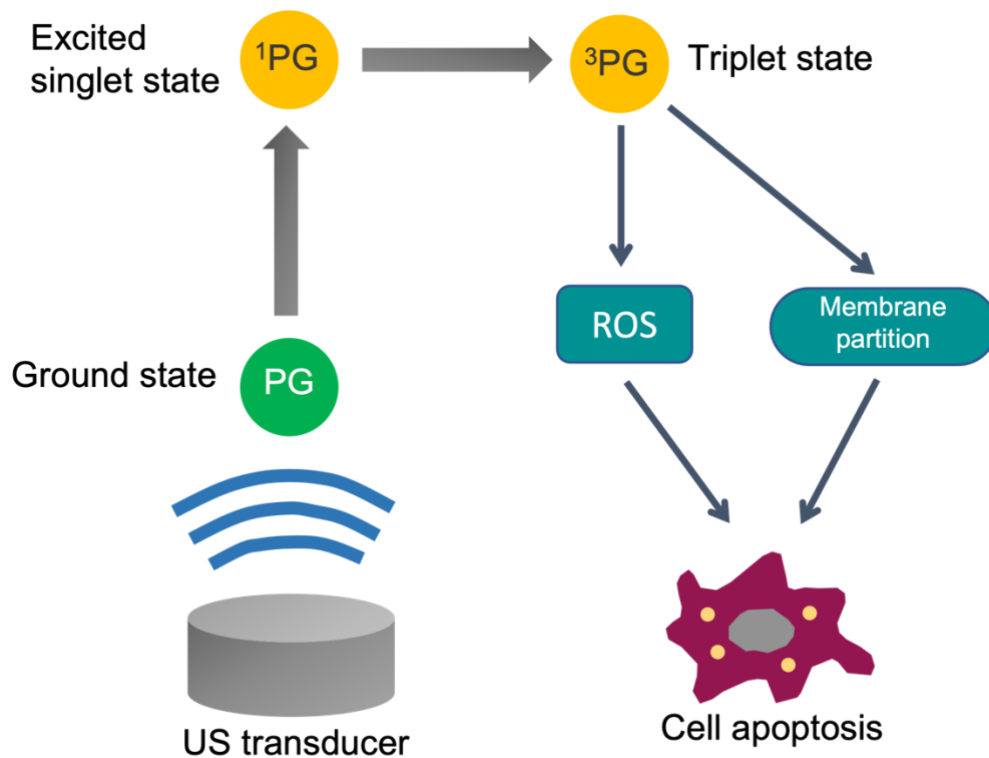


Fig. 3.11 Proposed mechanism of the synergistic inactivation of bacteria based on combined HFU and PG treatment. This enhanced inactivation is attributed to membrane damage and the generation of oxidative stress induced by the synergistic combination of HFU+PG.

5. Conclusions

The combination of HFU and PG synergistically enhanced the inactivation rate of the targeted Gram-negative *E. coli* O157:H7 and the Gram-positive *L. innocua*. The PI dye results together with SEM morphology analysis confirm the higher susceptibility of *E. coli* O157:H7 to the combined HFU + PG treatment than *L. innocua*. This study confirmed a higher level of membrane damage in SAT treated Gram-negative *E. coli* O157:H7 compared to *L. innocua*. Moreover, the generation of ROS from the combined HFU and PG was confirmed through the reduction of total intracellular thiol content and the quenching effect of the addition of free radical scavengers. The results obtained in this work provide a proof-of-concept of an alternative non-thermal food processing approach for the decontamination of juice products. Further research is needed to identify the causes of oxidative stress experienced by bacteria treated with SAT as well as the effectiveness and scalability of the combined HFU and PG for juice processing.

Acknowledgments

This project was supported by the Agriculture and Food Research Initiative by grant no. 2014-67017-21642 from the USDA National Institute of Food and Agriculture (USDA-NIFA) Program in Improving Food Quality (A1361) and by grant no. 2015-68003- 23411 from the USDA-NIFA Program Enhancing Food Safety through Improved Processing Technologies (A4131).

The *Escherichia coli* O157: H7 (ATCC 700728, Manassas, VA, USA) and *Listeria innocua* (ATCC 33090, Manassas, VA, USA) were kindly provided by Dr. Linda Harris and Dr. Trevor Suslow, respectively, at the University of California, Davis

Bibliography

- Abid, M., Jabbar, S., Wu, T., Hashim, M. M., Hu, B., Lei, S., Zhang, X., & Zeng, X. (2013). Effect of ultrasound on different quality parameters of apple juice. *Ultrasonics Sonochemistry*, *20*(5), 1182–1187. <https://doi.org/10.1016/j.ultsonch.2013.02.010>
- Alves, F., Pavarina, A. C., Mima, E. G. de O., McHale, A. P., & Callan, J. F. (2018). Antimicrobial sonodynamic and photodynamic therapies against *Candida albicans*. *Biofouling*, *34*(4), 357–367. <https://doi.org/10.1080/08927014.2018.1439935>
- Aneja, K. R., Dhiman, R., Aggarwal, N. K., & Aneja, A. (2014). Emerging preservation techniques for controlling spoilage and pathogenic microorganisms in fruit juices. *International Journal of Microbiology*, *2014*. <https://doi.org/10.1155/2014/758942>
- Arroyo, C., & Lyng, J. G. (2017). The Use of Ultrasound for the Inactivation of Microorganisms and Enzymes. In *Ultrasound in Food Processing* (pp. 255–286). John Wiley & Sons, Ltd. <https://doi.org/10.1002/9781118964156.ch9>
- Ashokkumar, M. (2011). The characterization of acoustic cavitation bubbles – An overview. *Ultrasonics Sonochemistry*, *18*(4), 864–872. <https://doi.org/10.1016/j.ultsonch.2010.11.016>
- Ashokkumar, M. (2015). Applications of ultrasound in food and bioprocessing. *Ultrasonics Sonochemistry*, *25*(1), 17–23. <https://doi.org/10.1016/j.ultsonch.2014.08.012>
- Bai, W. K., Shen, E., & Hu, B. (2012). Induction of the apoptosis of cancer cell by sonodynamic therapy: A review. *Chinese Journal of Cancer Research*, *24*(4), 368–373. <https://doi.org/10.1007/s11670-012-0277-6>
- Barbosa-Cánovas, G. V., & Rodríguez, J. J. (2002). Update on non-thermal food processing technologies: Pulsed electric field, high hydrostatic pressure, irradiation and ultrasound. *Food Australia*, *54*(11), 513–520.

- Bigelow, W. D., & Esty, J. R. (1920). The thermal death point in relation to typical thermophilic organisms. *Journal of Infectious Diseases*, *27*, 602–602.
- Borges, A., Ferreira, C., Saavedra, M. J., & Simões, M. (2013). Antibacterial Activity and Mode of Action of Ferulic and Gallic Acids Against Pathogenic Bacteria. *Microbial Drug Resistance*, *19*(4), 256–265. <https://doi.org/10.1089/mdr.2012.0244>
- Chen, H., Zhou, X., Gao, Y., Zheng, B., Tang, F., & Huang, J. (2014). Recent progress in development of new sonosensitizers for sonodynamic cancer therapy. *Drug Discovery Today*, *19*(4), 502–509. <https://doi.org/10.1016/J.DRUDIS.2014.01.010>
- Costley, D., Nesbitt, H., Ternan, N., Dooley, J., Huang, Y.-Y. Y., Hamblin, M. R., McHale, A. P., & Callan, J. F. (2017). Sonodynamic inactivation of Gram-positive and Gram-negative bacteria using a Rose Bengal–antimicrobial peptide conjugate. *International Journal of Antimicrobial Agents*, *49*(1), 31–36. <https://doi.org/10.1016/j.ijantimicag.2016.09.034>
- Dadjour, M. F., Ogino, C., Matsumura, S., Nakamura, S., & Shimizu, N. (2006). Disinfection of *Legionella pneumophila* by ultrasonic treatment with TiO₂. *Water Research*, *40*(6), 1137–1142. <https://doi.org/10.1016/j.watres.2005.12.047>
- Davies, B. W., Kohanski, M. A., Simmons, L. A., Winkler, J. A., Collins, J. J., & Walker, G. C. (2009). Hydroxyurea Induces Hydroxyl Radical-Mediated Cell Death in *Escherichia coli*. *Molecular Cell*, *36*(5), 845–860. <https://doi.org/10.1016/j.molcel.2009.11.024>
- De Oliveira, E. F., Cossu, A., Tikekar, R. V., Nitin, N., Björkroth, J., Oliveira, E. F. de, Cossu, A., Tikekar, R. V., & Nitin, N. (2017). Enhanced Antimicrobial Activity Based on a Synergistic Combination of Sublethal Levels of Stresses Induced by UV-A Light and Organic Acids. *Applied and Environmental Microbiology*, *83*(11), AEM.00383-17. <https://doi.org/10.1128/AEM.00383-17>

- del Valle, P., García-Armesto, M. R., de Arriaga, D., González-Donquiles, C., Rodríguez-Fernández, P., & Rúa, J. (2016). Antimicrobial activity of kaempferol and resveratrol in binary combinations with parabens or propyl gallate against *Enterococcus faecalis*. *Food Control*, *61*, 213–220.
<https://doi.org/10.1016/j.foodcont.2015.10.001>
- Drakopoulou, S., Terzakis, S., Fountoulakis, M. S., Mantzavinos, D., & Manios, T. (2009). Ultrasound-induced inactivation of gram-negative and gram-positive bacteria in secondary treated municipal wastewater. *Ultrasonics Sonochemistry*, *16*(5), 629–634.
<https://doi.org/10.1016/J.ULTSONCH.2008.11.011>
- Farmer, D., Burcham, P., & Marin, P. (2006). The ability of thiourea to scavenge hydrogen peroxide and hydroxyl radicals during the intra-coronal bleaching of bloodstained root-filled teeth. *Australian Dental Journal*, *51*(2), 146–152. <https://doi.org/10.1111/j.1834-7819.2006.tb00418.x>
- Foti, J. J., Devadoss, B., Winkler, J., Collins, J., & Walker, G. (2012). Oxidation of the Guanine Nucleotide Pool Underlies Cell Death by Bactericidal Antibiotics. *Science*, *336*(April), 315–319.
- Geeraerd, A. H., Valdramidis, V. P., & Van Impe, J. F. (2005). GlnaFiT, a freeware tool to assess non-log-linear microbial survivor curves. *International Journal of Food Microbiology*, *102*(1), 95–105.
<https://doi.org/10.1016/j.ijfoodmicro.2004.11.038>
- Giuntini, F., Foglietta, F., Marucco, A. M., Troia, A., Dezhkunov, N. V., Pozzoli, A., Durando, G., Fenoglio, I., Serpe, L., & Canaparo, R. (2018). Insight into ultrasound-mediated reactive oxygen species generation by various metal-porphyrin complexes. *Free Radical Biology and Medicine*, *121*, 190–201. <https://doi.org/10.1016/j.freeradbiomed.2018.05.002>
- Guerrero, S. N., Ferrario, M., Schenk, M., & Carrillo, M. G. (2017). Hurdle Technology Using Ultrasound for Food Preservation. *Ultrasound: Advances for Food Processing and Preservation*, 39–99.
<https://doi.org/10.1016/B978-0-12-804581-7.00003-8>

- Guo, S., Sun, X., Cheng, J., Xu, H., Dan, J., Shen, J., Zhou, Q., Zhang, Y., Meng, L., Cao, W., & Tian, Y. (2013). Apoptosis of THP-1 macrophages induced by protoporphyrin IX-mediated sonodynamic therapy. *International Journal of Nanomedicine*, *8*, 2239–2246.
<https://doi.org/10.2147/IJN.S43717>
- Hirofumi Shibata, K. K., Ryo Katsuyama, Kazuyoshi Kawazoe. (2016). Alkyl Gallates, Intensifiers of β -Lactam Susceptibility in Methicillin-Resistant *Staphylococcus aureus*. *49(2)*, 3018–3022.
<https://doi.org/10.1128/AAC.49.2.549>
- Holland-Letz, T., Gunkel, N., Amtmann, E., & Kopp-Schneider, A. (2018). Parametric modeling and optimal experimental designs for estimating isobolograms for drug interactions in toxicology. *Journal of Biopharmaceutical Statistics*, *28(4)*, 763–777.
<https://doi.org/10.1080/10543406.2017.1397005>
- Ji, R., Pflieger, R., Viot, M., & Nikitenko, S. I. (2018). Multibubble Sonochemistry and Sonoluminescence at 100 kHz: The Missing Link between Low- and High-Frequency Ultrasound. *The Journal of Physical Chemistry B*, *122(27)*, 6989–6994. <https://doi.org/10.1021/acs.jpccb.8b04267>
- Jingfei, G., & H. P. Vasantha, R. (2012). Nutritional, Physicochemical and Microbial Quality of Ultrasound-Treated Apple-Carrot Juice Blends. *Food and Nutrition Sciences*, *2012*.
<https://doi.org/10.4236/fns.2012.32031>
- Khandpur, P., & Gogate, P. R. (2016). Evaluation of ultrasound based sterilization approaches in terms of shelf life and quality parameters of fruit and vegetable juices. *Ultrasonics Sonochemistry*, *29*, 337–353. <https://doi.org/10.1016/j.ultsonch.2015.10.008>
- Kohanski, M. A., DePristo, M. A., & Collins, J. J. (2010). Sublethal Antibiotic Treatment Leads to Multidrug Resistance via Radical-Induced Mutagenesis. *Molecular Cell*, *37(3)*, 311–320.
<https://doi.org/10.1016/j.molcel.2010.01.003>

- Komori, C., Okada, K., Kawamura, K., Chida, S., & Suzuki, T. (2009). The Sonodynamic Antitumor Effect of Methylene Blue on Sarcoma180 Cells In Vitro. *Anticancer Research*, 29(6), 2411–2415.
<https://ar.iiarjournals.org/content/29/6/2411>
- Kundi, H., Ates, I., Kiziltunc, E., Cetin, M., Cicekcioglu, H., Neselioglu, S., Erel, O., & Ornek, E. (2015). A novel oxidative stress marker in acute myocardial infarction; Thiol/disulphide homeostasis. *American Journal of Emergency Medicine*, 33(11), 1567–1571.
<https://doi.org/10.1016/j.ajem.2015.06.016>
- Liu, B., Wang, D.-J., Liu, B.-M., Wang, X., He, L.-L., Wang, J., & Xu, S.-K. (2011). *The influence of ultrasound on the fluoroquinolones antibacterial activity.*
<https://doi.org/10.1016/j.ultsonch.2011.02.001>
- Lou, Z., Li, P., Sunz, X., Yang, S., Wang, B., & Han, K. (2013). A fluorescent probe for rapid detection of thiols and imaging of thiols reducing repair and H₂O₂ oxidative stress cycles in living cells. *Chemical Communications*, 49(4), 391–393. <https://doi.org/10.1039/c2cc36839k>
- Markovsky, E., Baabur-Cohen, H., & Satchi-Fainaro, R. (2014). Anticancer polymeric nanomedicine bearing synergistic drug combination is superior to a mixture of individually-conjugated drugs. *Journal of Controlled Release*, 187, 145–157. <https://doi.org/10.1016/j.jconrel.2014.05.025>
- Martínez-Flores, H. E., Garnica-Romo, Ma. G., Bermúdez-Aguirre, D., Pokhrel, P. R., & Barbosa-Cánovas, G. V. (2015). Physico-chemical parameters, bioactive compounds and microbial quality of thermo-sonicated carrot juice during storage. *Food Chemistry*, 172, 650–656.
<https://doi.org/10.1016/j.foodchem.2014.09.072>
- Nakamura, K., Ishiyama, K., Sheng, H., Ikai, H., Kanno, T., & Niwano, Y. (2015). Bactericidal Activity and Mechanism of Photoirradiated Polyphenols against Gram-Positive and -Negative Bacteria. *Journal of Agricultural and Food Chemistry*, 63(35), 7707–7713.
<https://doi.org/10.1021/jf5058588>

- Nakonechny, F., Nisnevitch, M., Nitzan, Y., & Nisnevitch, M. (2013). Sonodynamic Excitation of Rose Bengal for Eradication of Gram-Positive and Gram-Negative Bacteria. *BioMed Research International*, 2013. <https://doi.org/10.1155/2013/684930>
- Nakoneczna, J., Michta, E., Rybicka, M., Grinholc, M., Gwizdek-Wiśniewska, A., & Bielawski, K. P. (2010). Superoxide dismutase is upregulated in Staphylococcus aureus following protoporphyrin-mediated photodynamic inactivation and does not directly influence the response to photodynamic treatment. *BMC Microbiology*, 10, 323–323. <https://doi.org/10.1186/1471-2180-10-323>
- Nakoneczna, J., Wolnikowska, K., Ogonowska, P., Neubauer, D., Bernat, A., & Kamysz, W. (2018). Rose bengal-mediated photoinactivation of multidrug resistant pseudomonas aeruginosa is enhanced in the presence of antimicrobial peptides. *Frontiers in Microbiology*, 9(AUG). <https://doi.org/10.3389/fmicb.2018.01949>
- Nguyen, C., Rai, R., Yang, X., Tikekar, R. V., & Nitin, N. (2021). Synergistic inactivation of bacteria based on a combination of low frequency, low-intensity ultrasound and a food grade antioxidant. *Ultrasonics Sonochemistry*, 74, 105567. <https://doi.org/10.1016/j.ultsonch.2021.105567>
- Pang, X., Li, D., Zhu, J., Cheng, J., & Liu, G. (2020). Beyond Antibiotics: Photo/Sonodynamic Approaches for Bacterial Theranostics. *Nano-Micro Letters*, 12(1), 1–23. <https://doi.org/10.1007/s40820-020-00485-3>
- Pang, X., Xiao, Q., Cheng, Y., Ren, E., Lian, L., Zhang, Y., Gao, H., Wang, X., Leung, W., Chen, X., Liu, G., & Xu, C. (2019). Bacteria-Responsive Nanoliposomes as Smart Sonotheranostics for Multidrug Resistant Bacterial Infections. *ACS Nano*, 13(2), 2427–2438. <https://doi.org/10.1021/acsnano.8b09336>

- Pang, X., Xu, C., Jiang, Y., Xiao, Q., & Leung, A. W. (2016). Natural products in the discovery of novel sonosensitizers. *Pharmacology & Therapeutics*, *162*, 144–151.
<https://doi.org/10.1016/J.PHARMTHERA.2015.12.004>
- Pedraza-Chaverri, J., Barrera, D., Maldonado, P. D., Chirino, Y. I., Macías-Ruvalcaba, N. A., Medina-Campos, O. N., Castro, L., Salcedo, M. I., & Hernández-Pando, R. (2004). S-allylmercaptocysteine scavenges hydroxyl radical and singlet oxygen in vitro and attenuates gentamicin-induced oxidative and nitrosative stress and renal damage in vivo. *BMC Clinical Pharmacology*, *4*(1), 5.
<https://doi.org/10.1186/1472-6904-4-5>
- Piyasena, P., Mohareb, E., & McKellar, R. C. (2003). Inactivation of microbes using ultrasound: A review. *International Journal of Food Microbiology*, *87*(3), 207–216. [https://doi.org/10.1016/S0168-1605\(03\)00075-8](https://doi.org/10.1016/S0168-1605(03)00075-8)
- Pourhajibagher, M., Rahimi esboei, B., Hodjat, M., & Bahador, A. (2020). Sonodynamic excitation of nanomicelle curcumin for eradication of *Streptococcus mutans* under sonodynamic antimicrobial chemotherapy: Enhanced anti-caries activity of nanomicelle curcumin. *Photodiagnosis and Photodynamic Therapy*, *30*, 101780.
<https://doi.org/10.1016/j.pdpdt.2020.101780>
- Repine, J. E., Fox, R. B., & Berger, E. M. (1981). Hydrogen peroxide kills *Staphylococcus aureus* by reacting with staphylococcal iron to form hydroxyl radical. *Journal of Biological Chemistry*, *256*(14), 7094–7096.
- Serpe, L., & Giuntini, F. (2015). Sonodynamic antimicrobial chemotherapy: First steps towards a sound approach for microbe inactivation. *Journal of Photochemistry and Photobiology B: Biology*, *150*, 44–49. <https://doi.org/10.1016/J.JPHOTOBIO.2015.05.012>

- Shibata, H., Nakano, T., Parvez, M. A. K., Furukawa, Y., Tomoishi, A., Niimi, S., Arakaki, N., & Higuti, T. (2009). Triple combinations of lower and longer alkyl gallates and oxacillin improve antibiotic synergy against methicillin-resistant *Staphylococcus aureus*. *Antimicrobial Agents and Chemotherapy*, *53*(5), 2218–2220. <https://doi.org/10.1128/AAC.00829-08>
- Simonsen, M. E., Muff, J., Bennedsen, L. R., Kowalski, K. P., & Sjøgaard, E. G. (2010). Photocatalytic bleaching of p-nitrosodimethylaniline and a comparison to the performance of other AOP technologies. *Journal of Photochemistry and Photobiology A: Chemistry*, *216*(2–3), 244–249. <https://doi.org/10.1016/j.jphotochem.2010.07.008>
- Strippoli, V., D'auria, F. D., Tecca, M., Callari, A., & Simonetti, G. (2000). Propyl gallate increases in vitro antifungal imidazole activity against *Candida albicans*. In *International Journal of Antimicrobial Agents* (No. 09248579/00; Vol. 16, pp. 73–76). www.ischemo.org
- Tachibana, K., Feril, L. B., & Ikeda-Dantsuji, Y. (2008). Sonodynamic therapy. *Ultrasonics*, *48*(4), 253–259. <https://doi.org/10.1016/j.ultras.2008.02.003>
- Takai, E., Hirano, A., & Shiraki, K. (2011). Effects of alkyl chain length of gallate on self-association and membrane binding. *Journal of Biochemistry*, *150*(2), 165–171. <https://doi.org/10.1093/jb/mvr048>
- Vasantha Rupasinghe, H. P., & Juan, L. (2012). Emerging Preservation Methods for Fruit Juices and Beverages. *Food Additive*, May 2014. <https://doi.org/10.5772/32148>
- Wang, H., Wang, X., Zhang, S., Wang, P., Zhang, K., & Liu, Q. (2014). Sinoporphyrin sodium, a novel sensitizer, triggers mitochondrial-dependent apoptosis in ECA-109 cells via production of reactive oxygen species. *International Journal of Nanomedicine*, *9*(1), 3077–3090. <https://doi.org/10.2147/IJN.S59302>

- Wang, Q., De Oliveira, E. F., Alborzi, S., Bastarrachea, L. J., & Tikekar, R. V. (2017). On mechanism behind UV-A light enhanced antibacterial activity of gallic acid and propyl gallate against *Escherichia coli* O157:H7. *Scientific Reports*, 7(1), 1–11. <https://doi.org/10.1038/s41598-017-08449-1>
- Wang, X., Ip, M., Leung, A. W., Wang, P., Zhang, H., Hua, H., & Xu, C. (2016). Sonodynamic action of hypocrellin B on methicillin-resistant *Staphylococcus aureus*. *Ultrasonics*, 65, 137–144. <https://doi.org/10.1016/j.ultras.2015.10.008>
- Wang, X., Ip, M., Leung, A. W., Yang, Z., Wang, P., Zhang, B., Ip, S., & Xu, C. (2015). Sonodynamic action of curcumin on foodborne bacteria *Bacillus cereus* and *Escherichia coli*. *Ultrasonics*, 62, 75–79. <https://doi.org/10.1016/j.ultras.2015.05.003>
- Xu, C., Dong, J., Ip, M., Wang, X., & Leung, A. W. (2016). Sonodynamic action of chlorin e6 on *Staphylococcus aureus* and *Escherichia coli*. *Ultrasonics*, 64, 54–57. <https://doi.org/10.1016/j.ultras.2015.07.010>
- Yang, X., Rai, R., Huu, C. N., & Nitin, N. (2019). *Synergistic Antimicrobial Activity by Light or Thermal Treatment and Lauric Arginate: Membrane Damage and Oxidative Stress*. <https://doi.org/10.1128/AEM.01033-19>
- Zhuang, D., Hou, C., Bi, L., Han, J., Hao, Y., Cao, W., & Zhou, Q. (2014). Sonodynamic effects of hematoporphyrin monomethyl ether on *Staphylococcus aureus* in vitro. *FEMS Microbiology Letters*, 361(2), 174–180. <https://doi.org/10.1111/1574-6968.12628>
- Zou, Y., Jiang, A., Zou, Y., & Jiang, A. (2016). Effect of ultrasound treatment on quality and microbial load of carrot juice. *Food Science and Technology*, 36(1), 111–115. <https://doi.org/10.1590/1678-457X.0061>

Chapter 4

Synergistic Treatment of *L. innocua* and Multispecies Biofilms Using Sonodynamic Antimicrobial

Treatment with a Food Grade Compound

Cuong Nguyen Huu^a, Rohan V. Tikekar^b, Nitin Nitin^{a, c}

^a Department of Food Science and Technology, University of California, Davis, CA, USA.

^b Department of Nutrition and Food Science, University of Maryland, College Park, MD, USA.

^c Department of Biological and Agricultural Engineering, University of California, Davis, CA, USA.

Address correspondence to Nitin Nitin, nnitin@ucdavis.edu, Robert Mondavi Institute South, Room 2221, Hilgard Ln, Davis, CA 95616

Keywords: High-frequency ultrasound, propyl gallate, sonodynamic antimicrobial treatment, synergistic antimicrobial treatment, multispecies biofilm

Abstract

The study evaluates the effects of a synergistic antimicrobial combination of high-frequency ultrasounds (HFU) and a food-grade antioxidant, propyl gallate (PG), against mono-species biofilms from a gram-positive bacterium (*Listeria innocua*) and multispecies biofilms formed using a raw milk sample in combination with *Listeria innocua*. Combined treatment of HFU + PG significantly (more than 5 log CFU/mL, $P < 0.05$) enhanced the inactivation of both *L. innocua* and multispecies biofilm as compared to single treatments of HFU or PG, after 30 minutes of treatment time. Furthermore, the combined treatments also significantly improved the detachment of bacteria from the biofilm matrix (approximately 80%, $p < 0.05$) and subsequently led to the inactivation of the dispersed planktonic bacteria from both biofilm models (over 5 log CFU/mL, $P < 0.05$). SEM-based morphological analysis shows a detrimental effect of the combined HFU + PG treatments on the biofilm's matrix. Additionally, HFU + PG significantly suppressed the metabolic activity of biofilms in comparison to HFU or PG single treatments. Overall, the study illustrates the synergistic inactivation of biofilm as well as enhanced detachment and metabolic activity suppression using the combination of HFU + PG. This study demonstrates the potential use of high-frequency ultrasound in combination with a food-grade compound for enhanced sanitation of food contact surfaces and to improve the inactivation of bacterial biofilms.

1. Introduction

Biofilm formation and persistence in a food environment are favored due to a combination of biological, physical, and chemical factors (Araújo et al., 2011; Azeredo et al., 2017). Biological factors that favor the formation and persistence of biofilms include the presence of multiple microbial species and the biological response of microbes to environmental factors (Abdallah et al., 2014; Carrascosa et al., 2021). The biological response may result in changes in motility and surface hydrophobicity of microbes, activation of prophage elements (Abdallah et al., 2014), and expression of ECM components such as curli and bacterial cellulose (Carrascosa et al., 2021). The key physical factors of the environment that affect the forming of biofilm include the diversity of physicochemical properties, the surface roughness of food contact materials, wear and tear at specific locations on these surfaces, joints, and the lack of sanitary design in legacy food processing equipment (Winkelstroter, 2015). The major chemical factors include the presence of food biopolymers and essential nutrients that can support both the attachment and persistence of microbes on surfaces (Zhao et al., 2017a). Thus, the combination of biological, chemical, and physical factors in a food production environment can enable the formation of robust multispecies biofilms that can resist removal and sanitation.

Biofilm formation and its persistence on food contact surfaces are key risk factors for the safety of food products (Marchand et al., 2012). To address the food safety risks due to biofilm formation, sanitation practices in the food industry have focused on an extensive combination of mechanical and chemical methods to remove biofilms and inactivate microbes in a biofilm matrix (Zhao et al., 2017b). Mechanical treatments, such as brushing, scrubbing, flushing, etc. are also commonly used in the food industry (Yu et al., 2020). For example, high-pressure washing is normally applied to flush surfaces of equipment and floors. Although these approaches are effective in improving the hygiene of the processing facility, their effectiveness can be limited in removing biofilms that may form in crevices and

cracks on the surfaces. Further without adequate sanitizers, some of these processes may lead to the dispersal of microbes (Branck et al., 2017; Wille & Coenye, 2020).

For the removal and inactivation of biofilms, chemical sanitizers are commonly used in the food industry with and without mechanical scrubbing. Common disinfectants include chlorine, ozone, peracetic acid, and quaternary ammonium compounds (Araújo et al., 2011; Bridier et al., 2011), with chlorine being the most widely employed compound against biofilm. (Folsom & Frank, 2006; Zhu et al., 2020). However, the use of these sanitizers has limitations. The corrosive, flammable, or strong oxidizing properties of these conventional sanitizers result in a significant impact on the safety of the workforce (Galié et al., 2018). Similarly, reactions of conventional sanitizers such as chlorine with natural organic matter can result in the formation of carcinogenic halogenated disinfection by-products (DBP), like trihalomethanes (THMs) and haloacetic acids (HAAs) (Hua & Reckhow, 2007). Additionally, the residue of these conventional sanitizers in spent waters can impact the environment (Ölmez & Kretzschmar, 2009). With extensive use of sanitizers, especially chlorine-based disinfectant, studies have reported the development of potential resistance in bacterial biofilms against conventional chlorine treatment (Araújo et al., 2011; Bridier et al., 2011; Zhu et al., 2020). Ryu *et al.* (Ryu & Beuchat, 2005) reported an enhanced resistant of biofilm formed by curli producing *E. coli* O157:H7 strain biofilm to chlorine treatment up to 200 mg/mL and 5 minutes of treatment time. Folsom *et al.* (Folsom & Frank, 2006) reported a significant higher level of resistant of 11 subtype of *Listeria monocytogenes* strain against chlorine treatment up to 60 ppm compared to planktonic bacteria of the same subtype.

To address some of these limitations, low-frequency ultrasound (US) has been evaluated as a process intensification technology in combination with chemical sanitizers such as sodium hypochlorite, both to enhance the rate of removal of biofilms and efficiency of removal and inactivation of biofilms (Bang et al., 2017; Baumann et al., 2009; Berrang et al., 2008; Lee et al., 2014; Sagong et al., 2011). The rate of removal of biofilm may be enhanced by the hydrodynamic cavitation effects of the US process. In

addition, the US may enhance the inactivation of bacteria in a biofilm both by improving their dispersal in sanitizer solution as well as enhancing the rate of mass transport of chemicals to the biofilm. In these applications, most of the studies have focused on low-frequency US (20 to 40 kHz) and high-intensity US (100 W/cm² to 750 W/cm²) to achieve enhanced removal of microbes from biofilms (Yu et al., 2020). Despite the use of high-intensity US, the enhancement achieved by the combination of the US and conventional sanitizers is limited to 2 log CFU/ cm² (Abdallah et al., 2014; Bang et al., 2017; Carmen et al., 2004, 2005; Dong et al., 2013). Furthermore, non-uniform removal of biofilm from the surface with the US is a potential limitation as it can lead to the re-growth of biofilm (Yu et al., 2020). In addition to the limitations of using conventional sanitizers, the combination of high intensity and the low-frequency US with chemical sanitizers can result in potential damage to the equipment by extensive cavitation and the corrosive action of sanitizers. Moreover, the power level of high-intensity ultrasound treatment in previous studies ranged from 100 W/cm² to 750 W/cm², which could potentially increase the utility cost for the food industry over time. Thus, there is an unmet need to improve the efficacy of the combined treatment of US and chemicals for the inactivation of bacteria in biofilms while reducing the impact of these treatments on the environment, utility cost, and potential damage to the food contact surface.

To address some of these limitations, this study evaluated the synergistic combination of low power high-frequency US (1 MHz, 1.6 W/cm²) and food-grade antioxidants to achieve removal and inactivation of *L. innocua* and multispecies biofilms, an approach that is known as sonodynamic antimicrobial treatment or SAT. High-frequency US with low intensity was selected to reduce the risk of mechanical damage to the equipment and promote deeper US penetration (Fan et al., 2021). The synergistic combination of high-frequency US with food-grade polyphenolic antioxidants (propyl gallate, PG) was selected based on the results of our previous study that illustrated its potential to synergistically enhance the inactivation of planktonic cells (Nguyen et al., 2021). For the formation of biofilms, we selected two model systems. In the first approach, biofilms were formed using a surrogate of a

foodborne pathogenic strain, *Listeria innocua*. In the second approach, the biofilms were formed by the combination of the selected *Listeria* strain with commensal microbes from raw milk. This approach was selected to mimic some of the conditions in the food industry, such as biofilm formation in the dairy industry (Marchand et al., 2012; Oliveira et al., 2019; Weiler et al., 2013), where multiple microbes from environmental or food sources may combine with foodborne pathogens to form a problematic multispecies biofilm. In addition, the presence of food components such as milk proteins can condition the food contact surface to promote the adhesion and deposition of microbes on the food contact surface (Marchand et al., 2012; Weber et al., 2019). Stainless steel 304-grade coupons were used as a model food contact surface to form biofilms. In summary, this study illustrates the application of high-frequency ultrasound and its synergistic combination with a food-grade antioxidant to inactivate mono and multispecies biofilms on a model food contact surface.

2. Material And Methods

2.1. Material

Propyl Gallate (PG), was purchased from Invitrogen by Thermo Fisher Scientific (Waltham, MA, USA). Luria-Bertani (LB) broth, Tryptic Soy Broth (TSB), Tryptic Soy Agar (TSA), Phosphate-buffered Saline (PBS), and Tris-hydrochloride (1 M; Tris-HCl) were purchased from Fisher BioReagents (Pittsburgh, PA, USA). Ultrapure water was obtained using a Milli-Q filtration system (EDM Millipore; Billerica, MA, USA).

2.2. Study design

To investigate synergistic combinations of the combined HFU and PG treatment for the inactivation of *L. innocua* biofilm and multispecies biofilm of *L. innocua* with commensal microbes from raw milk, the sample size was determined using a power analysis. For this analysis, the following parameters were selected: number of treatment groups = 4, significance level = 0.05, power level = 0.8

and f value = 1.2. Based on the power analysis, a sample size of $n = 3$ for each treatment group was determined.

Briefly, each SS coupon that has either *L. innocua* or multispecies biofilm was added to each well of a round-bottom 24-well plate (Corning, Falcon™, USA) and randomly assigned into four treatment groups:

- Group 1. Control (Ctl) without any treatment
- Group 2. Incubated with PG 10 mM at room temperature for 30 min in the dark.
- Group 3. HFU; The wells containing stainless steel (SS) coupons were exposed to ultrasound waves at a frequency of 1 MHz and 1.6 W/cm². Treatment time ranges from 15 to 30 minutes
- Group 4. HFU + PG; To evaluate the influence of combined treatments based on PG at 10 mM and high-frequency ultrasound energy. The SS coupons with biofilm were added to the PG solution and immediately exposed to ultrasound (1 MHz, 1.6 W/cm²)

The detailed experimental design is also illustrated in Fig. 1. The concentration of PG was fixed at 10 mM based on the results of our previous study (Nguyen et al., 2021).

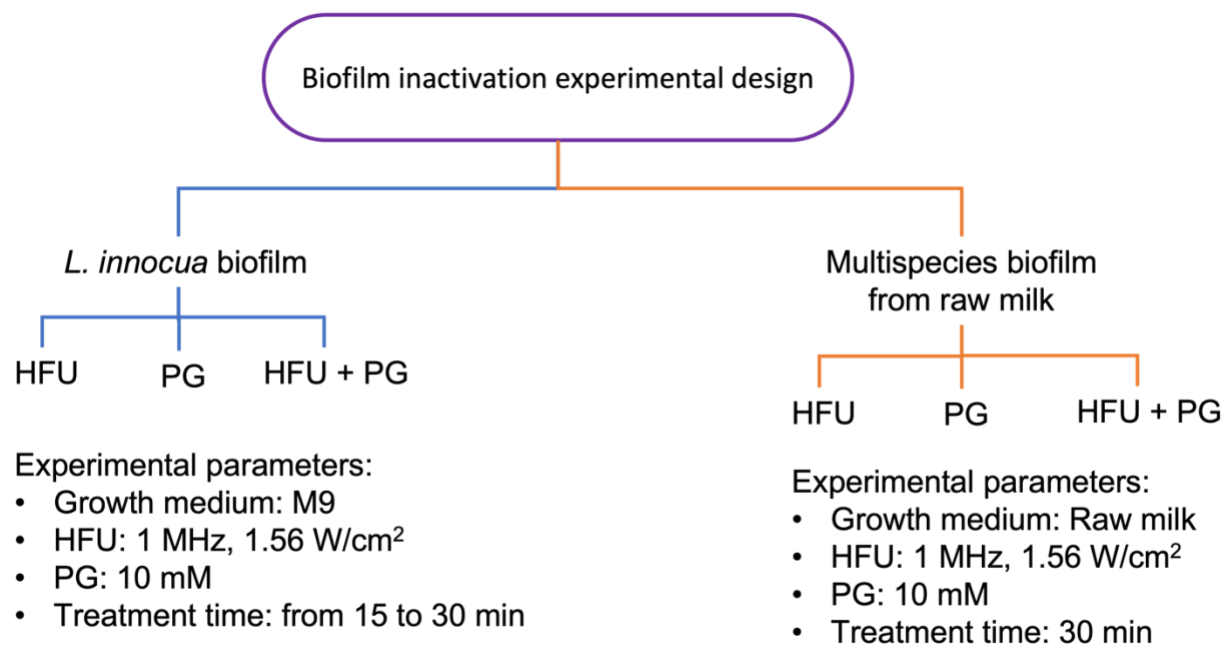


Fig. 4.1 Experimental design of the sonodynamic antimicrobial treatment (SAT) to inactivate biofilm from *L. innocua* and multispecies biofilm from raw milk with added *L. innocua*

2.3. Bacterial cultures

Rifampin (RIF)-resistant induced *L. innocua* strain (ATCC 33090, Manassas, VA, USA), was cultured in tryptic soy broth (TSB) (Sigma-Aldrich, St. Louis, MO, USA) with RIF (50 µg/ml) and grown at 37°C at 150 rpm for 24 hours. A bacterial culture with an absorbance at 600 nm of 1.5 (1 x 10⁹ CFU/ml assessed by plate count) was used for further experiments.

2.4. *L. innocua* biofilm formation

The *L. innocua* culture was grown overnight in TSB broth containing Rifampicin 50 µg mL⁻¹ at 37°C and 150 rpm. A 10 mL overnight culture was collected, and cell pellets were washed one time with PBS to remove traces of Rifampicin. After washing, *L. innocua* culture was diluted to a final concentration of 1 × 10⁷ CFU/ml using an M9 media (10% (vol/vol) water–1× M9 medium with minimal

salts (Sigma-Aldrich, St. Louis, MO, USA) with added 0.4% glucose and 0.4% tryptone. M9 is a minimal growth medium that facilitates the formation of biofilm as a survival mechanism when a bacterium is cultivated in a nutrition depletion condition. Briefly, 1 ml of the diluted bacterial suspension was then aliquoted into individual wells of a 24-well plate containing a stainless steel (304 grade) coupon of dimensions 1 cm × 1 cm. The plate was then incubated for 96 hours or four days at room temperature under dark conditions. The coupon is then recovered from the well and washed with 1 ml of sterile phosphate-buffered saline (PBS) (USB Co. Ltd., Cleveland, OH, USA) with gentle vortexing to remove planktonic cells.

2.5. Multispecies biofilm-forming method

The *L. innocua* culture was grown overnight in TSB broth containing Rifampicin 50 µg mL⁻¹ as described in section 2.4. The overnight culture was collected, and cell pellets were washed one time with PBS to remove traces of Rifampicin. After washing, the cell pellets (10⁹ CFU/mL) were resuspended in raw milk with a 1:2 (v/v) dilution. The bacterial concentration after dilution was 5 × 10⁸ CFU/mL. Then, sterilized SS coupons (1x1 cm²) were placed in a 24-well plate and a 1 mL aliquot of the raw milk inoculum (5 × 10⁸ CFU/mL) was added to each well. Biofilm was grown at room temperature for 24 hours before treatment. The shorter incubation time of 24 hours for the multispecies biofilm model was selected as the raw milk sample contains a high concentration of nutrients that can cause extensive biofouling of the contact surface. Furthermore, this period also aligns with the conditions in the industry where food contact surfaces are periodically sanitized after 12-24 hours of operation.

2.6. Sonodynamic antimicrobial treatment of biofilms

An ultrasound (Chattanooga medical supply, TN, USA) equipment with intensity and frequency ranges between 1 to 2.5 W/cm² and 1 to 3 MHz respectively was used for the high-frequency ultrasound treatment in this study. Based on our preliminary experiments, we determined that the lower

frequency, i.e., 1 MHz, was more effective than the higher frequency, i.e 3 MHz for bacterial inactivation, and the selected power of 1.6 W/cm² was sublethal to the target bacteria. Selection of sub-lethal levels of the US intensity was critical to demonstrate the synergistic impact of the selected compound and US treatment for the inactivation and the removal of bacteria from biofilms.

The 4-day-old biofilm of *L. innocua* growing on the SS coupon was removed from the M9 media and was washed two times with 2 ml of PBS buffer. After the washing steps, the coupon side with the biofilm was positioned downward on the bottom of a 24-well plate filled with treating solution. The biofilm side was facing the ultrasound transducer. The transducer was immersed in a water bath positioned 2 cm from the bottom of the well plate and supported by a custom platform as depicted in Fig. 2, with the well plate floating above the water. Total treatment times were set at 15 and 30 minutes.

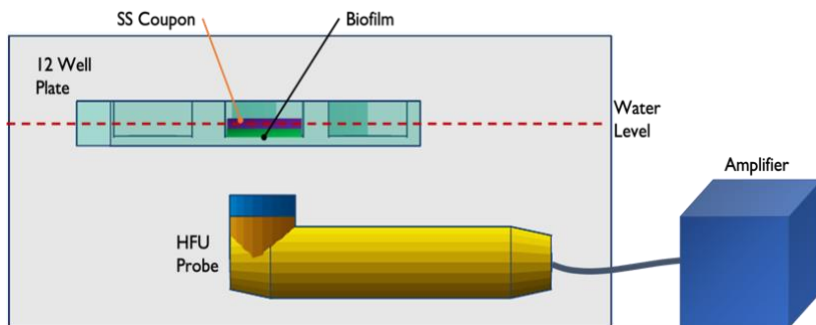


Fig. 4.2 SAT setup with a high-frequency probe sonicator for biofilm treatment. The probe was immersed in a water bath, and the temperature was monitored during the experiments with a

thermocouple. The probe has a diameter of 5 cm and was placed directly under the 24-well plate at a distance of 2 cm using a customized mechanical stage.

2.7. Enumeration of bacterial inactivation in treated biofilms

The SS coupons, after being treated with HFU, PG, or the combination of HFU + PG were then gently washed with PBS one time to remove any residual amount of PG. The coupons were then placed into a 50 mL Falcon tube with a 10 mL of maximum recovery diluent (MRD) solution. The tube was vigorously vortexed for 1 min and the recovered bacteria were spread plated on PCA and TSA plates using the serial dilution method. The Plate Count Agar (PCA) method was used to cultivate the total commensal microbes from the SS coupon and selective TSA plates with 50 ppm rifampicin were used to isolate the rifampicin-resistant *L. innocua* bacterial fraction. Plates were incubated at 37 °C for 48 hours before counting the number of bacterial CFU.

2.8. Crystal violet assay

The treated *L. innocua* biofilm or multispecies biofilm were removed from PG solution and washed two times with PBS. The washed biofilm was heat-fixed at 65°C for one hour before staining with crystal violet. Then, crystal violet was added and incubated for 5 minutes. After staining, the coupon was washed again two times with a PBS buffer. The crystal violet-stained biofilm biomass was then diluted with acetic acid (33%) and measured with a spectrophotometer at 570 nm.

2.9. Scanning electron microscopy (SEM) analysis of biofilms

Following ultrasound treatment, the SS coupons were washed one time with PBS, and the biofilm on the surface was fixed at 4 °C for 2 hours with 2.5 % glutaraldehyde–water. Post fixing, the SS coupons were exposed to 1% osmium tetroxide (OsO₄) for 1 h and then were dehydrated with increasing ethanol percentages (35%, 50%, 75%, 2 × 90%, and 2 × 100%) for 30 min in each solution.

Samples were then placed in a desiccator for 12 h. Finally, the disk samples were placed on a copper tape and sputter-coated with a thin layer of gold (100 Å) before SEM analysis (Huang et al., 2018). The scanning electron microscope used for this study was the Philips XL-30, which was operated at 10 kV accelerating voltage. Images were acquired at a 25,000x magnification level. Ten SEM images were obtained per sample.

2.10. Statistical analysis

Statistical analysis was performed using GraphPad Prism software V.9.3.1 (Graphpad Software, Inc., La Jolla, CA). To analyze differences between multiple experimental groups, a one-way analysis of variance ($P < 0.05$) was conducted to evaluate the statistical significance of the results. This statistical approach was used for the analysis of biofilm inactivation, biomass removal efficiency, and inactivation of the dispersed bacteria fraction.

3. Results

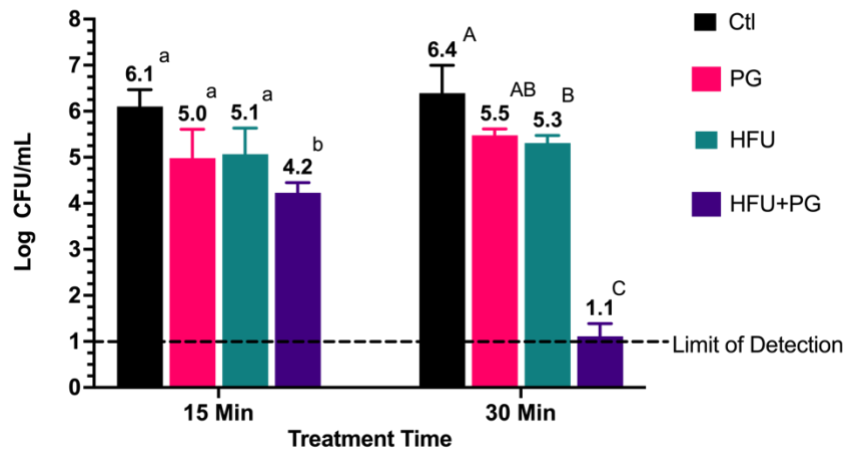
3.1. Biofilm inactivation data

The bactericidal effect of the combined HFU + PG treatment using (4 days old) *L. innocua* biofilm was evaluated and depicted in Fig. 3A. The results show a synergistic 5.5 log inactivation of the bacteria ($p < 0.01$) from a biofilm with an initial bacterial population of 6.4 log CFU/cm² following the treatment with HFU + PG for 30 min. In contrast to the synergistic effect of HFU + PG treatment, the individual treatments (HFU or PG) for 30 min resulted in only a one-log reduction of the bacteria from the *L. innocua* biofilm.

A multispecies environmental biofilm was formed to complement the evaluation of the *L. innocua* biofilm, as described in the materials and methods section. Due to the presence of milk components, including commensal microbes, inoculation of the *L. innocua* strain resulted in the formation of a multispecies environmental biofilm within a day of incubation. This multispecies biofilm

had approximately the same total bacterial count as a four-day-old mono-species *L. innocua* biofilm, as confirmed by the total plate count results in Fig. 3-A and 3-B. The multispecies biofilms were treated with the synergistic combination of HFU + PG as well as the individual treatments of HFU or PG for a fixed time of 30 min. This time was selected based on the results of the treatment of *L. innocua* biofilm, as illustrated in Fig. 3-A. The effect of the synergistic treatment on the multispecies biofilm was evaluated using a combination of the total plate count assay and specific colony count of *Listeria* cells with rifampicin as a selective media. The results in Fig. 3B illustrate a synergistic 5.2 log total reduction in the total bacterial population from an initial total population of 6.3 log CFU/cm². Within this total reduction, *L. innocua* levels were reduced by a 4.2 log CFU/cm² (p<0.01). In contrast, treatment of the multispecies biofilm with either HFU or PG for 30 min only resulted in less than one log reduction of both the total and *L. innocua* fractions of the multispecies biofilm.

A.



B.

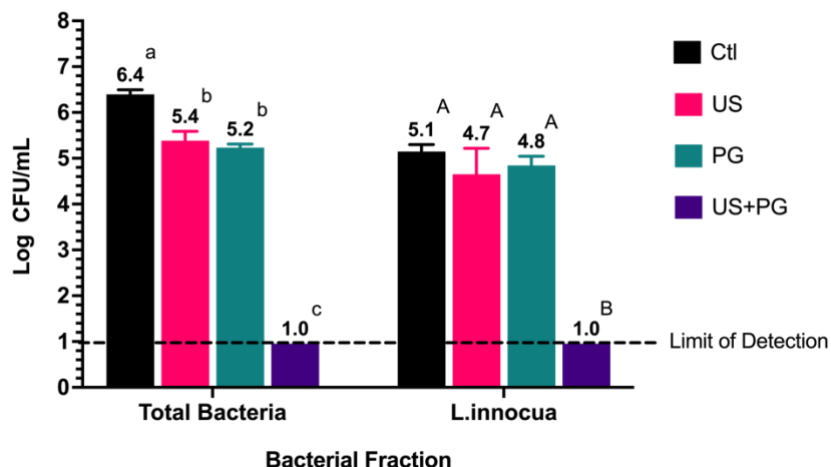


Fig. 4.3 (A) Biofilm inactivation data of sonodynamic antimicrobial treatment treated *L. innocua* biofilm from 15 to 30 minutes, **(B)** Biofilm inactivation data of SAT treated multispecies biofilm with added *L. innocua* strain for 30 minutes. Note: Mean denoted by a different letter indicates significant differences between treatments ($p < 0.05$). Sample abbreviation: Ctl – Control, HFU – High-frequency ultrasound treatment, PG – Propyl gallate treatment, HFU + PG – combined High-frequency ultrasound and PG treatment. The limit of detection is 10 CFU/mL.

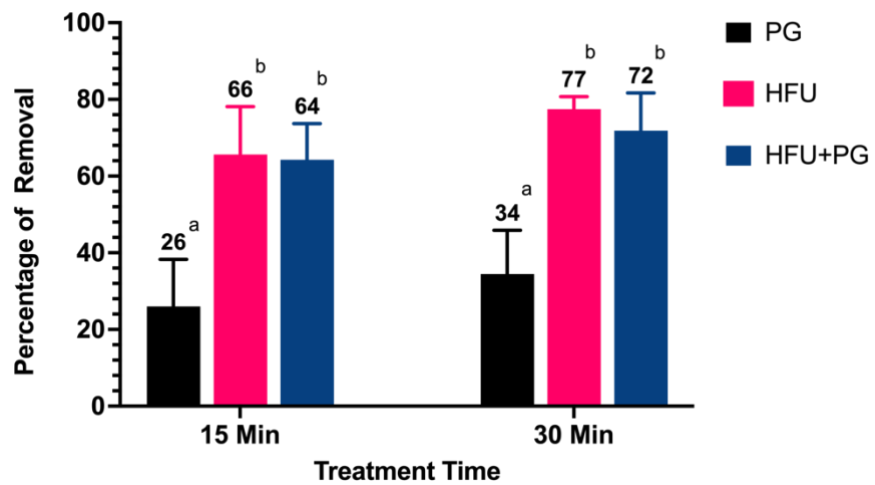
3.2. Biomass removal efficiency and detached bacterial inactivation

US approaches have been used to enhance the removal of biofilms from the treatment surface. In this study, the removal of biofilm mass was characterized using crystal violet staining of the biomass for both the model *L. innocua* and multispecies biofilms. For this characterization, biomass retention on the surface was measured for the synergistic combination of HFU + PG treatment. These results from the synergistic combination study were compared with the individual treatment of HFU or PG. The results in Fig. 4A show that the removal efficiency of combined HFU + PG treatment was similar to the HFU treatment alone for *L. innocua* biofilm. In contrast, PG treatment alone had a relatively smaller contribution to the removal of biomass. Furthermore, the results show that significant removal of the

biomass was achieved within the first 15 min of treatment, and the removal of biomass only increased marginally with an extended treatment time of 30 min.

The influence of selected treatments on the removal of biomass from a target surface was also assessed for the multispecies biofilm. The results in Fig. 4B show that HFU + PG treatment, as well as HFU treatment alone, resulted in the removal of over 60% of the biofilm biomass. This result is similar ($p>0.05$) to the results of a *L. innocua* biofilm treated with HFU + PG or HFU treatment. The removal efficiency of these treatments (HFU + PG or HFU) was significantly higher ($p<0.01$) than achieved using PG treatment alone.

A.



B.

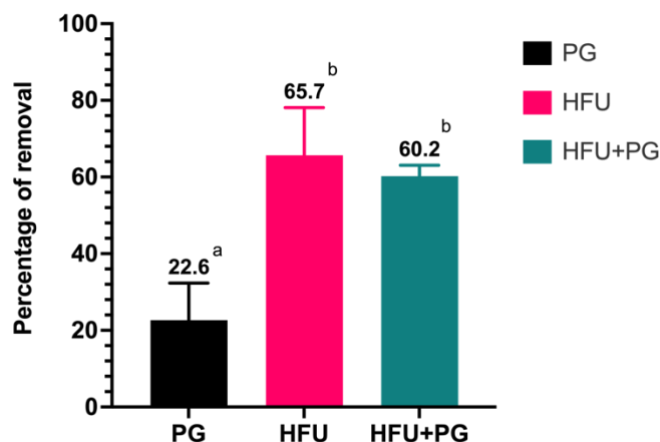


Fig. 4.4 Biomass Removal efficiency data of sonodynamic antimicrobial treatment treated *L. innocua* biofilm **(A)** with two different treatment times of 15 and 30 minutes, and multispecies biofilm **(B)** after 30 minutes of treatment time. Note: Mean denoted by a different letter indicates significant differences between treatments ($p < 0.05$). Sample abbreviation: Ctl – Control, HFU – High-frequency ultrasound treatment, PG – Propyl gallate treatment, HFU + PG – combined High-frequency ultrasound and PG treatment

3.3. Changes in biofilm morphology

The SEM images of the biofilm before and after treatment were acquired to characterize changes in biofilm morphology. In the case of *L. innocua* biofilm (Fig. 5), both the HFU and HFU + PG treatments enhanced bacteria removal from the SS surface compared to the control and PG treatments alone. In the case of HFU + PG, the residual bacterial cells on the surface show evidence of cell wall damage, as illustrated by their concave shape and deformed cell wall envelopes observed in the SEM images. In contrast, the HFU-treated samples show no significant visual evidence of bacterial cell damage in residual bacterial cells on the surface, although similar levels of reduction in the biomass were observed in both cases.

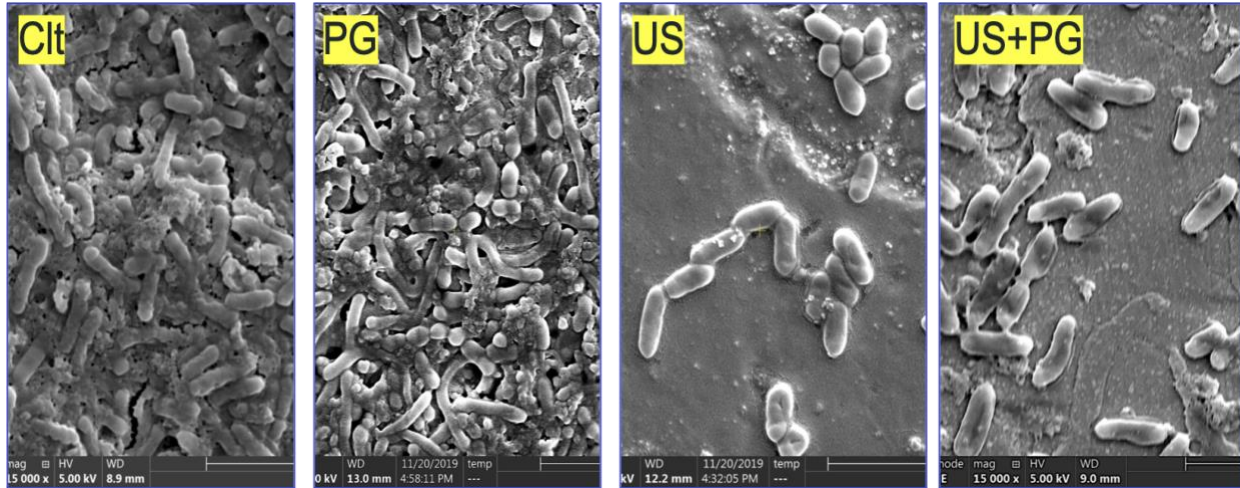


Fig. 4.5 Morphology observation of ultrasound treated *L. innocua* biofilm using SEM technique, HFU – High-frequency ultrasound treatment, PG – Propyl gallate treatment, HFU + PG – combined High-frequency ultrasound and PG treatment

Fig. 6 illustrates the effect of synergistic treatment on the multispecies biofilm formed by the combination of *Listeria* strain with commensal microbes from raw milk samples. The presence of *Listeria* was confirmed by the plate counting method in the presence of an antibiotic-resistant marker selective for the *L. innocua* strain. The results show that the combined HFU + PG treatment was more effective in dispersing bacterial cells from the food contact surface compared to the single treatment of HFU or PG alone. Compared to the results in Fig. 4, the results from Fig. 6 illustrate qualitatively more removal of the cells from the contact surface with HFU + PG treatment compared to HFU alone or PG alone. Due to a thick deposition of milk fouling layer biofilm formation, it was difficult to evaluate the integrity of cells in a multispecies biofilm using SEM imaging. To address these constraints and validate the qualitative difference in residual bacteria and their viability on the contact surface with the selected treatments, the bacterial cell counts on the surface and dispersed phase were measured using standard colony counting assays.

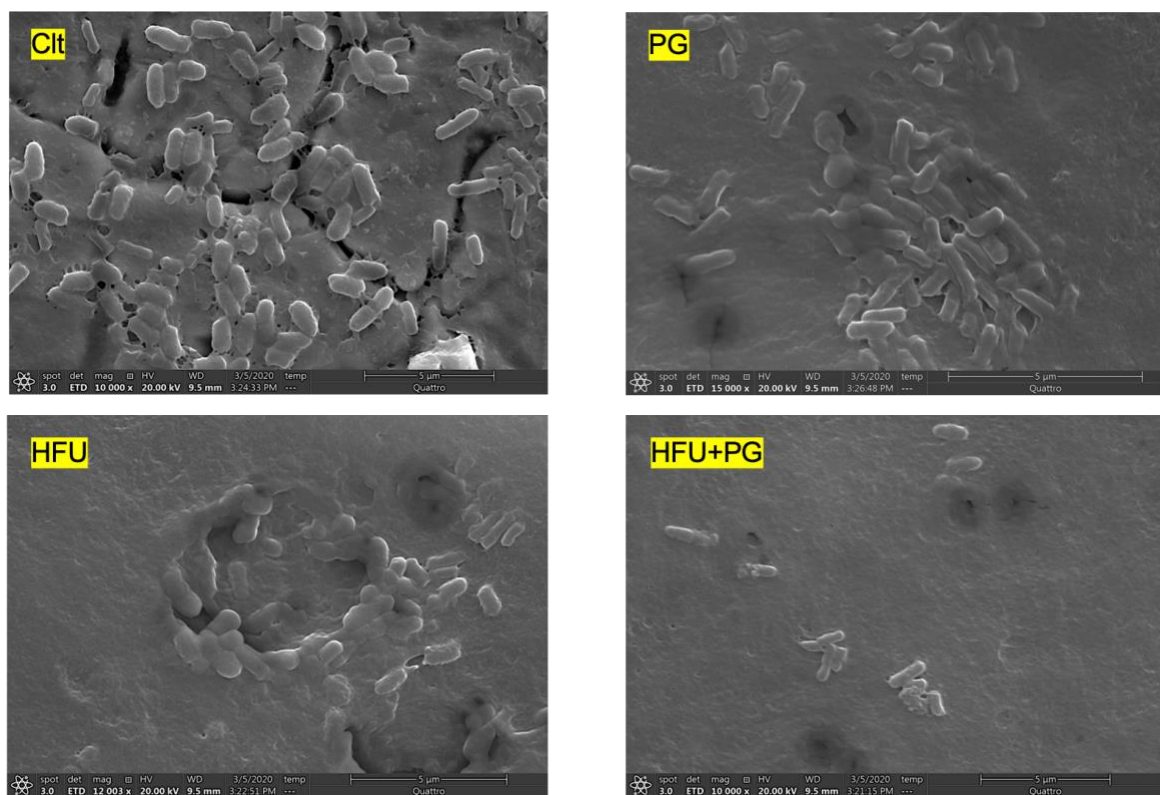


Fig. 4.6 Morphology observation of ultrasound treated multispecies biofilm with added *L. innocua* strain, using SEM technique, HFU – High-frequency ultrasound treatment, PG – Propyl gallate treatment, HFU + PG – combined High-frequency ultrasound and PG treatment

3.4. Dispersal of bacteria from biofilms and the viability of the dispersed bacteria

To further understand the decrease in the viable bacteria in biofilms following the selected treatments, the viability of the bacteria in the treatment medium was also characterized. This characterization is important as ultrasound treatment can result in the dispersal of the bacteria. The viability of bacteria released from biofilms to the treatment medium was measured for the HFU + PG, HFU, or PG treatments after 30 min of treatment of *L. innocua* biofilm, and the results were compared with the control *Listeria* biofilm without any ultrasound or chemical treatment. The results in Table 1 illustrate that the HFU + PG treated samples had less than one log of viable bacterial cells in the aqueous phase samples collected after ultrasonic treatment of *Listeria* and multispecies biofilm samples

respectively. In contrast, the biofilm samples treated with either HFU or PG treatments alone had approximately 2 log CFU of viable bacteria in the aqueous phase. Together with the results in Fig. 3A and Fig. 3B, this data set suggests that most of the bacteria population were inactivated within a biofilm after HFU + PG treatment and could not be detected in the aqueous phase. In contrast, HFU or PG treatments of the biofilms resulted in limited inactivation but increased the dispersal of the bacteria in the aqueous phase. Compared to the results in Fig. 4, these results also illustrate that although the dispersal of biomass with HFU or HFU + PG treatments may be similar, the level of inactivation of bacteria with HFU + PG treatment was significantly higher than the HFU or PG treatments alone.

Table 4.1 Biofilm inactivation data of sonodynamic antimicrobial treatment treated *L. innocua* biofilm model accounted for the detached bacterial fraction in the wells

	<i>L. innocua</i>	Multispecies	
	Bacterial count (CFU/mL)	Total count (CFU/mL)	<i>L. innocua</i> (CFU/mL)
Ctrl	0	0	0
PG	2.0 ^a ± 0.391	2 ^a ± 0.175	1.4 ^a ± 0.04
HFU	2.2 ^a ± 0.252	2.6 ^a ± 0.134	1.7 ^a ± 0.06
HFU+PG	<1 ^b	<1 ^b	<1 ^b

Note: Mean denoted by a different letter indicates significant differences between treatments ($p < 0.05$). Sample abbreviation: Ctrl – Control, HFU – High-frequency ultrasound treatment, PG – Propyl gallate treatment, HFU + PG – combined High-frequency ultrasound and PG treatment

4. Discussion

4.1. Biofilm inactivation and removal efficiency compared to a low-frequency US (LFU) process

The predominant role of the US during conventional sanitation of biofilms is limited to enhanced dispersal of the biofilm. To achieve efficient dispersion, LFU is commonly used at high power levels to disperse the biomass attached to the surface. Previous studies have reported that LFU can induce the removal of greater than 85% - 90% of the biomass (Erriu et al., 2014; Oulahal-Lagsir et al., 2000). The dispersed biomass is then inactivated by chemical sanitizers in the aqueous phase. Despite the effectiveness of the US in improving the dispersal of biofilm biomass, this approach is not commonly used in the industry. The possible limitations include limited improvement in the overall biofilm inactivation efficacy with this approach as previous studies have shown only 2-3 log improvements in the activation of biofilms using a combination of LFU and chemical sanitizers after 10 to 60 minutes of treatment time (Bang et al., 2017; Baumann et al., 2009; Berrang et al., 2008; Lee et al., 2014; Sagong et al., 2011) and to the best of our knowledge, none of these previous studies have evaluated multispecies biofilms. In addition, operational considerations such as coupling of the low frequency and high-intensity US with existing equipment and uniformity of the treatment can also be potential limitations as removal efficiency can vary across the surface. To address these limitations, this current study has focused on using low-intensity high-frequency US in combination with a food-grade antioxidant for the treatment of biofilms. The results illustrate relatively rapid (within 30 min) and effective (~5 log or higher) levels of inactivation of both *L. innocua* and multispecies biofilm on the food contact surface using a combination of HFU and PG treatment. In addition, a combined treatment of HFU + PG also reduced the dispersal of the viable bacteria in the aqueous suspension compared to HFU or PG treatment alone. Achieving higher levels of inactivation on the food contact can also enhance uniformity of the treatment as it reduces the viable bacterial population and also the risk of reseeded of the biofilm. In addition, this approach eliminates the need for conventional chemical sanitizer use and

promotes the use of food-grade compounds for the sanitation process. Furthermore, the process only requires a low-intensity US process compared to the high-intensity US process used in the conventional approach. The use of a low-intensity ultrasound process also reduces the energy cost required for the deployment of the US process in the industry and the lack of extensive cavitation with the high-frequency US may also reduce potential damage to the processing equipment. Further studies are required to validate these results using different food contact surfaces as well as translation of this approach with realistic food processing equipment.

4.2. Mode of action of the synergistic bacterial inactivation

The enhanced inactivation effects of HFU + PG were attributed to the ability of HFU to improve PG transport into biofilms, the ability of PG to partition in the bacterial membrane, and the generation of ROS by the combination of HFU + PG. HFU ultrasound-induced mixing and micro-jet streams can increase the mass transport of the PG to the biofilm surface and the biofilm matrix. This enhanced mass-transfer effect was confirmed by previous studies evaluating the combination of HFU (500 kHz to 1MHz) and an antibiotic (vancomycin) or microbubble for biofilm treatments (Bharatula et al., 2018; Dong et al., 2013, 2017; Fu et al., 2019; Goh et al., 2015; Guo et al., 2017; Hu et al., 2018; Johnson et al., 2012; Ronan et al., 2016). Due to the complexity of the EPS structure, bacterial cells residing within the biofilm are protected by the limited infiltration of the antibiotic compound. However, when ultrasound was co-applied, it is plausible that the barriers to mass transport were significantly reduced (Erriu et al., 2014). The ability of PG to partition lipid membranes, as evaluated in our previous studies (Nguyen et al., 2021), provides an advantage that can result in the enrichment of PG in bacterial cells in the biofilm. This advantage combined with the generation of oxidative stress induced by synergistic interactions with HFU treatment results in significantly enhanced inactivation of bacterial cells both in the biofilm as well as the planktonic cells released from the biofilm. The combination of HFU + PG also induces significant

damage to the membrane as observed in our previous study with planktonic cells (Nguyen et al., 2021), and is not influenced by the presence of food materials such as apple juice. In addition, both *L. innocua* and multispecies biofilms' metabolic activity were suppressed to some extent by the combined HFU + PG (result not shown); however, the effect is more noticeable in *L. innocua* biofilm and not the multispecies biofilm. Hence, metabolic activity suppression is not the decisive factor for both biofilm models' inactivation, but one of its contributing factors.

The results of this study illustrate that synergistic interactions of PG with HFU are effective for the inactivation of both *L. innocua* and multispecies biofilms. For food industries, such as the dairy industry, biofilm formation is a fundamental problem, because raw milk contains a wide variety of microorganisms and dairy products are susceptible to microbial spoilage. Even if primary biofilm formers are neither spoilage organisms nor pathogens, established biofilms can be a favorable environment for pathogenic organisms like *L. monocytogenes* (Weber et al., 2019; Weiler et al., 2013). The multispecies biofilm model used in this study simulated the established biofilm in a milk processing environment using a combination of commensal microbes in milk and *L. innocua*, and the combined HFU + PG treatment was able to significantly reduce both the overall microbial plate count and the viability of *L. innocua*. These results illustrate the potential of the sonodynamic antimicrobial treatment approach developed in this study for applications in a food processing environment to inactivate an established multispecies biofilm. To summarize, the inactivation mechanism of the synergistic bacterial inactivation of the HFU + PG treatment used in this study is suggested in Fig. 7.

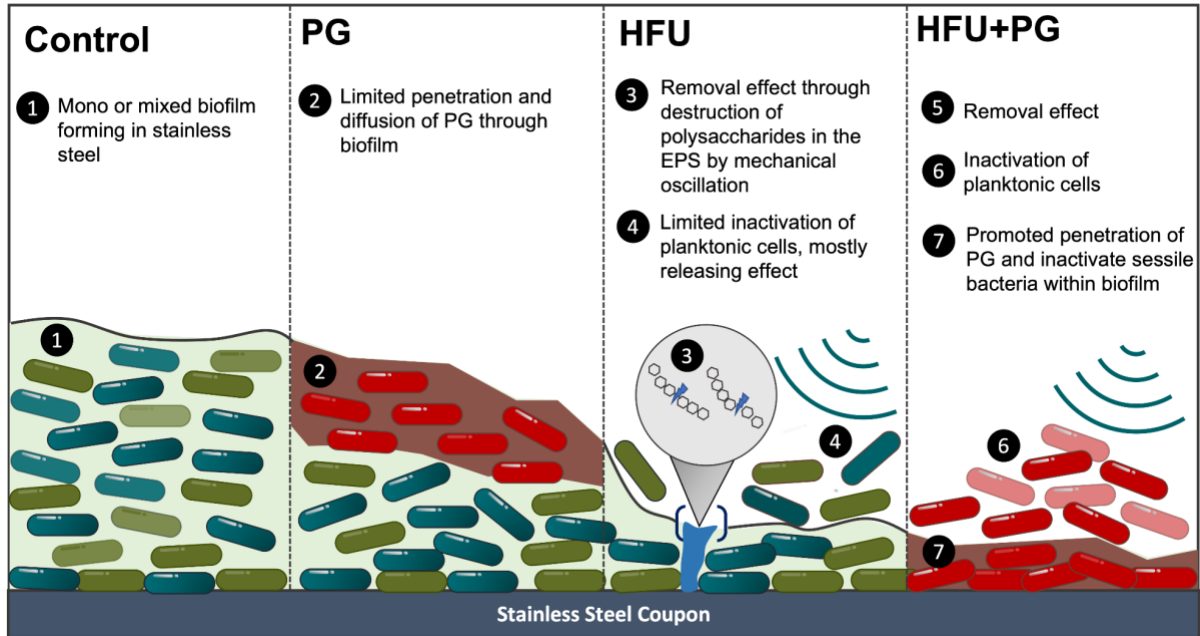


Fig. 4.7 Suggested modes of action of the sonodynamic antimicrobial treatment on biofilm (both *L. innocua* and multispecies) formed on a surface of a stainless-steel coupon

4.3. Conclusion

The combined HFU + PG treatment achieved a 5-log reduction in both *L. innocua* and multispecies biofilms within 30 min of treatment time. The combination treatment was also effective at eliminating biofilm biomass. Inactivation of biofilms and removal of biofilm biomass was accompanied by the changes in morphology, in response to HFU, PG, and a combination of these two treatments. Single treatment of either HFU or PG did not significantly affect biofilm viability; however, HFU showed significantly higher removal efficiency than PG treatment alone and was similar to the combined HFU+PG treatment. HFU + PG also reduced the population of dispersed planktonic cells from *L. innocua* and multispecies biofilm models to less than the detection limit. Using a combination of HFU and PG, the study illustrates the synergistic inactivation of established biofilms on a food processing surface. A possible mechanism of action underlying the high efficacy of the combined treatment was also

suggested by this study. An approach such as this may be relevant in areas such as food processing and packaging where biofilms are a persistent impediment.

Acknowledgments

This project was supported by the Agriculture and Food Research Initiative by grant no. 2016-67017-24599 from the USDA National Institute of Food and Agriculture (USDA-NIFA) Program in Improving Food Quality (A1361) and by grant no. 2015-68003- 23411 from the USDA-NIFA Program Enhancing Food Safety through Improved Processing Technologies (A4131).

The *Listeria innocua* (ATCC 33090, Manassas, VA, USA) were kindly provided by Dr. Linda Harris and Dr. Trevor Suslow, respectively, at the University of California, Davis

Bibliography

- Abdallah, M., Benoliel, C., Drider, D., Dhulster, P., & Chihib, N.-E. (2014). Biofilm formation and persistence on abiotic surfaces in the context of food and medical environments. *Archives of Microbiology*, *196*(7), 453–472. <https://doi.org/10.1007/s00203-014-0983-1>
- Araújo, P., Lemos, M., Mergulhão, F., Melo, L., & Simões, M. (2011). *Antimicrobial resistance to disinfectants in biofilms*.
- Azeredo, J., Azevedo, N. F., Briandet, R., Cerca, N., Coenye, T., Costa, A. R., Desvaux, M., Di Bonaventura, G., Hébraud, M., Jaglic, Z., Kačániová, M., Knøchel, S., Lourenço, A., Mergulhão, F., Meyer, R. L., Nychas, G., Simões, M., Tresse, O., & Sternberg, C. (2017). Critical review on biofilm methods. *Critical Reviews in Microbiology*, *43*(3), 313–351. <https://doi.org/10.1080/1040841X.2016.1208146>
- Bang, H.-J., Park, S. Y., Kim, S. E., Md Furkanur Rahaman, M., & Ha, S.-D. (2017). Synergistic effects of combined ultrasound and peroxyacetic acid treatments against *Cronobacter sakazakii* biofilms on fresh cucumber. *LWT*, *84*, 91–98. <https://doi.org/10.1016/J.LWT.2017.05.037>

- Baumann, A. R., Martin, S. E., & Feng, H. (2009). Removal of *Listeria monocytogenes* Biofilms from Stainless Steel by Use of Ultrasound and Ozone MATERIALS AND METHODS. In *Journal of Food Protection* (Vol. 72, Issue 6, pp. 1306–1309). http://meridian.allenpress.com/jfp/article-pdf/72/6/1306/1680690/0362-028x-72_6_1306.pdf
- Berrang, M. E., Frank, J. F., & Meinersmann, R. J. (2008). Effect of Chemical Sanitizers with and without Ultrasonication on *Listeria monocytogenes* as a Biofilm within Polyvinyl Chloride Drain Pipes†. *Journal of Food Protection*, 71(1), 66–69. <https://doi.org/10.4315/0362-028X-71.1.66>
- Bharatula, L. D., Marsili, E., Rice, S., & Kwan, J. J. (2018). The effects of high intensity focused ultrasound on biofilms formed by *Pseudomonas aeruginosa*. *The Journal of the Acoustical Society of America*, 143(3), 1928–1928. <https://doi.org/10.1121/1.5036297>
- Branck, T. A., Hurley, M. J., Prata, G. N., Crivello, C. A., & Marek, P. J. (2017). Efficacy of a Sonicating Swab for Removal and Capture of *Listeria monocytogenes* in Biofilms on Stainless Steel. *Applied and Environmental Microbiology*, 83(11), e00109-17. <https://doi.org/10.1128/AEM.00109-17>
- Bridier, A., Briandet, R., Thomas, V., & Dubois-Brissonnet, F. (2011). Resistance of bacterial biofilms to disinfectants: A review. *Biofouling*, 27(9), 1017–1032. <https://doi.org/10.1080/08927014.2011.626899>
- Carmen, J. C., Roeder, B. L., Nelson, J. L., Beckstead, B. L., Runyan, C. M., Schaalje, G. B., Robison, R. A., & Pitt, W. G. (2004). Ultrasonically enhanced vancomycin activity against *Staphylococcus epidermidis* biofilms in vivo. *Journal of Biomaterials Applications*, 18(4), 237–245. <https://doi.org/10.1177/0885328204040540>
- Carmen, J. C., Roeder, B. L., Nelson, J. L., Robison Ogilvie, R. L., Robison, R. A., Schaalje, G. B., & Pitt, W. G. (2005). Treatment of biofilm infections on implants with low-frequency ultrasound and antibiotics. *American Journal of Infection Control*, 33(2), 78–82. <https://doi.org/10.1016/j.ajic.2004.08.002>

- Carrascosa, C., Raheem, D., Ramos, F., Saraiva, A., & Raposo, A. (2021). Microbial Biofilms in the Food Industry—A Comprehensive Review. *International Journal of Environmental Research and Public Health*, *18*(4), 2014. <https://doi.org/10.3390/ijerph18042014>
- Davies, D. (2003). Understanding biofilm resistance to antibacterial agents. *Nature Reviews Drug Discovery*, *2*(2), 114–122. <https://doi.org/10.1038/nrd1008>
- Dong, Y., Chen, S., Wang, Z., Peng, N., & Yu, J. (2013). Synergy of ultrasound microbubbles and vancomycin against *Staphylococcus epidermidis* biofilm. *The Journal of Antimicrobial Chemotherapy*, *68*(4), 816–826. <https://doi.org/10.1093/jac/dks490>
- Dong, Y., Xu, Y., Li, P., Wang, C., Cao, Y., & Yu, J. (2017). Antibiofilm effect of ultrasound combined with microbubbles against *Staphylococcus epidermidis* biofilm. *International Journal of Medical Microbiology*, *307*(6), 321–328. <https://doi.org/10.1016/j.ijmm.2017.06.001>
- Erriu, M., Blus, C., Szmukler-Moncler, S., Buogo, S., Levi, R., Barbato, G., Madonnaripa, D., Denotti, G., Piras, V., & Orrù, G. (2014). Microbial biofilm modulation by ultrasound: Current concepts and controversies. *Ultrasonics Sonochemistry*, *21*(1), 15–22. <https://doi.org/10.1016/j.ultsonch.2013.05.011>
- Fu, Y.-Y., Zhang, L., Yang, Y., Liu, C.-W., He, Y.-N., Li, P., & Yu, X. (2019). Synergistic antibacterial effect of ultrasound microbubbles combined with chitosan-modified polymyxin B-loaded liposomes on biofilm-producing *Acinetobacter baumannii*. *International Journal of Nanomedicine*, *14*, 1805–1815. <https://doi.org/10.2147/IJN.S186571>
- Galié, S., García-Gutiérrez, C., Miguélez, E. M., Villar, C. J., & Lombó, F. (2018). Biofilms in the Food Industry: Health Aspects and Control Methods. *Frontiers in Microbiology*, *9*. <https://doi.org/10.3389/fmicb.2018.00898>

- Gilbert, P., Allison, D. g., & McBain, A. j. (2002). Biofilms in vitro and in vivo: Do singular mechanisms imply cross-resistance? *Journal of Applied Microbiology*, *92*(s1), 985-110S.
<https://doi.org/10.1046/j.1365-2672.92.5s1.5.x>
- Goh, B. H. T., Conneely, M., Kneuper, H., Palmer, T., Klaseboer, E., Khoo, B. C., & Campbell, P. (2015). High-Speed Imaging of Ultrasound-Mediated Bacterial Biofilm Disruption. In I. Lacković & D. Vasic (Eds.), *6th European Conference of the International Federation for Medical and Biological Engineering* (Vol. 45, pp. 533–536). Springer International Publishing.
https://doi.org/10.1007/978-3-319-11128-5_133
- Guo, H., Wang, Z., Du, Q., Li, P., Wang, Z., & Wang, A. (2017). Stimulated phase-shift acoustic nanodroplets enhance vancomycin efficacy against methicillin-resistant *Staphylococcus aureus* biofilms. *International Journal of Nanomedicine*, *12*, 4679–4690.
<https://doi.org/10.2147/IJN.S134525>
- Hu, X., Huang, Y. Y., Wang, Y., Wang, X., & Hamblin, M. R. (2018). Antimicrobial photodynamic therapy to control clinically relevant biofilm infections. *Frontiers in Microbiology*, *9*(JUN).
<https://doi.org/10.3389/fmicb.2018.01299>
- Hua, G., & Reckhow, D. A. (2007). Comparison of disinfection byproduct formation from chlorine and alternative disinfectants. *Water Research*, *41*(8), 1667–1678.
<https://doi.org/10.1016/j.watres.2007.01.032>
- Huang, K., Wrenn, S., Tikekar, R., & Nitin, N. (2018). Efficacy of decontamination and a reduced risk of cross-contamination during ultrasound-assisted washing of fresh produce. *Journal of Food Engineering*, *224*, 95–104. <https://doi.org/10.1016/J.JFOODENG.2017.11.043>
- Johnson, L. L., Peterson, R. V., Pitt, W. G., & Building, C. (2012). *Treatment of bacterial biofilms on polymeric biomaterials using antibiotics and ultrasound*.
<https://doi.org/10.1163/156856298X00712>

- Lee, N.-Y., Kim, S.-W., & Ha, S.-D. (2014). Synergistic Effects of Ultrasound and Sodium Hypochlorite (NaOCl) on Reducing *Listeria monocytogenes* ATCC19118 in Broth, Stainless Steel, and Iceberg Lettuce. *Foodborne Pathogens and Disease*, *11*(7), 581–587.
<https://doi.org/10.1089/fpd.2013.1722>
- Mah, T.-F. C., & O'Toole, G. A. (2001). Mechanisms of biofilm resistance to antimicrobial agents. *Trends in Microbiology*, *9*(1), 34–39. [https://doi.org/10.1016/S0966-842X\(00\)01913-2](https://doi.org/10.1016/S0966-842X(00)01913-2)
- Marchand, S., De Block, J., De Jonghe, V., Coorevits, A., Heyndrickx, M., & Herman, L. (2012). Biofilm Formation in Milk Production and Processing Environments; Influence on Milk Quality and Safety. *Comprehensive Reviews in Food Science and Food Safety*, *11*(2), 133–147.
<https://doi.org/10.1111/j.1541-4337.2011.00183.x>
- Nguyen, C., Rai, R., Yang, X., Tikekar, R. V., & Nitin, N. (2021). Synergistic inactivation of bacteria based on a combination of low frequency, low-intensity ultrasound and a food grade antioxidant. *Ultrasonics Sonochemistry*, *74*, 105567. <https://doi.org/10.1016/j.ultsonch.2021.105567>
- Oliveira, G. S., Lopes, D. R. G., Andre, C., Silva, C. C., Baglinière, F., & Vanetti, M. C. D. (2019). Multispecies biofilm formation by the contaminating microbiota in raw milk. *Biofouling*, *35*(8), 819–831. <https://doi.org/10.1080/08927014.2019.1666267>
- Ölmez, H., & Kretschmar, U. (2009). Potential alternative disinfection methods for organic fresh-cut industry for minimizing water consumption and environmental impact. *LWT - Food Science and Technology*, *42*(3), 686–693. <https://doi.org/10.1016/j.lwt.2008.08.001>
- Oulahal-Lagsir, N., Martial-Gros, A., Boistier, E., Blum, L. J., & Bonneau, M. (2000). The development of an ultrasonic apparatus for the non-invasive and repeatable removal of fouling in food processing equipment. *Letters in Applied Microbiology*, *30*(1), 47–52. Scopus.
<https://doi.org/10.1046/j.1472-765x.2000.00653.x>

- Ronan, E., Edjiu, N., Kroukamp, O., Wolfaardt, G., & Karshafian, R. (2016). USMB-induced synergistic enhancement of aminoglycoside antibiotics in biofilms. *Ultrasonics*, *69*, 182–190.
<https://doi.org/10.1016/j.ultras.2016.03.017>
- Sagong, H.-G., Lee, S.-Y., Chang, P.-S., Heu, S., Ryu, S., Choi, Y.-J., & Kang, D.-H. (2011). Combined effect of ultrasound and organic acids to reduce Escherichia coli O157:H7, Salmonella Typhimurium, and Listeria monocytogenes on organic fresh lettuce. *International Journal of Food Microbiology*, *145*(1), 287–292. <https://doi.org/10.1016/J.IJFOODMICRO.2011.01.010>
- Sharma, N., Arya, G., Kumari, R., Gupta, N., & Nimesh, S. (2019). Evaluation of Anticancer activity of Silver Nanoparticles on the A549 Human Lung Carcinoma Cell Lines through Alamar Blue Assay. *Bio-Protocol*, *9*(1), 1–9. <https://doi.org/10.21769/bioprotoc.3131>
- Simões, M., Simões, L. C., & Vieira, M. J. (2010). A review of current and emergent biofilm control strategies. *LWT - Food Science and Technology*, *43*(4), 573–583.
<https://doi.org/10.1016/j.lwt.2009.12.008>
- Singh, S., Singh, S. K., Chowdhury, I., & Singh, R. (2017). Understanding the Mechanism of Bacterial Biofilms Resistance to Antimicrobial Agents. *The Open Microbiology Journal*, *11*, 53–62.
<https://doi.org/10.2174/1874285801711010053>
- Weber, M., Liedtke, J., Plattes, S., & Lipski, A. (2019). Bacterial community composition of biofilms in milking machines of two dairy farms assessed by a combination of culture-dependent and – independent methods. *PLOS ONE*, *14*(9), e0222238.
<https://doi.org/10.1371/journal.pone.0222238>
- Weiler, C., Iffland, A., Naumann, A., Kleta, S., & Noll, M. (2013). Incorporation of Listeria monocytogenes strains in raw milk biofilms. *International Journal of Food Microbiology*, *161*(2), 61–68.
<https://doi.org/10.1016/j.ijfoodmicro.2012.11.027>

- Wille, J., & Coenye, T. (2020). Biofilm dispersion: The key to biofilm eradication or opening Pandora's box? *Biofilm*, 2, 100027. <https://doi.org/10.1016/j.bioflm.2020.100027>
- Winkelstroter, L. K. (2015). Microbial Biofilms: The Challenge of Food Industry. *Biochemistry & Molecular Biology Journal*, 1(1). <https://doi.org/10.21767/2471-8084.100005>
- Yu, H., Liu, Y., Li, L., Guo, Y., Xie, Y., Cheng, Y., & Yao, W. (2020). Ultrasound-involved emerging strategies for controlling foodborne microbial biofilms. *Trends in Food Science and Technology*, 96, 91–101. <https://doi.org/10.1016/j.tifs.2019.12.010>
- Zhao, X., Zhao, F., Wang, J., & Zhong, N. (2017a). Biofilm formation and control strategies of foodborne pathogens: Food safety perspectives. *RSC Advances*, 7(58), 36670–36683. <https://doi.org/10.1039/C7RA02497E>
- Zhao, X., Zhao, F., Wang, J., & Zhong, N. (2017b). Biofilm formation and control strategies of foodborne pathogens: Food safety perspectives. *RSC Advances*, 7(58), 36670–36683. <https://doi.org/10.1039/C7RA02497E>

CHAPTER 5

Screening of polyphenolic compounds for antimicrobial photodynamic and sonodynamic treatments

Lihua Fan^{a,b} and Cuong Nguyen Huu^a, Donghong Liu^b, Nitin Nitin^{a,c,*}

^aDepartment of Food Science and Technology, University of California, Davis, CA, USA.

^bDepartment of Food Science and Nutrition, Zhejiang Key Laboratory for Agro-Food Processing, Zhejiang University, Hangzhou, Zhejiang, China.

^cDepartment of Biological and Agricultural Engineering, University of California, Davis, CA, USA.

*Corresponding author. Email address: nnitin@ucdavis.edu.

Abstract

The antibacterial activity of a combination of UV-A light treatment or high-frequency (HFU) ultrasound treatment with three different classes of phenolic compounds (gallate derivatives, cinnamic acid derivatives, and other polyphenolic compounds such as quercetin, flavone, and grape seed extract) against *E. coli* O157:H7 and *L. innocua* was investigated in this study. Six photo-activated compounds were found to have a synergistic interaction with UV-A inactivating *E. coli* O157:H7, and four compounds were confirmed in the case of *L. innocua*, all of which belong to cinnamic acid derivatives. Of six photosensitizers confirmed in UV-A treatment, there were four retained their antimicrobial effectiveness when combined with HFU. Sinapic acid demonstrated the highest bacterial inactivation efficiency of the 18 chemicals tested when combined with either UV-A or HFU treatment. The various physiochemical reactions of the treated bacterial cells are not independent but rather interrelated processes. A "cause and effect" relationship between the physiological reactions was observed, where membrane damage might directly lead to intracellular oxidative stress and could also be a factor in the inactivation of membrane-associated dehydrogenase enzyme families. The robust bacterial inactivation and the food-grade nature of the screened compounds could facilitate the adaptation of APDT and ASDT in the food industry.

Keywords: *photodynamic therapy, sonodynamic therapy, phenolic acids, foodborne pathogen, oxidative stress*

1. Introduction

Antibacterial photodynamic therapy (APDT) is an emerging nonthermal technology used for surface (food and food processing surfaces) decontamination and bacterial inactivation in liquid media. APDT's working mechanism is based on the ROS generation mechanism from compounds that are excited by a certain wavelength of light, typically in the UV-A (320-400 nm) and visible wavelength range (400-700 nm) (Abrahamse and Hamblin, 2016). These compounds are termed photosensitizers (PSs). Specifically, the PSs are promoted from their ground states to excited states after being irradiated at specific wavelengths. When the compounds return to their ground state, the radiated energy and free electrons interact at the molecular level with oxygen molecules or other organic substrates, forming reactive oxygen species (ROS) such as superoxide, hydroxyl radicals, hydrogen peroxide, and singlet oxygen (Alves et al., 2014). These free radicals can oxidize a wide spectrum of functional molecules in the bacterial membrane and cytoplasm, causing irreversible damage and cell death (Pang et al., 2016a). APDT can be utilized as an alternative to chlorine-based sanitizers for surface cleaning applications because of its powerful ROS production mechanism. In addition, APDT has a substantial bacterial inactivation effect in liquid systems (Cossu et al., 2016; de Oliveira et al., 2018; Wang et al., 2017). However, when microorganisms are located within concealed or obscure areas such as stomata in the leafy green leaves (Doan *et al.*, 2020) or on surfaces that have irregular topography such as one a cantaloupe, the effect of light irradiation and the APDT treatment could be dampened. Furthermore, the success of APDT treatment is dependent on the transmission of light through the treated media, so the inactivation effect is diminished when the media is clouded or has a color that would otherwise absorb the light source wavelength.

Antimicrobial Sonodynamic Treatment (ASDT) was proposed to address the limitations of APDT when dealing with shady locations or non-transmitting issues. ASDT is an alternative to APDT that involves the use of a sonosensitizer (SS) and a low-intensity, high-frequency (0.5-1MHz) ultrasound

treatment (Serpe and Giuntini, 2015). Physically, ultrasound is similar to light irradiation in that both are non-ionizing irradiation waves (Duck and Leighton, 2018). As a result, the mode of action of ultrasound and light irradiation in activating sensitizers to generate ROS is comparable. When the sonosensitizer is exposed to a specific intensity and frequency of ultrasound, it is activated from the ground to an excited state. On returning to the ground state, it releases energy, which is transferred to oxygen to produce ROS, such as singlet oxygen and free radicals. These ROS can mediate apoptosis, thereby inhibiting the growth of pathological cells (Trendowski, 2014) It is worth noting that these sonosensitizers show low toxicity and no inhibitory effect, and they are bioactive only after being exposed to ultrasonic irradiation (Pang et al., 2016b). Although ASDT is conceptually similar to the well-established APDT (Dougherty et al., 1998), the former still exhibits several distinct advantages. Ultrasonic irradiation is superior to light irradiation in that the applied energy can be focused precisely on the specific location requiring treatment (Pang et al., 2016b). In addition, ultrasound is a type of mechanical wave that can penetrate samples to a greater extent than light. As a result, ultrasound can be used to treat deeply located diseases (Tachibana et al., 2008). Moreover, studies have shown that low-intensity ultrasound can alter the cell membrane through high shear stress, localized compression, and microjet stream that facilitates its permeability to sonosensitizers, resulting in cell death (Harrison & Balcer-Kubiczek, 1991).

One of the major barriers for translating the applications of APDT and ASDT in food processing are a lack of understanding of the operating mechanism of bacterial inactivation and the limited availability of food-grade sensitizers. The effects of the sensitizer's molecular configuration, as well as the type of ROS they generate, are largely unexplored among food grade compounds (Ghorbani et al., 2018; Hessling et al., 2017; Kvam and Benner, 2020). To the best of our knowledge, the effects of the APDT and ASDT on the physiology of microorganisms, including membrane damage, oxidative stress, as well as enzymatic activity, have not been extensively reported in the literature. Furthermore, there are limited number of food-grade sensitizers that have been discovered (Pang et al., 2016). One of the

preferred conditions for food grade applications of compound is the lack of significant color and flavor modification of the food with the addition of photo or sono-sensitizers. Many of the currently explored compounds can potentially influence the sensory properties of food either by altering its color, e.g. in the case of curcumin, chlorophyll derivatives and vitamin K compounds or influence the flavor of the food such as porphyrin from blood or hypocrellins from *hypocrella bambuase* (Pang et al., 2016).

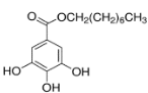
Given these challenges, there is a need to (i) broaden the selection of food-grade sensitizers for food processing applications, (ii) identify compounds with a neutral sensory feature that do not alter food product sensory qualities, and (iii) investigate the ROS generating mechanism as well as the molecular targets of these species in more details. Based on those requirements, we designed this screening study to investigate the effects of combining UV-A irradiation and HFU with three different classes of food-grade compounds, including gallate derivatives, cinnamic acid derivatives, and others (quercetin, flavone, and grape seed extract) on the inactivation of model bacteria *E. coli* O157:H7 and *L. innocua*. These compounds were chosen to demonstrate the impact of different molecular configurations including the changes in carbon chain lengths and the position of functional groups, such as hydroxyls and carboxylates, on ROS production capacity and bacterial inactivation. To investigate the effect of synergistic interaction on bacterial inactivation, both the selected chemical concentrations and the intensity levels of physical treatments are set at sub-lethal levels for the targeted bacteria. In addition to the bacterial inactivation experiments, assays were performed to assess the effect of the combined treatment on cellular targets such as bacterial membrane, intracellular oxidative damage, and enzymatic activity suppression. The results of this study will increase the number of food-grade compounds that can act in tandem with UV-A irradiation and high-frequency ultrasound and improve understanding of mechanisms of inactivation of bacteria by either APDT or ASDT. The findings of this study will aid in evaluation of the potential of APDT and ASDT with food grade compounds to improve food safety, quality, and nutrition retention.

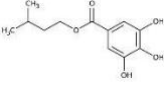
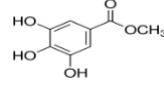
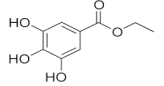
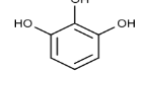
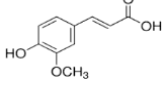
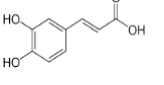
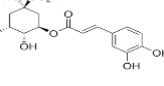
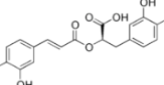
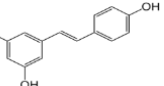
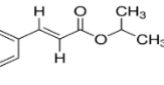
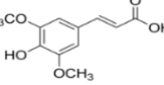
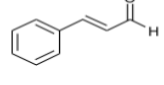
2. Materials and methods

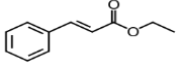
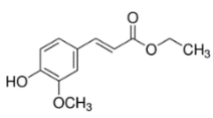
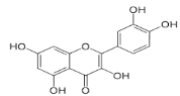
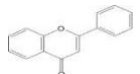
2.1 Reagent

Octyl gallate, isoamyl gallate, methyl gallate, ethyl gallate, pyrogalllic acid, ferulic acid, caffeic acid, chlorogenic acid, rosmarinic acid, resveratrol, isopropyl cinnamate, sinapic acid, trans-cinnamaldehyde, ethyl cinnamate, ethyl ferulate, quercetin, flavone, grape seed extracts, reduced L-glutathione (GSH), sodium chloride (NaCl), sodium dodecyl sulfate (SDS), ethylenediaminetetraacetic acid (EDTA), and Triton X-100 were all obtained from Sigma-Aldrich (St. Louis, MO, USA). Measure-iT™ Thiol Assay Kit, a thiol-reactive fluorescent probe, was purchased from Molecular Probes (Eugene, OR, USA). Zirconia-silica beads (0.1 mm diameter) were acquired from Biospec Products (Bartlesville, OK, USA). Luria-Bertani (LB) broth, tryptic soy broth (TSB), tryptic soy agar (TSA), phosphate-buffered saline (PBS), and Tris-hydrochloride (1M; Tris-HCl) were purchased from Fisher BioReagents (Pittsburgh, PA, USA). Ultrapure water was obtained using a Milli-Q filtration system (EDM Millipore; Billerica, MA, USA). Table 1 summarizes the molecular structure and antimicrobial ability demonstrated by MIC and IC of the compounds used in this study.

Table 1. Structure and antibacterial information of the 18 polyphenols studied

Category	Polyphenol	Chemical structure	MIC		IC ^b
			<i>E. coli</i>	<i>L. innocua</i>	
Gallates	Octyl gallate		~53 mM	~ 63.6 mM	150 μM

	Isoamyl gallate		>532 μM	>532 μM	1.5 mM
	Methyl gallate		2.5 mM	>2.5 mM	1.5 mM
	Ethyl gallate		2 mM	>2.5 mM	1.5 mM
	Pyrogalllic acid		2 mM	>2.5 mM	1.5 mM
Cinnamic acid derivative	Ferulic acid		2.32 mM	>6.44 mM	1.5 mM
	Caffeic acid		1.94 mM	16.1 mM	1.5 mM
	Chlorogenic acid		0.23 mM	0.13 mM	1.5 mM
	Rosmarinic acid		1.4 mM	1.8 mM	1 mM
	Resveratrol		1 mM	2.5 mM	1 mM
	Isopropyl cinnamate		139 μM	>164 μM	100 μM
	Sinapic acid		>2.0 mM	1.3 mM	1.5 mM
	Trans-Cinnamaldehyde		1.89 mM	>1.89 mM	1 mM

	Ethyl cinnamate		203 μM	>203 μM	150 μM
	Ethyl ferulate		>2 mM	>4 mM	1 mM
Others	Quercetin		2 mM	2 mM	1.5 mM
	Flavone		2 mM	2 mM	1.5 mM
	Grape seed extracts	--	--	--	2,000 ppm

^a, Structure and MIC information of the 18 polyphenols in Table 1 were obtained from references (Bordes et al., 2019; Guzman et al., 2014);

^b, IC, implemented concentration in the present study;

--, No information.

2.2 Bacterial strains and culture conditions

Escherichia coli O157: H7 (ATCC 700728, Manassas, VA, USA) and *Listeria innocua* (ATCC 33090, Manassas, VA, USA) are selected as models for the gram-negative and gram-positive bacteria inactivation. Both bacterial strains were modified with a Rifampicin resistance plasmid, allowing the selective cultivation of these strains in Rifampicin-containing culture media. Antibacterial experiments were performed against the stationary phase bacteria as described in a previous study (Huang et al., 2018). The standard plate counting method was used to assess changes in bacterial counts following single treatments of UV-A light irradiation, HFU, and incubation in phenolic compound solution, as well

as the combination of them and the control samples. The treated and control bacterial samples were serially diluted using a Phosphate-Buffered Saline (PBS) solution, followed by overnight cultivation on Rifampicin modified Tryptic Soy Agar (TSA) plates.

2.3 Sample preparation and inoculation

The working concentration of each compound for bacterial inactivation was determined based on their minimal inhibitory concentration (MIC), as suggested in previous studies. Each polyphenol was firstly dissolved in pure ethanol, and then diluted to the final concentration with 2% ethanol which is sublethal to either of the tested bacteria. Then, these solutions were kept in the dark at 4 °C. Then 0.5 mL of bacterial suspension was centrifuged at $13,000 \times g$ and 4 °C for 2 min, and the pellet was resuspended in one mL of fresh-prepared polyphenol solution. For microbial inactivation studies, the pathogen cocktail with a concentration of approximately 10^9 CFU/mL was used. The negative control was the pathogen suspension in sterile water.

2.4 UV-A light-mediated antibacterial activity of selected compounds

UV-A irradiation was performed in a chamber equipped with four lamps (18 W; Actinic BL, Philips, Holland) as previously reported (Erick Falcão de Oliveira, et al., 2018) (Fig. 1A). One mL of bacteria aliquot was removed to a sterile 24-well polystyrene plate. The plate was then exposed to UV-A lamps directly at the center of the chamber for 15 min. The available intensity of UV-A light at the center of the chamber was 6.8 ± 0.2 mW/cm². The controls were cells suspended in water and kept in the dark for 15 min. All the experiments were repeated in triplicate.

2.5 Ultrasound mediated antibacterial activity of selected compounds

A high-frequency ultrasound probe (Chattanooga medical supply, TN, USA) with an ultrasound intensity range between 1 to 2.5 W/cm² and a frequency between 1 to 3 MHz respectively was used. Based on our preliminary experiments and literature related to ASDT topics, a frequency value of 1 MHz

and an intensity level of 1.6 W/cm² were selected. This combination of ultrasound frequency and intensity level was identified as HFU treatment alone. The bacterial sample was inoculated in a 12-well plate and the HFU probe was fixed at a distance of 2 cm from the well plate bottom by a customized platform. The maximum temperature measured during processing in the exposed samples was 38.9 °C. The controls were the cell suspension in water incubated for 15 min. All the experiments were repeated in triplicate.

2.6 Microbial analysis

The plate count method was used to enumerate the number of pathogen cells. After treatment, one mL aliquot of samples was centrifuged at 13,000 ×g for 2 min, washed twice with PBS, and then the bacterial pellet was resuspended in one mL of PBS. The cell suspension was serially diluted with PBS. 0.1 mL of diluent was spread onto tryptic soy agar and incubated at 37 °C for 18±2 h.

2.7 Investigation of the bactericidal mechanism

2.7.1 Detection of exogenous ROS generation using RNO assay

A free radical sensitive dye *N,N*-dimethyl-4-nitrosoaniline (RNO) was added to the testing compound solutions and these solutions were exposed to UV-A irradiation and ultrasound treatment. The production of hydroxyl radical (HO·) and singlet oxygen (¹O₂) when PG was excited by HFU was determined by monitoring *N,N*-dimethyl-4-nitrosoaniline (RNO) bleaching, using a previously reported spectrophotometric method (Pedraza-Chaverrí *et al.*, 2004).

2.7.2 Detection of intracellular ROS generation

The intracellular ROS was quantified by a cellular assay probe the 5-(and-6)-chloromethyl-2',7'-dichlorodihydrofluorescein diacetate (CM-H₂DCFDA; Spectrum Chemical, Gardena, CA, USA) as described by a previous study (Park & Ha, 2020). After treatment, one mL of the pathogen cocktail was subjected to centrifugation (13,000 ×g, 2 min), washed twice with PBS, and finally, the cell pellet was

resuspended in one mL of PBS. The bacterial cells were incubated with CM-H₂DCFDA at a final concentration of 5 µM for 15 min at 37 °C. After incubation, the mixtures were centrifuged at 13,000 ×g for 2 min and washed twice with PBS. The green fluorescence intensity was measured with a spectrofluorometer (Tecan SPECTRAFluor Plus, Switzerland) at excitation and emission wavelengths of 495 and 520 nm, respectively.

2.7.3 Membrane damage measurement

The fluorescent dye propidium iodide (PI; Sigma-Aldrich, MO, USA) was employed to quantitatively evaluate the damage to the cell membrane induced by each treatment (Park & Ha, 2020). PI is a fluorescence probe that is not allowed to penetrate intact plasma membranes, and it only can enter cells with compromised membranes, binding to the nucleic molecule (Li, et al., 2017). Details on the experimental protocol are provided in supplemental materials.

2.7.4 Suppression of enzymatic activity assay

The activity of intracellular enzymes was investigated by using iodinitrotetrazolium chloride (INT; Sigma-Aldrich, MO, USA) as described by a previous study (Park & Ha, 2020). The detailed protocol is provided in the supplementary materials.

2.7 Statistical analysis

Each experiment was conducted in triplicate with duplicate samples. Statistical analyses were performed on the SPSS 20.0 software (SPSS Inc., Chicago, IL). Analysis of Variance (ANOVA) and Tukey's test was used for comparing the significance between the means, and a $P < 0.05$ was considered statistical significance.

3. Results

3.1 Bacterial inactivation effect of APDT and ASDT

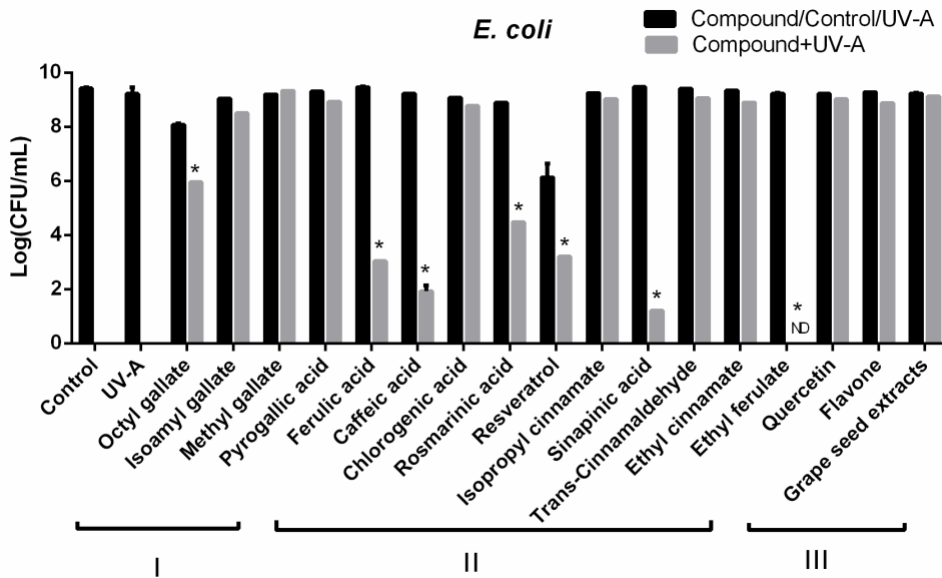
3.1.1 Screening of UV-A light-mediated antibacterial synergism

The efficacy of UV-A irradiation, selected plant based phenolic compounds, and the combined treatment of UV-A+ phenolic compounds for the inactivation of *E. coli* O157:H7 and *L. innocua* is shown in Fig. 1. Most individual compound treatments result in no significant bacterial inactivation ($p > 0.05$), with the exception of resveratrol, which results in a mild 2 log CFU/mL *E. coli* O157:H7 reduction and octyl gallate, which results in a 5 log CFU/mL *L. innocua* reduction. Similarly, treatment with UV-A irradiation single treatment showed no significant bactericidal effect in both tested bacteria ($p > 0.05$). In contrast, when UV-A and various compounds were combined, the inactivation of targeted bacteria was significantly increased ($P > 0.05$) (Fig. 1) compared to either UV-A or phenolic compound treatment alone. The amounts and duration of UV-A irradiation as well as the concentration of phenolic compounds were chosen to cause only limited inactivation (sub-lethal levels) of the target bacteria in order to determine the degree of synergism between the two. In the case of *E. coli* O157:H7, seven compounds out of a total of 18 showed enhanced bactericidal efficacy when coupled with UV-A, compared to five compounds in the case of *L. innocua*. All of the compounds that synergistically inactivated bacteria in combination with UV-A, achieved more than 6 log CFU reduction ($p < 0.01$) in the initial titer of inoculated bacteria (9 log CFU). The 10^9 CFU/mL inoculation level was selected to represent an extreme condition to identify lead compounds with significant potential for the synergistic inactivation of target bacteria. Among the selected compounds, ethyl ferulate, ferulic acid, caffeic acid, and sinapic acid, all of which belong to the cinnamic acid family, inactivated both bacteria when coupled with UV-A irradiation. With more than 9 log CFU inactivation ($p < 0.001$), ethyl ferulate was one of the leading compounds discovered in this screening assay. Rosmarinic acid and resveratrol also achieved a significant inactivation of *E. coli* O157:H7 (5-6 log CFU reduction) in combination UV-A light, but only a limited influence on *L. innocua* inactivation. Octyl gallate, on the other hand, had a significantly higher level of inactivation of *L. innocua*, resulting in 6 log CFU bacterial cell count compared to limited

inactivation of *E. coli* O157:H7. This is the only gallate derivative that works synergistically with UV-A treatment on *L. innocua* while also having a considerable bactericidal effect on *L. innocua* with a 4 log CFU bacterial reduction on its own.

As the goal of this set of experiments was to investigate the synergistic interaction between phenolic compounds and UV-A irradiation, the compounds that had a significant bactericidal effect on their own, such as octyl gallate at the selected concentration levels, were not further investigated. As a result, six compounds were selected that had a synergistic interaction with UV-A inactivating *E. coli* O157:H7, and four compounds were confirmed in the case of *L. innocua*. Ferulic acid, caffeic acid, rosmarinic acid, resveratrol, sinapic acid, and ethyl ferulate are the six photosensitizers associated with *E. coli* O157:H7 inactivation that will be employed in the subsequent sono-sensitivity screening. The four compounds associated with *L. innocua* inactivation are ferulic acid, caffeic acid, sinapic acid, and ethyl ferulate.

A.



B.

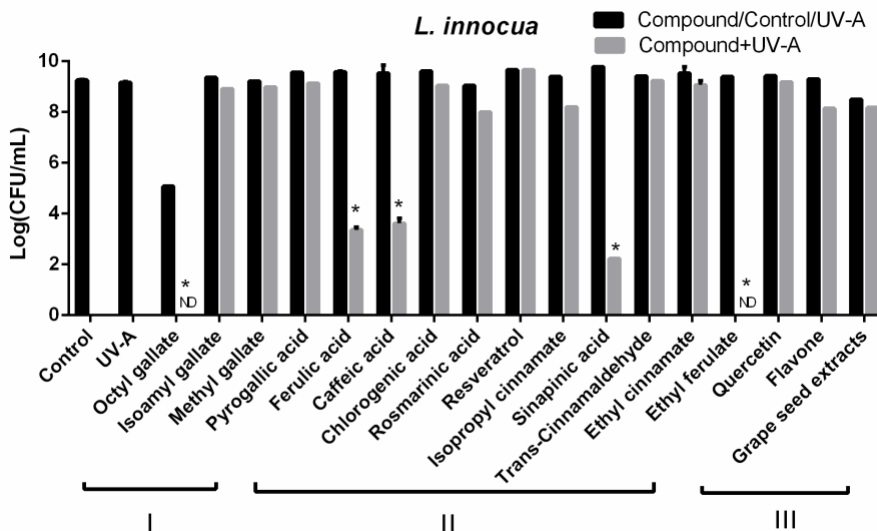


Fig. 5.1 Inactivation of *E. coli* O157:H7 (A) and *L. innocua* (B) by UV-A and three categories. (I) Gallates, (II) Cinnamic acid derivatives, and (III) Others. Each value is the mean of three measurements, plus the standard deviation. The asterisk * indicates a significant difference from the control sample ($P < 0.05$). ND stands for "not detected."

3.2 Ultrasound-mediated antimicrobial activity

The results of the sonosensitizer screening are illustrated in Fig. 2. Single treatment of HFU does not induce bactericidal effect on the targeted bacteria ($p > 0.05$). Similar to the results in Fig. 1, more compounds responded synergistically with HFU to inactivate *E. coli* O157:H7 than the synergistic inactivation of *L. innocua*. Interestingly, ethyl ferulate did not demonstrate any synergistic interaction with ultrasound treatment, as it did with UV-A light irradiation. Both the tested bacteria showed no significant decrease in cell viability after the combined HFU + EF treatment. When combined with HFU, four substances—ferulic acid, caffeic acid, rosmarinic acid, and sinapic acid—achieved a complete 9-log CFU inactivation of *E. coli* O157:H7 ($p < 0.01$). In the case of *L. innocua*, only caffeic acid and sinapic acid have an antibacterial effect when combined with HFU, resulting in a 4-log CFU and 5-log CFU reduction, respectively ($p < 0.05$). Between APDT and ASDT, there are differences in the number of effective

compounds and the degree of their efficacy, which demonstrate how these two approaches operate differently from one another. These operating mechanisms differ depending on the chemical and the type of bacteria being treated.

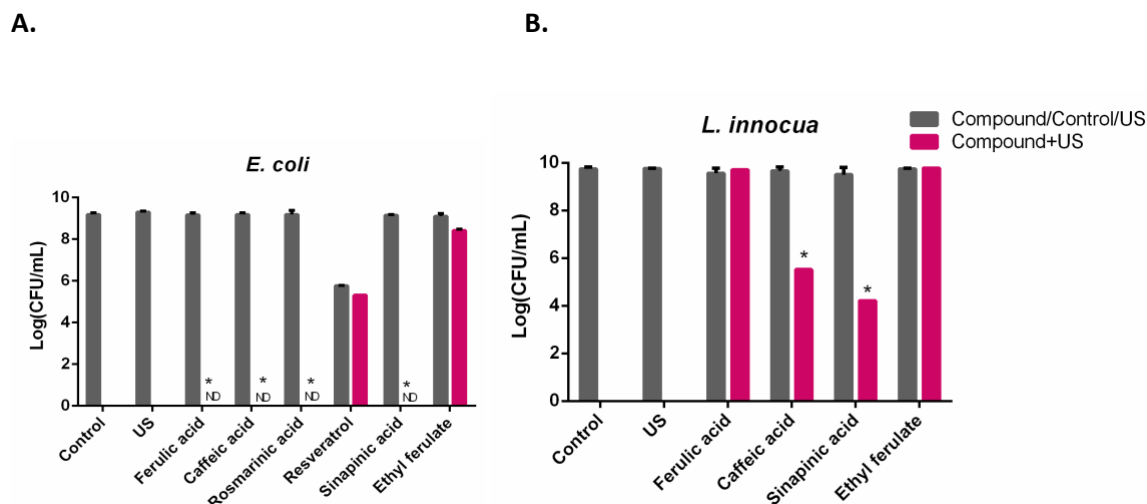


Fig. 5.2 Inactivation of *E. coli* O157:H7 (A) and *L. innocua* (B) by HFU. Each value is the mean of three measurements, plus the standard deviation. The asterisk * indicates a significant difference from the control sample ($P < 0.05$). ND stands for "not detected."

3.3 Mechanisms for photodynamic and sonodynamic inactivation of bacteria

3.3.1 Exogenous ROS generation in photodynamic antimicrobial measurement

One of the main suggested mechanisms for the synergistically antimicrobial activity of the compounds in the presence of light is the generation of ROS (Ghorbani et al., 2018). The four compounds that were effective against both targeted bacteria were selected to test for the presence of this mechanism. The ability to generate the hydroxyl radical (shown in Fig. 3A) and singlet oxygen (shown in Fig. 3B) were both investigated. The results illustrate that sinapic acid, ferulic acid, and caffeic acid generated hydroxyl radicals upon excitation with light and sinapic acid generated the highest level of hydroxyl radicals among these compounds. In contrast, ethyl ferulate generated significantly higher

level of singlet oxygen when being exposed to UV-A light treatment compared to the other compounds. Combined results from Fig. 3 and Fig. 1 suggest the role of exogenous ROS generation in bacterial inactivation in the form of hydroxyl radicals and singlet oxygen generation.

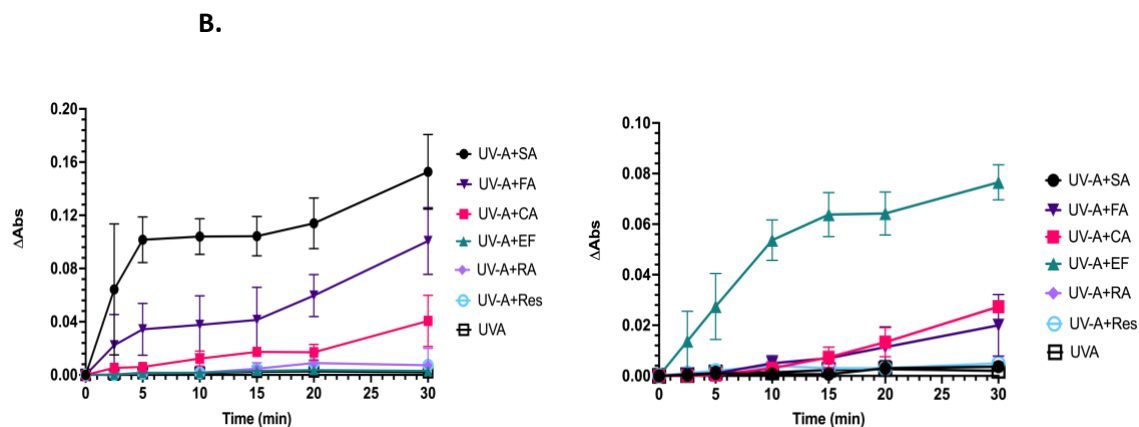


Fig 5.3 OH⁻ radical (A) and singlet oxygen (B) measurement of selected photosensitizer, where RA: rosmarinic acid, Cur: curcumin, FA: ferulic acid, CA: caffeic acid, SA: sinapic acid, EF: ethyl ferulate. Each value is the mean of triplicate measurements with the standard deviation.

3.4 Exogenous ROS generation in ASDT measurement

Figure 4 depicts the results of ASDT-mediated exogenous ROS production. The results illustrate that the combination of HFU and sinapic acid generates significantly more singlet oxygen than other compounds. Following the HFU+SA treatment, the yield of singlet oxygen increased steadily over the course of 30 minutes. (Fig. 4B). In contrast, no substantial quantity of hydroxyl radical production was observed in any of the investigated compounds when paired with HFU treatment (Fig. 4A). The differences in the ROS generation response of compounds with HFU excitation compared to UV-A irradiation suggest the existence of different inactivation mechanisms between these two processes. Thus, significant synergistic activity of sinapic acid with HFU for the inactivation of target bacteria could be attributed to singlet oxygen generation, based on these results in Fig. 4 and the inactivation data in Fig. 2. Sinapic acid was selected for further investigation as this compound was effective against both

target bacteria with UV-A and HFU, although the mechanisms involved in the inactivation may be different.

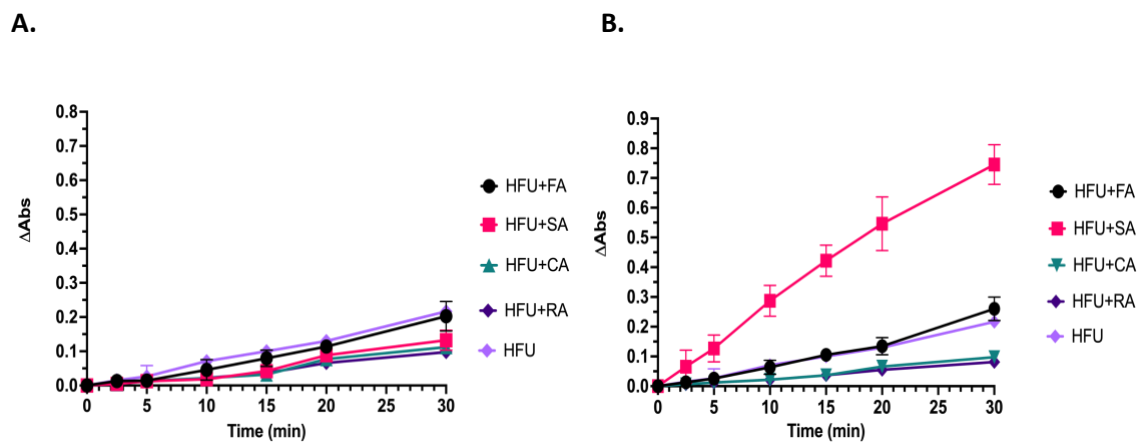


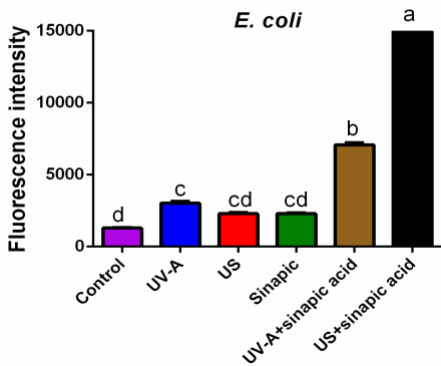
Fig 5.4 OH- (A) and singlet oxygen radical (B) measurement of selected sonosensitizer, where FA: Ferulic acid, SA: Sinapic acid, CA: Caffeic acid, RA: Rosmarinic acid. Each value is the mean of triplicate measurements with the standard deviation.

3.3.1 Intracellular oxidative stress measurement

Intracellular oxidative stress was assessed in order to validate the role ROS-induced lethal effect on bacteria upon treatment with the combination of UV-A radiation or HFU in the presence of SA. The CM-H2DCFDA dye was utilized to assess the intracellular oxidative stress generated by the combination treatments outlined above, and the fluorescence intensity of the oxidized product was measured. Higher fluorescence intensity in this assay corresponds to higher concentration of oxidized product resulting from the intracellular oxidative stress. The results are shown in Fig. 5. Figure 5A shows the enhancement in fluorescence signal upon treatment of *E. coli* bacteria with the combined treatment UV-A+SA compared to UVA or SA alone. The results show that the fluorescence intensity of the combined treatment was twice that of single treatments of either UV-A or SA ($p < 0.01$). Similarly, the combined treatment results in ~30% higher fluorescence intensity ($p < 0.05$) in *L. innocua* (Fig. 5B), compared to the individual treatment of UV-A or sinapic acid.

In contrast, the combination of HFU and sinapic acid only caused considerable oxidative stress in *E. coli* O157:H7 but not in *L. innocua*. In *E. coli* cells, the fluorescence signal when HFU coupled with sinapic acid is substantial, approximately 6 times higher than the single treatments of ultrasound and sinapic acid (Fig. 5A), and around 50% higher than the combined UV-A and sinapic acid treatment ($p < 0.01$). The level of intracellular oxidative damage is consistent with the results from Fig. 3B where a significant exogenous singlet oxygen generation was confirmed when sinapic acid was co-applied with HFU.

A.



B.

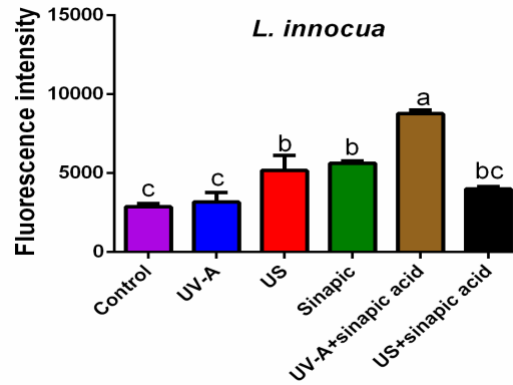


Fig. 5.5 Reactive oxygen species (ROS) levels in *E. coli* and *L. innocua* following different treatments.

Each value is the mean of triplicate measurements with the standard deviation. ND, not detected. The different letter indicates a significant difference among samples ($P < 0.05$)

3.3.2 Membrane damage assessment

Membrane damage was also evaluated to characterize the influence of synergistic treatment of SA with HFU or US compared to the individual treatments using both the selected bacteria. From the results shown in Fig 6A, the combined treatment of HFU+SA significantly increased membrane damage compared to single treatments ($p < 0.05$), in both bacteria. The combined treatment outperforms the HFU or sinapic acid single treatments by more than an order of magnitude in both selected bacteria. This observation reflects a strong synergistic bacterial membrane damage effect compared to individual

treatments. On the other hand, when UV-A was combined with sinapic acid, significant membrane damage ($p < 0.05$) was only observed in the Gram-positive *L. innocua* (Fig. 6B) but not in the Gram-negative *E. coli* O157:H7 (Fig. 6A). The fluorescence intensity when *L. innocua* was treated with the combined UV-A+SA treatment is more than two times higher than the individual treatments. This also resembles the synergistic bacterial membrane damage of the combined UV-A and sinapic acid treatment on the tested *L. innocua*.

In general, this experiment revealed two important observations. First, when compared to UV-A+SA treatment, the combined HFU+SA induced more synergistic membrane damage to the tested bacteria. Second, the Gram-positive *L. innocua* was more susceptible to the combined UV-A+SA treatment than the Gram-negative *E. coli* O157:H7, as evidenced by the fact that the combined UV-A and sinapic acid only affected the *L. innocua*'s membranes.

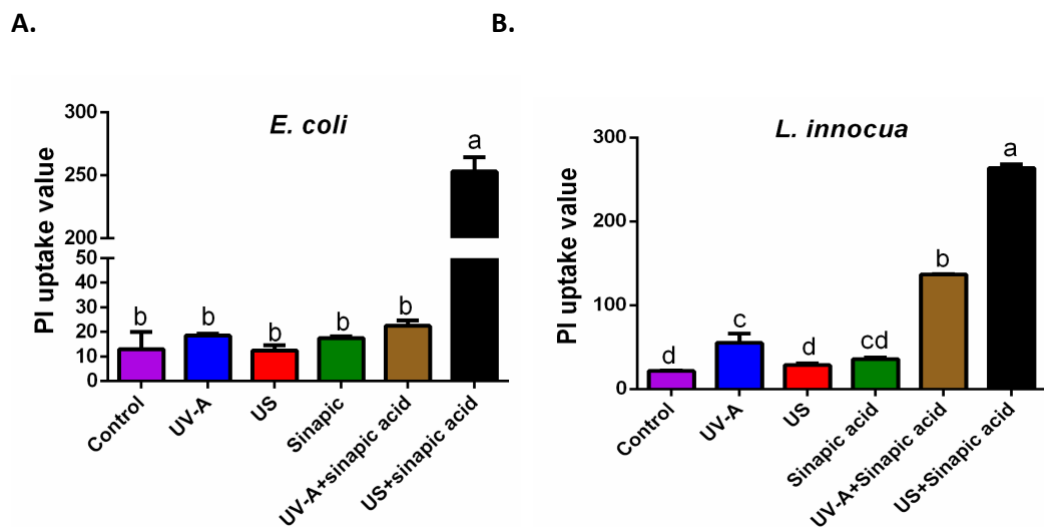
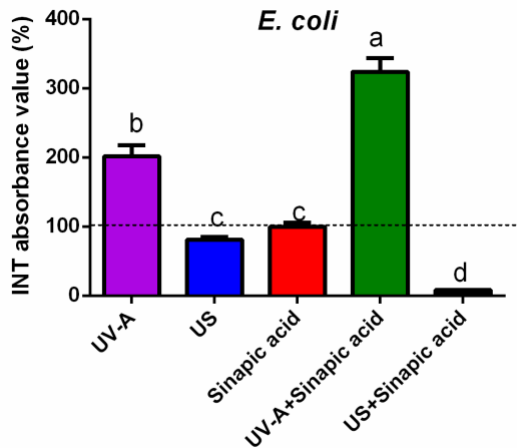


Fig. 5.6 Propidium iodide (PI) uptake values in *E. coli* (A) and *L. innocua* (B) after different treatments. Each value is the mean of triplicate measurements with the standard deviation. ND, not detected. The different letter indicates a significant difference among samples ($P < 0.05$)

3.3.3 Determination of bacterial respiratory dehydrogenase activity

The INT conversion test was utilized to determine the loss of dehydrogenase activity following different treatments (Fig. 7). The activity of bacterial respiratory chain dehydrogenase was verified by monitoring the conversion of colorless INT to red iodonitrotetrazolium formazan (INF) (Jeon & Ha, 2020; Park & Ha, 2020). The decreasing spectrophotometric value of INF indicates the loss in dehydrogenase activity. The combination of HFU and sinapic acid significantly ($p < 0.05$) reduced the dehydrogenase activity in both tested bacteria. This reduction in enzyme activity after the combined treatments of HFU+SA, was significantly higher than the individual treatments effect indicating the presence of synergistic interaction. On the other hand, the combined UV-A and sinapic acid caused a significant reduction ($p < 0.05$) of dehydrogenase activity in *L. innocua* (Fig. 7B) but not in *E. coli* O157:H7 (Fig. 7A). This reduction in *L. innocua* (Fig. 7B) was significantly greater than the effect of either UV-A or sinapic acid treatments alone, indicating a synergistic effect. Interestingly, the combined UV-A+SA and single treatment of UV-A increased the activity of dehydrogenase in *E. coli* O157:H7 (Fig. 7A) indicating the presence of self-defending mechanisms.

A.



B.

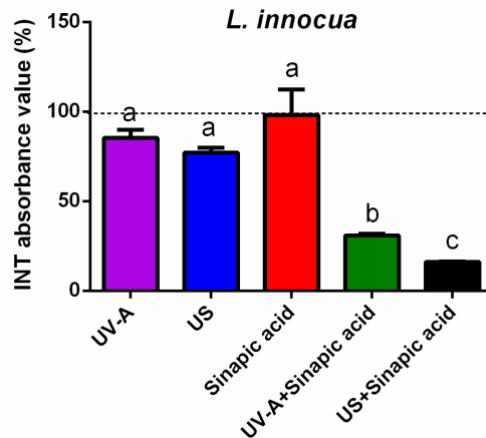


Fig. 5.7 Levels of intracellular enzyme inactivation in *E. coli* (A) and *L. innocua* (B) cells treated with different treatments. Each value is the mean of triplicate measurements with the standard deviation. ND, not detected. The different letter indicates a significant difference among samples ($P < 0.05$)

4. Discussion

4.1 Bacterial inactivation

As seen in Fig. 1, the combination of UV-A and the cinnamic acid derivatives significantly enhanced bacterial inactivation, resulting in an average of 8 to 9-log bacterial reduction. This level of bacterial reduction within 15 minutes of treatment time is comparable when compared with other more established PSs such as synthetic phenothiazinium dyes including toluidine blue (TB) and rose bengal (RB), natural pigment such as porphyrin derivatives as well as natural PSs includes coumarins, benzofurans, anthraquinones, and flavin derivatives. The dyes in phenothiazinium class are among the first generation of PSs and could reduce levels of both the Gram-negative (*E. coli*, *A. baumannii*) and Gram-positive (*S. aureus*, *MSSA*) bacteria in the range of ~3-5 logs reduction within 10 min of treatment time (Liu et al., 2015, Donnelly et al., 2009; Tardivo et al., 2005, Cahan et al., 2010; Vecchio et al., 2014). The concentrations used are considerably low, ranging from 10 - 800 μM , since the compounds in the phenothiazinium group are strong singlet oxygen generator (Ghorbani et al., 2018). Furthermore, one major drawback is that these synthetic dyes were not originally intended for use in food processing; rather, they were developed for the treatment of bacterial infections and cancers in vivo (Liu et al., 2015). Porphyrin is another well-known photosensitizer that has strong antimicrobial properties when combined with light or UV sources, inactivating both the Gram-negative (Alenezi et al., 2017; Alves et al., 2009) (*E. coli*, *P. aeruginosa*) and Gram-positive (Banfi et al., 2006; Sobotta et al., 2019; Zhuang et al., 2014) (*S. aureus*, *S. warneri*) bacteria with a level of effectiveness ranging from 1 to 4 log bacterial reduction (Sobotta et al., 2019) within 5 minutes of treatment time and a concentration of 10 - 100 μM .

Advantages like a high rate of singlet oxygen production and easy chemical modification make Porphyrins one of the most commonly used PSs. However, similar to the phenothiazinium group, porphyrin does not have food-grade status which prevent the utilization of this chemical class in food (Liu et al., 2015).

Unlike the synthetic dye PSs or porphyrin group of compounds, the natural PSs are considered less toxic to mammalian cells in several cell culture and animal studies (Ghorbani et al., 2018). The natural compounds including hypericin and curcumin have been extensively studied as photosensitizer over the years (Ghorbani et al., 2018). Curcumin is a cinnamic acid derivative that has been shown to have photo-induced antibacterial effects in gram-negative and gram-positive bacteria in our earlier research (de Oliveira, Tikekar, et al., 2018; de Oliveira, Tosati, et al., 2018), with a 5-log reduction in both model gram-negative and gram-positive bacteria. Other studies report that curcumin is capable of inhibiting drug-resistant bacterial strains through a photo-inactivation effect with more than 3-log bacterial reduction (Ribeiro et al., 2013). *S. aureus* is one of the most common resistant bacteria to antibiotic therapy which remains susceptible to curcumin-mediated inactivation (Ribeiro et al., 2013). Curcumin has demonstrated some antibacterial properties in absence of light irradiation by binding to *FtsZ* proteins and inhibiting the assembly of *FtsZ* protofilament in *Bacillus subtilis* (Rai et al., 2008). The current study broadened the discovery of PSs to include additional members of the cinnamic acid family in addition to curcumin, leading to a 9-log reduction in bacterial inactivation. The compounds used in this study are food-grade molecules that are often used as antioxidants in food processing.

In terms of the influence of bacterial phenotypes on APDT efficacy, most PSs studies using both types of bacteria found that gram-negative bacteria are more resistant to PSs than gram-positive bacteria since bacterial efflux pumps decrease PSs concentration in bacterial cells (Spengler et al., 2014; Tegos & Hamblin, 2006). This decreased concentration buys time for the antioxidant machinery of the bacteria to activate, resulting in less inactivation (Spengler et al., 2014). In this investigation, we found

that the gram-positive *L. innocua* was more resistant to APDT and ASDT than the gram-negative *E. coli* O157:H7, with seven compounds inactivating the *E. coli* strain in APDT compared to five compounds inactivating *L. innocua*, and four versus two in ASDT. The thicker peptidoglycan component of the *L. innocua* cell envelope may help to shield the cells from the combined therapy (Nguyen et al., 2021; Schleifer & Kandler, 1972). The higher susceptibility of gram-negative *E. coli* O157: H7 was explained in previous studies that looked at the partitioning of polyphenolic sensitizer to the bacterial outer membrane layer, weakening its structure, altering fluidity, and enhancing sensitizer uptake into the bacterial cytoplasm (E. Alves et al., 2013; de Oliveira et al., 2021; Nguyen et al., 2021; Yang et al., 2019).

Regardless of the type of targeted bacteria, there were compounds from our pool of cinnamic acid derivatives that works against both types of bacteria including ethyl ferulate, ferulic acid, caffeic acid, and sinapic acid, all of which belong to the cinnamic acid family. These compounds exhibit $\log P$ values of 2.41 for ethyl ferulate, 1.51 for ferulic acid, 1.53 for caffeic acid, and sinapic acid (Chemaxon database). The $\log P$ value is a physicochemical parameter that must be considered while designing new biochemicals such as photosensitizers and sonosensitizers (Chandrasekaran et al., 2018) because it has been shown to have a substantial influence on certain pharmacokinetic parameters such as ADMET (absorption, distribution, metabolism, excretion, and toxicity). Sensitizers with moderate to high lipophilicity (moderate to high $\log P$) are increasingly being developed to meet the needed potency against bacterial infection (Armstrong et al., 2017). The requirement arose primarily as a result of the lipid composition of bacterial targets (Chandrasekaran et al., 2018). High lipophilicity ($\log P > 5$) frequently contributes to high metabolic turnover, low solubility, and poor absorption, whereas compounds with a moderate $\log P$ (between 1 and 4), ideal value is 1.34 - 1.8, are more likely to have optimum physicochemical and ADME properties (Armstrong et al., 2017). As a result, the four most robust cinnamic acid derivatives' moderate $\log P$ values (1.5 - 2.4) will maximize their affinity and partition into the target bacterial membrane, enhancing the efficiency of the physical treatments.

Of six photosensitizers confirmed in UV-A treatment, there were four retained their antimicrobial effectiveness when combined with HFU. The proposed idea that a photosensitizer can also serve as a sonosensitizer, as stated in other investigations (Ghorbani et al., 2018; Pang et al., 2016; Yoon et al., 2013), is not universal and depends on the nature of the photosensitizer. Ultrasound has typically been used in conjunction with physical treatments such as thermal treatment (thermosonication) and high pressure (manosonication) or chemical disinfectants such as chlorine or quaternary ammonium compounds to increase bactericidal efficiency (Evelyn & Silva, 2015; Guzel et al., 2014; Lee et al., 2009; Paga'n et al., 1999; Ross et al., 2003). However, physical treatments and chemical sanitizers have inherent disadvantages in that they affect the nutritional and sensory quality aspects of food products (Awuah et al., 2007; Barbosa-Cánovas & Rodríguez, 2002; Simpson, 2009). Not to mention the incompetency of these combination treatments, which only achieved a 2 to 3-log bacterial reduction and required a longer treatment time of 30 to 60 minutes (Arroyo & Lyng, 2017; Ashokkumar, 2015; Barbosa-Cánovas & Rodríguez, 2002). In this study, when coupled with HFU, the four compounds ferulic acid, caffeic acid, rosmarinic acid, and sinapic acid reduced bacterial counts by 9 log CFU after 15 minutes. Previous research that paired curcumin with high frequency with similar ultrasonic frequency and intensity found a similar fast inactivation (Wang et al., 2014, 2015). There was a significant 6 log bacterial reduction observed (Wang et al., 2014, 2015). Even though fewer compounds were found to work with HFU compared to UV-A light, HFU still exhibits several distinct advantages. Ultrasonic irradiation is superior to light irradiation in that the applied energy can be focused precisely on the specific pathological location requiring treatment. In addition, ultrasound is a type of mechanical wave that can penetrate tissues to a greater extent than light. As a result, SDT can be used to treat deeply located diseases (Tachibana et al., 2008) Moreover, studies have shown that high-frequency and low-intensity ultrasound can alter the cell membrane, thus increasing its permeability to sonosensitizers (Gao et al., 2014; Rahimi et al., 2014).

In summary, the APDT and ASDT approach used in this study proved to be a very strong platform, with bacterial reductions of 8 to 9-log CFU. In comparison to *E. coli* O157:H7, gram-positive *L. innocua* was more resistant to the combined treatment. Finally, there are photosensitizers with sonosensitizing capacity, four with *E. coli* O157:H7 inactivation, and two with *L. innocua* inactivation.

4.2 Molecular configuration effect on ROS generation in APDT and antimicrobial ability

The lead compounds that inactivated both bacteria when paired with UV-A irradiation, based on the inactivation data, include ethyl ferulate, ferulic acid, caffeic acid, and sinapic acid, all of which belong to the cinnamic acid family. Based on a comparison of the structural features of the various phenolic acid groups, the presence of a propionic acid side chain (-CH=CH-COOH) in ethyl ferulate, ferulic acid, caffeic acid, and sinapic acid considerably boosts their synergistic antibacterial action (de Oliveira et al., 2021; Plaetzer et al., 2009). The double bond in the -CH=CH-COOH sidechain of the four cinnamic acid derivatives could stabilize the phenolic free radical via resonance (Baptista et al., 2017; Eslami et al., 2010; Yoon et al., 2013). When compared to other gallate group compounds with longer side chains, the -CH=CH-COOH may have a lesser electron-withdrawing capacity. As a result, the electron density of benzene rings is higher, and the dissociation energy of phenolic hydroxyl bonds is substantially lower (Baptista et al., 2017). As a result, cinnamic acid derivatives have a greater electron-donating capability. According to Functional Density Theory calculations (Giacomelli et al., 2004; Saqib et al., 2015), -CH=CH-COOH side chains reduce the ionization potential (IP) of cinnamic acid derivatives and enhance their HOMO energy when compared to benzoic acid derivatives. Due to combination of these two parameters, cinnamic acid derivatives outperform gallate derivatives in terms of electron-donating capabilities, resulting in a significantly higher synergistic interaction with UV-A irradiation.

In addition to the influence of the carboxylic acid side chain, the bacterial inactivation ability of cinnamic acid derivatives is linked to the aromatic ring's hydroxylation and methoxylation patterns (Zeb, 2021).

The amount and position of both the methoxyl and hydroxyl groups have a major impact on antibacterial efficacy (Koroleva et al., 2014). Within the four cinnamic acid derivatives, there are three levels of aromatic substitution: *p*-*dihydroxy* (caffeic acid), *p*-*hydroxymethoxy* (ferulic acid), and *p*-*hydroxydimethoxy* (sinapic acid). According to structure-activity relationships and DFT analysis (Natella et al., 1999; Zeb, 2021), the electron-donating sequence is *p*-*dihydroxy* (caffeic acid) < *p*-*hydroxymethoxy* (ferulic acid) < *p*-*hydroxydimethoxy* (sinapic acid), with a comparable order of antimicrobial effectiveness. This effect is supported by the results of Fig. 2 and the DFT calculation from the literature (Giacomelli et al., 2004; Saqib et al., 2015). When combined with the results from Fig. 3A, the order of ROS formation is sinapic acid followed by ferulic acid and caffeic acid. This is in line with the inactivation result in Fig. 1, which revealed sinapic acid had a stronger bactericidal ability when paired with UV-A irradiation.

The ability of ethyl ferulate to generate a much greater amount of singlet oxygen, as seen in Fig. 3B, is an example of a type II photosensitizer (Baptista et al., 2017). In Type II reactions, energy is transferred directly between the excited PS and the ground-state molecular oxygen, producing singlet oxygen that can interact with a large number of molecules in the cell to form oxidized products and cause cell death (F. Alves et al., 2021). The higher level of singlet oxygen generated by ethyl ferulate could partly explain the higher inactivation effect of ethyl ferulate (Fig. 1A) since singlet oxygen is considered the stronger form of radical compared to hydroxyl radical (Nakamura et al., 2012; Wang et al., 2017). To the best of our knowledge, this is the first study to reveal such behavior from ethyl ferulates, which are typically utilized as an antioxidant (Cunha et al., 2019; Nazaré et al., 2014). Due to its potential to transmit energy to other substances as an antioxidant, an antioxidant may change into a pro-oxidant molecule, resulting in significant ROS production under some circumstances (Eghbaliferiz & Iranshahi, 2016; Fukumoto & Mazza, 2000; Mazza, 2016; Saqib et al., 2015). This is a dose-dependent effect that requires the presence of chelating metals like Cu²⁺ or Mn²⁺ (Eghbaliferiz & Iranshahi, 2016).

In this situation, however, such a condition did not exist; instead, the stimulating effect of UV-A irradiation was present. To explain this phenomenon, further structure-activity correlations and DFT research is required.

4.3 ROS generation in ASDT and antimicrobial ability

The amount of singlet oxygen created by sinapic acid and HFU was much larger than that of other cinnamic derivatives. This was supported by Figs. 2A and 2B, which showed that cinnamic acid combined with HFU increased bacterial inactivation in *E. coli* O157:H7 and *L. innocua*. Sonoluminescence, which occurs as a result of acoustic cavitation, produces spectra similar to UV-A in the 400 nm range and excites sonosensitizer to form singlet oxygen ($^1\text{O}_2$), which is a well-known phenomenon (Kanthale et al., 2008). Previous research has revealed that singlet oxygen ($^1\text{O}_2$) has a major role in the inactivation of bacteria using a combination of sonosensitizers such as porphyrin, chlorin-e6, and rose bengal derivatives and the ultrasound treatment (Costley et al., 2017; Xu et al., 2016, p. 6; Zhuang et al., 2014). The results of this study illustrate that the combination of sinapic acid with HFU enhanced the generation of singlet oxygen (Fig. 2) which can induce oxidative stress in bacterial cells. Singlet oxygen can be produced in the extracellular environment from unbound sinapic acid molecules, as shown in Fig. 4B, or in the intracellular environment when sinapic acid partitioned into the bacterial cell wall and caused oxidative stress, as shown in Fig. 5A. Since singlet oxygen has a relatively short life time (10-320 ns) and a limited diffusion distance within the cell membrane of just 10-55 nm (Kvam and Benner, 2020), it is critical that a sonosensitizer have a good membrane partitioning capacity to maximize intracellular singlet oxygen formation. The improved partitioning ability of a sonosensitizer may arise from an optimized $\log P$ from 1 to 4 as discussed in the preceding section, or from the mass transfer effect of HFU. The later may play a more important role as HFU induced mass transfer (Arroyo & Lyng, 2017; Sango et al., 2014) can drive the sonosensitizer into a greater distant into bacterial membrane and potentially into cell cytoplasmic environment, resulted in an increasing

oxidative stress on the bacteria. This mass diffusion effect is not present in UV-A treatment (Birmpa et al., 2013), giving the HFU treatment a distinct advantage. In both APDT and ASDT, sinapic acid consistently outperformed other selected cinnamic derivatives and was the greatest photo and sonosensitizer in this investigation.

4.4 Biological change in bacteria after APDT and ASDT

The physiochemical responses of the targeted bacteria to the combined UV-A+SA and HFU+SA treatments are discussed in further detail in the sections that follow, including intracellular oxidative stress, membrane damage, and enzymatic activity suppression. We found an intriguing "cause and effect" relationship between the physiological reactions, wherein membrane damage might directly lead to intracellular oxidative stress and could also be a factor in the inactivation of membrane-associated dehydrogenase enzyme families. The various physiochemical reactions of the treated bacterial cells are not independent, unrelated occurrences, but rather interrelated processes.

4.4.1 Intracellular oxidative stress and membrane damage relationship

One of the proposed mechanisms for both photo and sonodynamic cytotoxic effects is the formation of ROS via the excitation of sensitizers by UV-A irradiation and sono-sensitization with ultrasound treatment (E. Alves et al., 2013; Costley et al., 2017). The generated ROS include singlet oxygen, hydroxyl radicals, the superoxide anion, and hydrogen peroxide (Costley et al., 2017; Dadjour et al., 2006; Giuntini et al., 2018; Guo et al., 2013; Nakonechny et al., 2013; Nakonieczna et al., 2018; Pang et al., 2016; Yumita et al., 2007). In a biological environment, high levels of these ROS species can stimulate oxidative stress on intracellular molecules and induce cell damage, leading to cell death (Harris et al., 2014). Enhanced ROS generation in *E. coli* O157:H7 treated with UV-A+SA or HFU+SA may be one of the possible mechanisms underlying the enhanced bactericidal effect of the combined treatments. Furthermore, the quantum yield of singlet oxygen following the combination of HFU+SA was

significantly higher than that of UV-A+SA (Fig. 3B and Fig. 4B). These results correlated with the higher oxidative stress that *E. coli* O157:H7 cells experienced following the HFU+SA compared to the UV-A treatment. Oxidative stress that cell experiences could be a product of membrane damage, especially in gram-negative bacteria species like *E. coli* O157:H7 (Stark, 2005; Yang et al., 2019). The bacterial membrane damage could result from the extracellular ROS generated by the combined HFU+SA treatment or by the mechanical effects of the physical treatments. The higher oxidative stress that *E. coli* O157:H7 experienced after HFU+SA treatment could be attributed to the fact that the combination generated more membrane damage than the UV-A+SA combination, as evidenced by the data in Fig. 6A. Thus in *E. coli* cells, both the higher singlet oxygen generation by the combined HFU+SA treatment and the higher membrane damage effect caused by the mechanical action of the HFU treatment can explain the resultant higher intracellular oxidative stress compared to the UV-A+SA treatment.

In contrast, *L. innocua* experiences less oxidative stress in HFU+SA treatments compared to UV-A+SA treatments, which could be attributed to *L. innocua* being more protected against ultrasonic mechanical effects. In a study that looked at the combination of curcumin and UV-A irradiation, *L. innocua* was found to be more susceptible to the combined UV-A+curcumin treatment than *E. coli* O157:H7, which could be due to the higher level of membrane damage that *L. innocua* experiences following UV-A treatment (de Oliveira, Tosati, et al., 2018). In contrast, in our previous study, *L. innocua* demonstrated a higher resistance than *E. coli* O157:H7 to the combined ultrasound and propyl gallate treatment as a result of *L. innocua* being better shielded from the mechanical effect of HFU treatment (Nguyen et al., 2021). A thicker and more rigid peptidoglycan layer as part of the *L. innocua* cell envelope, as opposed to a much thinner outer membrane comprised primarily of phospholipid in *E. coli* O157:H7, could explain *L. innocua*'s higher resistance to HFU treatment. (E. Alves et al., 2013; Clementi et al., 2014; Epand & Epand, 2009; Runyan et al., 2006; Stark, 2005; Yang et al., 2019). The thicker

peptidoglycan in *L. innocua* membrane could also prevent the penetration of exogenous single oxygen species and result in better protection against oxidative stress and membrane damage.

4.4.2 Enzymatic activity

In general, when bacteria are exposed to stressful circumstances that can damage respiratory enzyme systems, such as those caused by the APDT or ASDT, the bacteria may not be able to restore redox equilibrium and balance electron fluxes to fulfill metabolic and energetic demands of a cell and resulting in inactivation of cells, (Kaila & Wikström, 2021). Respiration has been linked to bacterial diseases such as tuberculosis and listeriosis (a condition caused by the foodborne bacterium *Listeria monocytogenes*) (Lugo, 2022). Previous studies showed that targeting the dehydrogenase enzyme system could render bacterial inactivation. Examples include the use of UV-A to damage the hydrogenase of *E. coli* K12 wide type (Bosshard, 2010) and the use of antibiotics to damage the hydrogenase of *L. monocytogenes* (Rivera-Lugo et al., 2022).

Figures 7A and 7B illustrate that the effect on the dehydrogenase enzyme system is not uniform and varies depending on the bacteria and the treatments. The activities of the dehydrogenase enzyme were increased in *E. coli* O157:H7 in both single UV-A and combination UV-A+SA treatments, with the latter treatment having a synergistic effect on enhancing enzymatic activity. Since UV-A is a mild treatment, *E. coli* cells may have ample time to boost the synthesis of dehydrogenase enzymes in order to improve energy production to feed defensive systems and preserve cellular homeostasis (E. Alves et al., 2013; Bosshard et al., 2010). However, when UV-A was coupled with SA treatment, membrane damage started to play a more critical role. Because the dehydrogenase enzymes are membrane-associated, they could be released into the medium after membrane damage/lysis and interact with the INT substrate, increasing the fluorescence signal, as seen in Fig. 7A. In contrast, ultrasound is well known for its enzyme inactivation effect (Arroyo & Lyng, 2017; Huang et al., 2017). The released dehydrogenase enzymes from *E. coli*'s cell membrane could be inactivated by the combined effect of mechanical actions

of HFU and the protein denaturation effect of the acidic state generated by SA, resulting in a decline in fluorescence intensity, as shown in Fig. 7A. In *L. innocua*, however, both UV+SA and HFU+SA treated samples revealed a similar pattern of decreased enzymatic activity following the combined treatments. Unlike *E. coli* O157:H7, which has a more extensive dehydrogenase group that includes NDH-1, NDH-2, succinate dehydrogenase, D-lactate dehydrogenase, and formate dehydrogenase (Shepherd & Poole, 2013), *Listeria* cells can only rely on NDH-2 to feed electrons into the respiratory chain (Russell, 2022). This difference in enzymatic composition could explain why *L. innocua* was unable to boost its respiratory enzymatic activity in order to counteract the UV-A+SA-induced stress. Nonetheless, HFU+SA causes a substantial reduction in enzymatic activity in *L. innocua*, as seen in Fig. 7B. The results shown in Figs. 7A and 7B showed that HFU treatment outperformed UV-A treatment in reducing respiratory enzymatic activities on both gram-negative *E. coli* O157:H7 and gram-positive *L. innocua*. In addition, the results of *E. coli* enzymatic inactivation (Fig. 7A) demonstrated that membrane damage could result in the release and inactivation of membrane-bound dehydrogenase enzymes, contributing to the overall inactivation effect of the combined treatments.

5. Conclusions

Among the 18 chemicals tested, cinnamic acid derivatives displayed the highest bacterial inactivation efficacy (8-9 log CFU reduction) in both the tested gram-negative and gram-positive bacteria, in both APDT and ASDT processes. Six photo-activated compounds were discovered to have a synergistic interaction with UV-A inactivating *E. coli* O157:H7, and four compounds were confirmed in the case of *L. innocua*. In comparison to UV-A treatment, there were fewer compounds in the cinnamic acid family that could also work synergistically with HFU treatment. The differences between *E. coli* O157:H7 inactivation and *L. innocua* inactivation are significant, with the gram-negative bacterium demonstrating more susceptibility toward ASDT. These discrepancies in antibacterial activity between treatments or strains suggested a different mode of action for APDT and ASDT. We discovered a "cause

and effect" relationship between the physiochemical responses of the targeted bacteria to the combined UV-A+SA and HFU+SA treatments, where intracellular oxidative stress could be a direct result of membrane damage, and membrane damage could also contribute to the inactivation of membrane-associated dehydrogenase enzyme families. The inactivation and bacterial response to the combined treatments are the results of a complex process that has yet to be fully understood, requiring further research into elements such as bacterial gene expression and regulation in stressful conditions caused by the combination treatments. Nonetheless, the robust bacterial inactivation and the food-grade nature of the screened compounds could facilitate the adaptation of APDT and ASDT in the food industry.

Acknowledgments

This project was supported by the Agriculture and Food Research Initiative by grant no. 2014-67017-21642 from the USDA National Institute of Food and Agriculture (USDA-NIFA) Program in Improving Food Quality (A1361) and by grant no. 2015-68003- 23411 from the USDA-NIFA Program Enhancing Food Safety through Improved Processing Technologies (A4131).

Bibliography

- Cunha, F. V. M., Coelho, A. G., Azevedo, P. S. da S., da Silva, A. A., Oliveira, F. de A., & Nunes, L. C. C. (2019). Systematic review and technological prospection: Ethyl ferulate, a phenylpropanoid with antioxidant and neuroprotective actions. *Expert Opinion on Therapeutic Patents*, 29(2), 73–83. <https://doi.org/10.1080/13543776.2019.1568410>
- Ghorbani, J., Rahban, D., Aghamiri, S., Teymouri, A., & Bahador, A. (2018). Photosensitizers in antibacterial photodynamic therapy: An overview. *Laser Therapy*, 27(4), 293–302. https://doi.org/10.5978/islsm.27_18-RA-01

- Koroleva, O., Torkova, A., Nikolaev, I., Khrameeva, E., Fedorova, T., Tsentalovich, M., & Amarowicz, R. (2014). Evaluation of the Antiradical Properties of Phenolic Acids. *International Journal of Molecular Sciences*, *15*(9), 16351–16380. <https://doi.org/10.3390/ijms150916351>
- Liu, Y., Qin, R., Zaat, S. A. J., Breukink, E., & Heger, M. (2015). Antibacterial photodynamic therapy: Overview of a promising approach to fight antibiotic-resistant bacterial infections. *Journal of Clinical and Translational Research*, *1*(3), 140–167. <https://doi.org/10.18053/jctres.201503.002>
- Natella, F., Nardini, M., Di Felice, M., & Scaccini, C. (1999). Benzoic and Cinnamic Acid Derivatives as Antioxidants: Structure–Activity Relation. *Journal of Agricultural and Food Chemistry*, *47*(4), 1453–1459. <https://doi.org/10.1021/jf980737w>
- Nazaré, A. C., de Faria, C. M. Q. G., Chiari, B. G., Petrônio, M. S., Regasini, L. O., Silva, D. H. S., Corrêa, M. A., Isaac, V. L. B., da Fonseca, L. M., & Ximenes, V. F. (2014). Ethyl Ferulate, a Component with Anti-Inflammatory Properties for Emulsion-Based Creams. *Molecules*, *19*(6), 8124–8139. <https://doi.org/10.3390/molecules19068124>
- Pang, X., Xu, C., Jiang, Y., Xiao, Q., & Leung, A. W. (2016). Natural products in the discovery of novel sonosensitizers. *Pharmacology & Therapeutics*, *162*, 144–151. <https://doi.org/10.1016/J.PHARMTHERA.2015.12.004>
- Trendowski, M. (2014). The promise of sonodynamic therapy. *Cancer and Metastasis Reviews*, *33*(1), 143–160. <https://doi.org/10.1007/s10555-013-9461-5>
- Zeb, A. (2021). *Phenolic Antioxidants in Foods: Chemistry, Biochemistry and Analysis*. Springer International Publishing. <https://doi.org/10.1007/978-3-030-74768-8>

- Alenezi, K., Tovmasyan, A., Batinic-Haberle, I., & Benov, L. T. (2017). Optimizing Zn porphyrin-based photosensitizers for efficient antibacterial photodynamic therapy. *Photodiagnosis and Photodynamic Therapy*, *17*, 154–159. <https://doi.org/10.1016/j.pdpdt.2016.11.009>
- Alves, E., Costa, L., Carvalho, C. M., Tomé, J. P., Faustino, M. A., Neves, M. G., Tomé, A. C., Cavaleiro, J. A., Cunha, Â., & Almeida, A. (2009). Charge effect on the photoinactivation of Gram-negative and Gram-positive bacteria by cationic meso-substituted porphyrins. *BMC Microbiology*, *9*(1), 70–70. <https://doi.org/10.1186/1471-2180-9-70>
- Alves, E., Santos, N., Melo, T., Maciel, E., Dória, M. L., Faustino, M. A. F., Tomé, J. P. C., Neves, M. G. P. M. S., Cavaleiro, J. A. S., Cunha, Â., Helguero, L. A., Domingues, P., Almeida, A., & Domingues, M. R. M. (2013). Photodynamic oxidation of Escherichia coli membrane phospholipids: New insights based on lipidomics. *Rapid Communications in Mass Spectrometry*, *27*(23), 2717–2728. <https://doi.org/10.1002/rcm.6739>
- Alves, F., Ayala, E. T. P., & Pratavieira, S. (2021). Sonophotodynamic Infection: The power of light and ultrasound in the battle against microorganisms. *Journal of Photochemistry and Photobiology*, 100039. <https://doi.org/10.1016/j.jpap.2021.100039>
- Armstrong, D., Li, S., Friauff, W., Martus, H.-J., Reilly, J., Mikhailov, D., Whitebread, S., & Urban, L. (2017). 2.04 - Predictive Toxicology: Latest Scientific Developments and Their Application in Safety Assessment. In S. Chackalamannil, D. Rotella, & S. E. Ward (Eds.), *Comprehensive Medicinal Chemistry III* (pp. 94–115). Elsevier. <https://doi.org/10.1016/B978-0-12-409547-2.12367-4>
- Arroyo, C., & Lyng, J. G. (2017). The Use of Ultrasound for the Inactivation of Microorganisms and Enzymes. In *Ultrasound in Food Processing* (pp. 255–286). John Wiley & Sons, Ltd. <https://doi.org/10.1002/9781118964156.ch9>

- Ashokkumar, M. (2015). Applications of ultrasound in food and bioprocessing. *Ultrasonics Sonochemistry*, 25(1), 17–23. <https://doi.org/10.1016/j.ultsonch.2014.08.012>
- Awuah, G. B., Ramaswamy, H. S., & Economides, A. (2007). Thermal processing and quality: Principles and overview. *Chemical Engineering and Processing: Process Intensification*, 46(6), 584–602. <https://doi.org/10.1016/j.cep.2006.08.004>
- Banfi, S., Caruso, E., Buccafurni, L., Battini, V., Zazzaron, S., Barbieri, P., & Orlandi, V. (2006). Antibacterial activity of tetraaryl-porphyrin photosensitizers: An in vitro study on Gram negative and Gram positive bacteria. *Journal of Photochemistry and Photobiology B: Biology*, 85(1), 28–38. <https://doi.org/10.1016/j.jphotobiol.2006.04.003>
- Baptista, M. S., Cadet, J., Di Mascio, P., Ghogare, A. A., Greer, A., Hamblin, M. R., Lorente, C., Nunez, S. C., Ribeiro, M. S., Thomas, A. H., Vignoni, M., & Yoshimura, T. M. (2017). Type I and Type II Photosensitized Oxidation Reactions: Guidelines and Mechanistic Pathways. *Photochemistry and Photobiology*, 93(4), 912–919. <https://doi.org/10.1111/php.12716>
- Barbosa-Cánovas, G. V., & Rodríguez, J. J. (2002). Update on nonthermal food processing technologies: Pulsed electric field, high hydrostatic pressure, irradiation and ultrasound. *Food Australia*, 54(11), 513–520.
- Birmpa, A., Sfika, V., & Vantarakis, A. (2013). Ultraviolet light and Ultrasound as non-thermal treatments for the inactivation of microorganisms in fresh ready-to-eat foods. *International Journal of Food Microbiology*, 167(1), 96–102. <https://doi.org/10.1016/J.IJFOODMICRO.2013.06.005>
- Bosshard, F., Bucheli, M., Meur, Y., & Egli, T. 2010. (2010). The respiratory chain is the cell's Achilles' heel during UVA inactivation in Escherichia coli. *Microbiology*, 156(7), 2006–2015. <https://doi.org/10.1099/mic.0.038471-0>

- Cahan, R., Swissa, N., Gellerman, G., & Nitzan, Y. (2010). Photosensitizer–Antibiotic Conjugates: A Novel Class of Antibacterial Molecules. *Photochemistry and Photobiology*, *86*(2), 418–425.
<https://doi.org/10.1111/j.1751-1097.2009.00674.x>
- Chandrasekaran, B., Abed, S. N., Al-Attaqchi, O., Kuche, K., & Tekade, R. K. (2018). Chapter 21—Computer-Aided Prediction of Pharmacokinetic (ADMET) Properties. In R. K. Tekade (Ed.), *Dosage Form Design Parameters* (pp. 731–755). Academic Press. <https://doi.org/10.1016/B978-0-12-814421-3.00021-X>
- Clementi, E. A., Marks, L. R., Roche-håkansson, H., & Håkansson, A. P. (2014). *Monitoring Changes in Membrane Polarity, Membrane Integrity, and Intracellular Ion Concentrations in Streptococcus pneumoniae Using Fluorescent Dyes. February*, 1–8. <https://doi.org/10.3791/51008>
- Costley, D., Nesbitt, H., Ternan, N., Dooley, J., Huang, Y.-Y. Y., Hamblin, M. R., McHale, A. P., & Callan, J. F. (2017). Sonodynamic inactivation of Gram-positive and Gram-negative bacteria using a Rose Bengal–antimicrobial peptide conjugate. *International Journal of Antimicrobial Agents*, *49*(1), 31–36. <https://doi.org/10.1016/j.ijantimicag.2016.09.034>
- Dadjour, M. F., Ogino, C., Matsumura, S., Nakamura, S., & Shimizu, N. (2006). Disinfection of *Legionella pneumophila* by ultrasonic treatment with TiO₂. *Water Research*, *40*(6), 1137–1142.
<https://doi.org/10.1016/j.watres.2005.12.047>
- de Oliveira, E. F., Tikekar, R., & Nitin, N. (2018). Combination of aerosolized curcumin and UV-A light for the inactivation of bacteria on fresh produce surfaces. *Food Research International*, *114*, 133–139. <https://doi.org/10.1016/j.foodres.2018.07.054>
- de Oliveira, E. F., Tosati, J. V., Tikekar, R. V., Monteiro, A. R., & Nitin, N. (2018). Antimicrobial activity of curcumin in combination with light against *Escherichia coli* O157:H7 and *Listeria innocua*: Applications for fresh produce sanitation. *Postharvest Biology and Technology*, *137*, 86–94.
<https://doi.org/10.1016/j.postharvbio.2017.11.014>

- de Oliveira, E. F., Yang, X., Basnayake, N., Huu, C. N., Wang, L., Tikekar, R., & Nitin, N. (2021). Screening of antimicrobial synergism between phenolic acids derivatives and UV-A light radiation. *Journal of Photochemistry and Photobiology B: Biology*, 214, 112081. <https://doi.org/10.1016/j.jphotobiol.2020.112081>
- Donnelly, R. F., Cassidy, C. M., Loughlin, R. G., Brown, A., Tunney, M. M., Jenkins, M. G., & McCarron, P. A. (2009). Delivery of Methylene Blue and meso-tetra (N-methyl-4-pyridyl) porphine tetra tosylate from cross-linked poly(vinyl alcohol) hydrogels: A potential means of photodynamic therapy of infected wounds. *Journal of Photochemistry and Photobiology B: Biology*, 96(3), 223–231. <https://doi.org/10.1016/j.jphotobiol.2009.06.010>
- Eghbaliferiz, S., & Iranshahi, M. (2016). Prooxidant Activity of Polyphenols, Flavonoids, Anthocyanins and Carotenoids: Updated Review of Mechanisms and Catalyzing Metals. *Phytotherapy Research*, 1391(March), 1379–1391. <https://doi.org/10.1002/ptr.5643>
- Epand, R. M., & Epand, R. F. (2009). Lipid domains in bacterial membranes and the action of antimicrobial agents. *Biochimica et Biophysica Acta - Biomembranes*, 1788(1), 289–294. <https://doi.org/10.1016/j.bbamem.2008.08.023>
- Eslami, A. C., Pasanphan, W., Wagner, B. A., & Buettner, G. R. (2010). Free radicals produced by the oxidation of gallic acid: An electron paramagnetic resonance study. *Chemistry Central Journal*, 4(1), 1–4. <https://doi.org/10.1186/1752-153X-4-15>
- Fukumoto, L. R., & Mazza, G. (2000). Assessing antioxidant and prooxidant activities of phenolic compounds. *Journal of Agricultural and Food Chemistry*, 48(8), 3597–3604. <https://doi.org/10.1021/jf000220w>
- Gao, S., Lewis, G. D., Ashokkumar, M., & Hemar, Y. (2014). *Inactivation of microorganisms by low-frequency high-power ultrasound: 1. Effect of growth phase and capsule properties of the bacteria*. <https://doi.org/10.1016/j.ultsonch.2013.06.006>

- Ghorbani, J., Rahban, D., Aghamiri, S., Teymouri, A., & Bahador, A. (2018). Photosensitizers in antibacterial photodynamic therapy: An overview. *Laser Therapy*, 27(4), 293–302.
https://doi.org/10.5978/islm.27_18-RA-01
- Giacomelli, C., da Silva Miranda, F., Gonçalves, N. S., & Spinelli, A. (2004). Antioxidant activity of phenolic and related compounds: A density functional theory study on the O-H bond dissociation enthalpy. *Redox Report*, 9(5), 263–269. <https://doi.org/10.1179/135100004225006038>
- Giuntini, F., Foglietta, F., Marucco, A. M., Troia, A., Dezhkunov, N. V., Pozzoli, A., Durando, G., Fenoglio, I., Serpe, L., & Canaparo, R. (2018). Insight into ultrasound-mediated reactive oxygen species generation by various metal-porphyrin complexes. *Free Radical Biology and Medicine*, 121, 190–201. <https://doi.org/10.1016/j.freeradbiomed.2018.05.002>
- Guo, S., Sun, X., Cheng, J., Xu, H., Dan, J., Shen, J., Zhou, Q., Zhang, Y., Meng, L., Cao, W., & Tian, Y. (2013). Apoptosis of THP-1 macrophages induced by protoporphyrin IX-mediated sonodynamic therapy. *International Journal of Nanomedicine*, 8, 2239–2246.
<https://doi.org/10.2147/IJN.S43717>
- Hamblin, M. R., & Hasan, T. (2004). Photodynamic therapy: A new antimicrobial approach to infectious disease? *Photochemical and Photobiological Sciences*, 3(5), 436–450.
<https://doi.org/10.1039/b311900a>
- Harris, F., Dennison, S. R., & Phoenix, D. A. (2014). Using sound for microbial eradication—Light at the end of the tunnel? *FEMS Microbiology Letters*, 356(1), 20–22. <https://doi.org/10.1111/1574-6968.12484>
- Huang, G., Chen, S., Dai, C., Sun, L., Sun, W., Tang, Y., Xiong, F., He, R., & Ma, H. (2017). Effects of ultrasound on microbial growth and enzyme activity. *Ultrasonics Sonochemistry*, 37, 144–149.
<https://doi.org/10.1016/j.ultsonch.2016.12.018>

- Jeon, M.-J., & Ha, J.-W. (2020). Inactivating foodborne pathogens in apple juice by combined treatment with fumaric acid and ultraviolet-A light, and mechanisms of their synergistic bactericidal action. *Food Microbiology*, *87*, 103387. <https://doi.org/10.1016/j.fm.2019.103387>
- Kaila, V. R. I., & Wikström, M. (2021). Architecture of bacterial respiratory chains. *Nature Reviews Microbiology*, *19*(5), 319–330. <https://doi.org/10.1038/s41579-020-00486-4>
- Kanthale, P., Ashokkumar, M., & Grieser, F. (2008). Sonoluminescence, sonochemistry (H₂O₂ yield) and bubble dynamics: Frequency and power effects. *Ultrasonics Sonochemistry*, *15*(2), 143–150. <https://doi.org/10.1016/j.ultsonch.2007.03.003>
- Liu, Y., Qin, R., Zaat, S. A. J., Breukink, E., & Heger, M. (2015). Antibacterial photodynamic therapy: Overview of a promising approach to fight antibiotic-resistant bacterial infections. *Journal of Clinical and Translational Research*, *1*(3), 140–167. <https://doi.org/10.18053/jctres.201503.002>
- Mazza, G. (2016). *Assessing Antioxidant and Prooxidant Activities of Phenolic Compounds †*. September 2000. <https://doi.org/10.1021/jf000220w>
- Nakonechny, F., Nisnevitch, M., Nitzan, Y., & Nisnevitch, M. (2013). Sonodynamic Excitation of Rose Bengal for Eradication of Gram-Positive and Gram-Negative Bacteria. *BioMed Research International*, *2013*. <https://doi.org/10.1155/2013/684930>
- Nakoneczna, J., Wolnikowska, K., Ogonowska, P., Neubauer, D., Bernat, A., & Kamysz, W. (2018). Rose bengal-mediated photoinactivation of multidrug resistant pseudomonas aeruginosa is enhanced in the presence of antimicrobial peptides. *Frontiers in Microbiology*, *9*(AUG). <https://doi.org/10.3389/fmicb.2018.01949>
- Nguyen, C., Rai, R., Yang, X., Tikekar, R. V., & Nitin, N. (2021). Synergistic inactivation of bacteria based on a combination of low frequency, low-intensity ultrasound and a food grade antioxidant. *Ultrasonics Sonochemistry*, *74*, 105567. <https://doi.org/10.1016/j.ultsonch.2021.105567>

- Pang, X., Xu, C., Jiang, Y., Xiao, Q., & Leung, A. W. (2016). Natural products in the discovery of novel sonosensitizers. *Pharmacology & Therapeutics*, *162*, 144–151.
<https://doi.org/10.1016/J.PHARMTHERA.2015.12.004>
- Park, J.-S., & Ha, J.-W. (2020). Synergistic antimicrobial effect of X-ray and curcumin against *Listeria monocytogenes* on sliced cheese. *Food Control*, *110*, 106986.
<https://doi.org/10.1016/j.foodcont.2019.106986>
- Plaetzer, K., Krammer, B., Berlanda, J., Berr, F., & Kiesslich, T. (2009). Photophysics and photochemistry of photodynamic therapy: Fundamental aspects. *Lasers in Medical Science*, *24*(2), 259–268.
<https://doi.org/10.1007/s10103-008-0539-1>
- Rahimi, M., Safari, S., Faryadi, M., & Moradi, N. (2014). Experimental investigation on proper use of dual high-low frequency ultrasound waves—Advantage and disadvantage. *Chemical Engineering and Processing: Process Intensification*, *78*, 17–26. <https://doi.org/10.1016/j.cep.2014.02.003>
- Rai, D., Singh, J. K., Roy, N., & Panda, D. (2008). Curcumin inhibits FtsZ assembly: An attractive mechanism for its antibacterial activity. *Biochemical Journal*, *410*(1), 147–155.
<https://doi.org/10.1042/BJ20070891>
- Ribeiro, A. P. D., Pavarina, A. C., Dovigo, L. N., Brunetti, I. L., Bagnato, V. S., Vergani, C. E., & de Souza Costa, C. A. (2013). Phototoxic effect of curcumin on methicillin-resistant *Staphylococcus aureus* and L929 fibroblasts. *Lasers in Medical Science*, *28*(2), 391–398.
<https://doi.org/10.1007/s10103-012-1064-9>
- Rivera-Lugo, R., Deng, D., Anaya-Sanchez, A., Tejedor-Sanz, S., Tang, E., Reyes Ruiz, V. M., Smith, H. B., Titov, D. V., Sauer, J.-D., Skaar, E. P., Ajo-Franklin, C. M., Portnoy, D. A., & Light, S. H. (2022). *Listeria monocytogenes* requires cellular respiration for NAD⁺ regeneration and pathogenesis. *ELife*, *11*, e75424. <https://doi.org/10.7554/eLife.75424>

- Runyan, C. M., Carmen, J. C., Beckstead, B. L., Nelson, J. L., Robison, R. A., & Pitt, W. G. (2006). Low-frequency ultrasound increases outer membrane permeability of *Pseudomonas aeruginosa*. *Journal of General and Applied Microbiology*, 52(5), 295–301.
<https://doi.org/10.2323/jgam.52.295>
- Russell, E. R. (2022). *The Role of Type II NADH Dehydrogenases in Listeria monocytogenes* [Thesis, University of Otago]. <https://ourarchive.otago.ac.nz/handle/10523/12847>
- Sango, D. M., Abela, D., Mcelhatton, A., & Valdramidis, V. P. (2014). Assisted ultrasound applications for the production of safe foods. *Journal of Applied Microbiology*, 116(5), 1067–1083.
<https://doi.org/10.1111/jam.12468>
- Saqib, M., Mahmood, A., Akram, R., Khalid, Dr. B., Afzal, S., & Kamal, G. M. (2015). Density Functional Theory for Exploring the Structural Characteristics and Their Effects on the Antioxidant Properties. *Journal of Pharmaceutical and Applied Chemistry*, 1, 65–71.
- Schleifer, K. H., & Kandler, O. (1972). Peptidoglycan types of bacterial cell walls and their taxonomic implications. *Bacteriological Reviews*, 36(4), 407–477.
<http://www.ncbi.nlm.nih.gov/pubmed/4568761>
- Shepherd, M., & Poole, R. K. (2013). Bacterial Respiratory Chains. In G. C. K. Roberts (Ed.), *Encyclopedia of Biophysics* (pp. 172–177). Springer. https://doi.org/10.1007/978-3-642-16712-6_30
- Simpson, R. (Ed.). (2009). Principles of Thermal Processing: Pasteurization. In *Engineering Aspects of Thermal Food Processing*. CRC Press.
- Sobotta, L., Skupin-Mrugalska, P., Piskorz, J., & Mielcarek, J. (2019). Porphyrinoid photosensitizers mediated photodynamic inactivation against bacteria. *European Journal of Medicinal Chemistry*, 175, 72–106. <https://doi.org/10.1016/J.EJMECH.2019.04.057>
- Spengler, G., Takács, D., Horváth, Á., Szabó, Á. M., Riedl, Z., Hajós, G., Molnár, J., & Burián, K. (2014). Efflux Pump Inhibiting Properties of Racemic Phenothiazine Derivatives and their Enantiomers

- on the Bacterial AcrAB-TolC System. *In Vivo*, 28(6), 1071–1075.
<https://iv.iarjournals.org/content/28/6/1071>
- Stark, G. (2005). Functional consequences of oxidative membrane damage. *Journal of Membrane Biology*, 205(1), 1–16. <https://doi.org/10.1007/s00232-005-0753-8>
- Tachibana, K., Feril, L. B., & Ikeda-Dantsuji, Y. (2008). Sonodynamic therapy. *Ultrasonics*, 48(4), 253–259.
<https://doi.org/10.1016/j.ultras.2008.02.003>
- Tardivo, J. P., Del Giglio, A., de Oliveira, C. S., Gabrielli, D. S., Junqueira, H. C., Tada, D. B., Severino, D., de Fátima Turchiello, R., & Baptista, M. S. (2005). Methylene blue in photodynamic therapy: From basic mechanisms to clinical applications. *Photodiagnosis and Photodynamic Therapy*, 2(3), 175–191. [https://doi.org/10.1016/S1572-1000\(05\)00097-9](https://doi.org/10.1016/S1572-1000(05)00097-9)
- Tegos, G. P., & Hamblin, M. R. (2006). Phenothiazinium Antimicrobial Photosensitizers Are Substrates of Bacterial Multidrug Resistance Pumps. *Antimicrobial Agents and Chemotherapy*, 50(1), 196–203.
<https://doi.org/10.1128/AAC.50.1.196-203.2006>
- Vecchio, D., Bhayana, B., Huang, L., Carrasco, E., Evans, C. L., & Hamblin, M. R. (2014). Structure–function relationships of Nile blue (EtNBS) derivatives as antimicrobial photosensitizers. *European Journal of Medicinal Chemistry*, 75, 479–491.
<https://doi.org/10.1016/j.ejmech.2014.01.064>
- Wainwright, M. (1998). Photodynamic antimicrobial chemotherapy (PACT). *Journal of Antimicrobial Chemotherapy*, 42(1), 13–28. <https://doi.org/10.1093/jac/42.1.13>
- Wang, X., Ip, M., Leung, A. W., & Xu, C. (2014). Sonodynamic inactivation of methicillin-resistant *Staphylococcus aureus* in planktonic condition by curcumin under ultrasound sonication. *Ultrasonics*, 54(8), 2109–2114. <https://doi.org/10.1016/j.ultras.2014.06.017>

- Wang, X., Ip, M., Leung, A. W., Yang, Z., Wang, P., Zhang, B., Ip, S., & Xu, C. (2015). Sonodynamic action of curcumin on foodborne bacteria *Bacillus cereus* and *Escherichia coli*. *Ultrasonics*, *62*, 75–79. <https://doi.org/10.1016/j.ultras.2015.05.003>
- Xu, C., Dong, J., Ip, M., Wang, X., & Leung, A. W. (2016). Sonodynamic action of chlorin e6 on *Staphylococcus aureus* and *Escherichia coli*. *Ultrasonics*, *64*, 54–57. <https://doi.org/10.1016/j.ultras.2015.07.010>
- Yang, X., Rai, R., Huu, C. N., & Nitin, N. (2019). *Synergistic Antimicrobial Activity by Light or Thermal Treatment and Lauric Arginate: Membrane Damage and Oxidative Stress*. <https://doi.org/10.1128/AEM.01033-19>
- Yoon, I., Li, J. Z., & Shim, Y. K. (2013). Advance in Photosensitizers and Light Delivery for Photodynamic Therapy. *Clinical Endoscopy*, *46*(1), 7–23. <https://doi.org/10.5946/ce.2013.46.1.7>
- Yumita, N., Okuyama, N., Sasaki, K., & Umemura, S. I. (2007). Sonodynamic therapy on chemically induced mammary tumor: Pharmacokinetics, tissue distribution and sonodynamically induced antitumor effect of gallium-porphyrin complex ATX-70. *Cancer Chemotherapy and Pharmacology*, *60*(6), 891–897. <https://doi.org/10.1007/s00280-007-0436-5>
- Zhuang, D., Hou, C., Bi, L., Han, J., Hao, Y., Cao, W., & Zhou, Q. (2014). Sonodynamic effects of hematoporphyrin monomethyl ether on *Staphylococcus aureus* in vitro. *FEMS Microbiology Letters*, *361*(2), 174–180. <https://doi.org/10.1111/1574-6968.12628>

Chapter 6

Conclusion

The findings of Chapters 2, 3, 4, and 5 supported the study's main hypothesis that the simultaneous application of sub-lethal ultrasonic treatments and sub-lethal concentrations of sonosensitizers can cause synergistic bacterial damages, including membrane damage and intracellular oxidation, and result in rapid and synergistic inactivation of bacteria in model aqueous and food systems. The specific objectives of the planned research were met, and a high level of bacterial inactivation was attained when the synergistic inactivation between ultrasound therapy and sonosensitizers was translated into a food model system. The knowledge base gained from this research project will provide a promising alternative to address some of the key limitations of both physical processing and chemical preservatives.

1. Synergistic inactivation of bacteria based on a combination of low frequency, low-intensity ultrasound and a food-grade antioxidant

The inactivation rates of the gram-negative *E. coli* O157:H7 and the gram-positive *L. innocua* are increased by a synergistic interaction between low-frequency ultrasound (LFU) and propyl gallate (PG). One of the main causes of the reported increased inactivation of bacteria, as determined by studies made using both liposomes and bacterium cells, is the rapid interaction of PG with lipid membranes. Through this interaction, the bacterial membrane was altered and becomes more permeable. LFU and PG together further increased membrane permeability in bacterial cells during an extended treatment period. The outcomes of the bacterial membrane damage experiment supported the SEM imaging findings. In contrast, a lack of significant change in the intracellular thiol content as well as a lack of protective effect from exogenous antioxidants to the antibacterial effect indicate that oxidative stress

generation was not a leading mechanism responsible for the enhanced antimicrobial effect. Overall, these results illustrate a novel approach to achieve more than 5 log inactivation of bacteria using a synergistic combination of PG with a low intensity and a low-frequency ultrasound process.

2. Combination of high-frequency ultrasound with a food-grade antioxidant for enhancing the inactivation of bacteria in water and a model food system

The inactivation rate of the targeted Gram-negative *E. coli* O157:H7 and the Gram-positive *L. innocua* was improved by the synergistic interaction of HFU and PG. The PI dye results, and SEM morphological analysis support the finding that *E. coli* O157:H7 is more susceptible to the combined HFU + PG treatment than *L. innocua*. This investigation confirmed that SAT-treated Gram-negative *E. coli* O157:H7 had more membrane damage than *L. innocua*. Furthermore, the decrease in total intracellular thiol content and the quenching impact of the addition of free radical scavengers were evidence that ROS were produced by the combination of HFU and PG. The results obtained in this work provide a proof-of-concept of an alternative non-thermal food processing approach for the decontamination of juice products. Further research is needed to identify the causes of oxidative stress experienced by bacteria treated with SAT as well as the effectiveness and scalability of the combined HFU and PG for juice processing.

3. Synergistic Treatment of *L. innocua* and Multispecies Biofilms Using Sonodynamic Antimicrobial Treatment with a Food Grade Compound

Within 30 minutes of treatment, the combination HFU + PG therapy reduced *L. innocua* and multispecies biofilms by 5 logs. The removal of biofilm biomass was also accomplished by the combination treatment. In response to HFU, PG, and a combination of these two treatments, changes in morphology were observed along with the inactivation of biofilms and removal of biofilm biomass.

Biofilm viability was not significantly impacted by a single HFU or PG treatment, however HFU demonstrated much greater removal efficiency than PG therapy alone and was comparable to the combination HFU+PG treatment. The number of dispersed planktonic cells from multispecies and *L. innocua* biofilm models was also reduced by HFU + PG to below the detection limit. Using a combination of HFU and PG, the study illustrates the synergistic inactivation of established biofilms on a food processing surface. A possible mechanism of action underlying the high efficacy of the combined treatment was also suggested by this study. An approach such as this may be relevant in areas such as food processing and packaging where biofilms are a persistent impediment.

4. Screening compounds for antimicrobial photodynamic and sonodynamic treatment for the inactivation of *Escherichia coli* O157:H7 and *Listeria innocua*

When gram-positive and gram-negative bacteria were targeted in both APDT and ASDT processes, cinnamic acid derivatives showed the highest bacterial inactivation efficacy (8–9 log CFU reduction) among the 18 compounds studied. Four of the photo-activated compounds were confirmed in the case of *L. innocua*, and six photo-activated compounds were found to interact synergistically with UV-A in inactivating *E. coli* O157:H7. There were fewer molecules in the cinnamic acid family that could work synergistically with HFU treatment than with UV-A treatment. *L. innocua* inactivation differs significantly from *E. coli* O157:H7 inactivation in that the gram-negative bacterium exhibits greater susceptibility to ASDT. These variations in antibacterial effectiveness between treatments or strains showed that APDT and ASDT may operate in different ways. We discovered a "cause and effect" relationship between the physiochemical responses of the targeted bacteria to the combined UV-A+SA and HFU+SA treatments, where intracellular oxidative stress could be a direct result of membrane damage, and membrane damage could also contribute to the inactivation of membrane-associated dehydrogenase enzyme families. The inactivation and bacterial response to the combined treatments are the results of a complex process that has yet to be fully understood, requiring further research into

elements such as bacterial gene expression and regulation in stressful conditions caused by the combination treatments. Nonetheless, the robust bacterial inactivation and the food-grade nature of the screened compounds could facilitate the adaptation of APDT and ASDT in the food industry.